

Resistance of Clay Brick Masonry Façades to Wind-Driven Rain

Repointing of Eroded Mortar Joints

MOHAMMAD KAHANGI | FACULTY OF ENGINEERING | LUND UNIVERSITY



Resistance of Clay Brick Masonry Façades to Wind-Driven Rain

Repointing of Eroded Mortar Joints

by Mohammad Kahangi



LUND
UNIVERSITY

LICENTIATE THESIS

Faculty opponent

Dr. Carl-Magnus Capener

RISE – Research Institute of Sweden

To be defended, by due permission of the Faculty of Engineering, Lund University, Sweden, in the lecture hall A:C, A-Huset, Sölvegatan 24, Lund, on Friday, the 1st of October 2021 at 13:00.

Organization LUND UNIVERSITY Department of Building and Environmental Technology Division of Structural Engineering Box 118, SE-221 00 LUND, Sweden		Document name Licentiate Thesis	
		Date of disputation 2021-10-01	
Author(s) Mohammad Kahangi		Sponsoring organization	
Title and subtitle Resistance of clay brick masonry façades to wind-driven rain: Repointing of eroded mortar joints			
Abstract <p>Clay brick masonry façades are commonly used due to their high-performance durability. However, exposure to climate agents such as wind-driven rain (WDR), freeze-thaw cycles, and wind abrasion cause deterioration of masonry façades over time. WDR as a significant source of moisture may contribute to the erosion of mortar joints and lead to increased moisture content and risk of water penetration. Accordingly, a maintenance technique, repointing of eroded mortar joints, is recommended as a measure to mitigate moisture/water penetration related to WDR. Repointing is a labor-intensive and costly measure, and there are today no established criteria to determine when repointing is necessary. As such, to enable rational decision-making in maintenance, there is a need for a systematic approach to assessing the need for repointing.</p> <p>Water penetration in masonry exposed to WDR is dependent on a wide range of parameters such as rain intensity, wind velocity, building geometry, the presence of cracks, the profile of mortar joints, the type and quality of masonry units, the compatibility of units and mortar, and the workmanship. There are several experimental methods available through standards and research studies aiming to study water penetration in masonry. Nevertheless, the test conditions, including water spray rate and differential air pressure, of those methods are rather extreme and not representative of actual conditions.</p> <p>In this regard, a new test setup has been developed to study water absorption and penetration in masonry. The key feature is to enable uniform water spray exposure at considerably lower water application rates than in existing standards while continuously recording both the amount of absorbed and penetrated water. Further, the test setup was equipped with a digital camera to record visible dampness, enabling the damp area on the backside of the specimen to be monitored over time. The test setup was used in two experimental campaigns to study the interaction of clay brick masonry and WDR, providing a fundamental basis for developing a framework for rational repointing of clay brick masonry façades.</p> <p>In the first experimental campaign, two series of clay brick masonry specimens were prepared, with two different types of bricks and three different mortar joint profiles. As a representative of eroded mortar joints, specimens with the raked joint profiles were prepared to study how eroded mortar joints might affect WDR related water absorption and penetration. The tests were conducted at zero differential air pressure, at water spray rates varying between 1.7 and 3.8 l/m²/h. In the second experimental campaign, the water spray rate was increased to around 6.3 l/m²/h; yet no air pressure was applied. Further, compared to the first campaign, three different types of bricks with different water absorption properties were considered.</p> <p>The obtained results indicate that water absorption and penetration are highly dependent on the water spray rate and water absorption properties of bricks, whereas the effect of mortar joint profile on water absorption and penetration is negligible. It should be mentioned that no considerable amount of water penetration in the first campaign was recorded; hence, only the results regarding water absorption and damp patches are presented for the first campaign. The newly developed test setup might facilitate verification of moisture simulations and provide a basis for rational decision-making concerning clay brick masonry design and maintenance.</p>			
Keywords: clay brick masonry façade, wind-driven rain, water absorption, water penetration, damp patches			
Classification system and/or index terms (if any)			
Supplementary bibliographical information		Language English	
ISSN and key title 0349-4969		ISBN 978-91-87993-20-6	
Recipient's notes		Number of pages 63	Price
		Security classification	

I, the undersigned, being the copyright owner of the abstract of the above-mentioned thesis, hereby grant to all reference sources permission to publish and disseminate the abstract of the above-mentioned dissertation.

Signature



Date 2021-08-23

Resistance of Clay Brick Masonry Façades to Wind-Driven Rain

Repointing of Eroded Mortar Joints

by Mohammad Kahangi



LUND
UNIVERSITY

Front and back cover photos by Mohammad Kahangi

© pp 1-63 Mohammad Kahangi 2021

Paper 1 © Taylor & Francis

Paper 2 © Elsevier

Paper 3 © Canada Masonry Design Center

Faculty of Engineering
Department of Building & Environmental Technology
Division of Structural Engineering

Report: TVBK-1055
ISBN: 978-91-87993-20-6
ISSN: 0349-4969
ISRN: LUTVDG/TVBK-21/1055 (63)

Printed in Sweden by Media-Tryck, Lund University
Lund 2021



Media-Tryck is a Nordic Swan Ecolabel
certified provider of printed material.
Read more about our environmental
work at www.mediatryck.lu.se

MADE IN SWEDEN 

Table of Contents

Preface	7
List of Publications	8
Summary	9
1 Introduction	11
1.1 Background	11
1.2 Objectives.....	12
1.3 Limitations	12
1.4 Outline of the thesis.....	13
2 Theoretical Framework	14
2.1 Repointing	14
2.2 Wind-driven rain	17
2.2.1 Measurements and calculations.....	17
2.2.2 WDR intensities at four sites in Sweden	20
2.2.3 Input to test design.....	22
2.3 Moisture transport	23
2.3.1 Unsaturated flow	24
2.3.2 Saturated flow.....	26
2.3.3 Rain penetration of brick masonry façades	27
3 Methods and materials.....	29
3.1 Test setup	29
3.2 Test conditions	31
3.3 Materials.....	32
3.3.1 Bricks.....	32
3.3.2 Mortars	34
3.3.3 Masonry specimens	34

4 Experimental results	38
4.1 General observations	38
4.2 Water absorption	39
4.2.1 First campaign (A).....	39
4.2.2 Second campaign (B)	41
4.3 Damp patches	44
4.4 Water penetration	46
5 Summary of the appended papers	52
6 Conclusions	54
7 Future Research.....	56
References	58

Preface

The presented thesis is submitted for the licentiate degree at Lund University. The author conducted the research described herein under the supervision of Dr. Miklós Molnár at the Division of Structural Engineering, Lund University, between September 2019 and September 2021.

I would like to express my gratitude to my main supervisor, Dr. Miklós Molnár, and assistant supervisor, Tekn. Lic. Tomas Gustavsson, who drew the outline of the project. Constructive supervision, patience, and support of Miklós have helped me to accomplish my study goals. Thank you so much for all your encouragement, sharing knowledge, and always providing helpful feedback. Further, I would like to thank my co-supervisor, Dr. Jonas Niklewski, a caring friend and patient colleague with exceptional input and golden hands in programming and image analysis. I would like to thank my assistant supervisors, Tekn. Lic. Tomas Gustavsson, Dr. Eva Frühwald Hansson, and Dr. Ivar Björnsson, for their excellent guidance and support during this project. I am also grateful for the support given by Per-Olof Rosenkvist, without whose cooperation I would not have been able to conduct the experimental part of the project. I also wish to thank all the reference group members.

The project would not have been possible to be carried out without the financial support of the Development Fund of the Swedish Construction Industry (SBUF) and the Masonry and Render Construction Association (TMPB).

To my other colleagues, Amro, Iman, and Oskar, at the Division of Structural Engineering: I would like to thank you for your outstanding cooperation as well. It was always helpful to bat ideas about my research around with you. I also benefitted from debating issues with my friends and family.

Mohammad Kahangi

List of Publications

- I. **Shahreza, S., Molnár, M., Niklewski, J., Björnsson, I., & Gustavsson, T. (2020). Making decision on repointing of clay brick facades on the basis of moisture content and water absorption tests results—a review of assessment methods. In the proceedings of the 17th International Brick/Block Masonry Conference (17th IB2MaC 2020), Kraków, Poland, (pp. 617-623). CRC Press/Balkema.**
- II. **Shahreza, S. K., Niklewski, J., & Molnár, M. (2021). Experimental investigation of water absorption and penetration in clay brick masonry under simulated uniform water spray exposure, *Journal of Building Engineering*, vol. 43, p. 102583, 2021, doi: <https://doi.org/10.1016/j.jobe.2021.102583>.**
- III. **Shahreza, S., Molnár, M., & Niklewski, J. (2021). Water absorption and penetration in clay brick masonry exposed to uniform water spray. In the proceedings of the 14th Canadian Masonry Symposium (14th CMS), Montreal, Quebec, Canada, 16–20 May 2021.**

Summary

Clay brick masonry is a building material commonly used in façades because of its high durability and a reduced need for costly maintenance. While being a comparatively slow process, brick masonry façades deteriorate over time due to climate agents such as cyclic freezing-thawing and wind-driven rain (WDR), making continual monitoring and frequent maintenance of masonry façades necessary. WDR is a significant source of moisture and a leading cause of mortar joint erosion in Nordic countries. High levels of moisture and water penetration resulting from WDR can cause corrosion of reinforcement, promote microbiological growth, and compromise indoor air quality. Accordingly, maintenance techniques such as repointing of eroded joints can be used to control moisture content and water penetration and to protect moisture-sensitive parts of the building envelope.

There are several benefits to repointing. Primarily, it is expected that repointing can reduce the risk of issues stemming from the increased penetration of WDR caused by eroded mortar joints. Further, repointing may lead to improving the aesthetics and maintain the integrity of the façade. However, there are also several risks related to improper repointing, such as the risk of damaging the bricks or the existing mortar. In addition, repointing is both a laborious and expensive measure.

Repointing should not be carried out in situations when it is not required. Today, repointing is generally carried out at regular intervals ranging between 40-50 years, even if not necessary. In order to improve current practice, more well-established criteria to assess the actual need for repointing are required. In order to do so, the resistance of masonry façades to frequent WDR events encountered in Nordic countries should be understood. Secondly, the effects of erosion and repointing of mortar joints need to be established. This information can ultimately be used in a cost-benefit analysis to enable rational decisions on the maintenance of clay brick façades.

There are many parameters affecting moisture content and water penetration of masonry façades. The first group of parameters consists of characteristics of rain and wind, including rain intensity, raindrop size, wind velocity, and wind direction. The second group is related to the characteristics of the masonry, including material properties (absorption properties of brick and mortar), joint profile, mortar water content, and joint thickness. However, masonry walls with the same prescribed characteristics may differ widely in performance due to workmanship during construction.

The primary goal of the studies presented in this thesis is to investigate the resistance of clay brick masonry façades exposed to realistic WDR events, providing basic knowledge to make rational decisions on maintenance techniques, with a focus on repointing. Experimental campaigns were designed to explore the masonry-water interaction during exposure to WDR. The test parameters include water spray rate,

water absorption properties of bricks, and mortar joint profiles. A newly developed test setup capable of producing a wide range of WDR intensities with a uniform water spray is designed. The test conditions are adapted to be representative of WDR events encountered on the west coast of Sweden.

The results indicate that mortar joint erosion may not affect to a significant degree water absorption and penetration in masonry exposed to WDR. Furthermore, the benefit gained from the water absorption capacity of clay brick masonry to buffer and thus postpone water penetration is of great importance. Considering frequent WDR events where the average WDR intensity usually varies between 1–2 mm/h, and wind speed is less than 5 m/s, equivalent to 20 Pa pressure difference, clay brick masonry façades are capable of absorbing most of the raindrops prior to water penetration.

There are several techniques available that may reveal the real need for repointing or postpone costly maintenance techniques. Washing the masonry façade gently with water and cleaning microbiological growth might reveal the depth of erosion and cracks. Washing might also reduce the fixation of water to clay brick façades. Further, hairline cracks that are not deep through the masonry wall can be treated by so-called surface grouting, expected to reduce water absorption during WDR events.

Based on the previous observations and analyses of climate data, usually, one or two faces of a building are exposed to more wind-driven rain than the other faces. Therefore, partial repointing can be considered as an alternative, reducing the maintenance costs compared to full repointing.

1 Introduction

1.1 Background

Clay brick masonry is one of the most common building materials used in external walls and building façades, with a history spanning many thousands of years and applications throughout the world. Its longevity and ubiquitous use provide some insight into clay brick masonry's excellent durability and long-term performance. In addition to the impacts of material properties and workmanship on the durability of masonry, performance degradation due to exposure to climate agents such as wind-driven rain (WDR) and freeze-thaw cycles is notable. WDR is a significant source of moisture ingress and a leading cause of the erosion of mortar joints, further associated with elevated moisture accumulation and increased risk of water penetration.

The co-occurrence of wind and rain giving rise to an oblique driving rain vector, that together with the presence of deficiencies like cracks, voids, and pores, may result in water penetration. Water penetration through façades depends on several parameters categorized into two groups. The first group is related to the WDR deposition rate on building façades, including rain intensity, raindrop size, wind velocity and its direction, building geometry and its height, and topography. The second group of parameters is related to the façade characteristics such as the presence of cracks, the profile of mortar joints, the type and quality of masonry units, the type of mortar and its consistency, the compatibility of units and mortar, joint thickness, and the workmanship.

In addition to the impact of WDR on the aesthetics of masonry façades, high levels of moisture and water penetration resulting from WDR can cause corrosion of reinforcement and promote microbiological growth, leading to the physical deterioration of the envelope and of the quality of indoor air through the emission of mycotoxins and organic volatiles [1]. Performing maintenance is thus necessary to ensure the long-term performance of the structure, reduce the speed of deterioration, and guarantee the comfort of its users.

A typical maintenance technique to mitigate moisture/water penetration related to WDR in brick masonry façade is repointing, recommended being carried out after 40–50 years of the façade erection. Repointing is the process of raking out the eroded/cracked mortar joints to a certain depth and replacing it with new mortar.

The motivation for repointing is often brought up when eroded mortar joints, cracks in the mortar, gaps between the mortar and masonry unit, damp surfaces on the masonry, and water infiltration on the interior walls are observed [2].

On the one hand, repointing of the eroded joints may improve the resistance of the masonry façade to WDR and keep the integrity of the masonry. On the other hand, repointing only to improve the aesthetics of the façade may also be unsuitable owing to the high costs and relatively complex procedures for carrying out repointing. Additionally, repointing can lead to premature deterioration of the mortar and the masonry unit, such as erosion of the edges of soft masonry units and discoloration of the masonry units if it is not done properly. Hence, there is a need to shed light on how the erosion of mortar joints influences water uptake and penetration exposed to WDR, providing a basis for making rational decisions on repointing. In order to do so, there is a need to understand the basic interaction of clay brick masonry exposed to realistic WDR intensities.

Various test setups have been proposed in different standards and research studies to explore water penetration in masonry [3-10], yet the applied water spray and air pressure rates represent rather extreme WDR conditions [3-9, 11-14]. Hence, several authors have pointed out the need to develop a simple test setup able to operate at considerably lower water application rates [6, 9, 15-18]. Accordingly, several studies were carried out with adjusting test conditions, including differential air pressure [5, 12, 19, 20] and water spray rate [18, 21, 22]. Therefore, to better understand brick masonry resistance to WDR, there is a need to adapt the test parameters of the available standards.

1.2 Objectives

The primary objective of the presented thesis is to provide an adequate understanding of the clay brick masonry response exposed to more realistic and frequently encountered WDR events. It is expected that the outcomes lead to solid and scientific knowledge to be used in the context of assessing repointing needs. In doing so, water absorption and penetration in masonry as a function of brick and mortar material properties were studied. Additionally, the effect of mortar joint erosion on water absorption and penetration in masonry was investigated.

1.3 Limitations

The experimental investigation presented here is limited to studying the exposure of small-scale brick masonry specimens to uniform water spray, whereas a masonry

façade includes windows, joints, and other connections that are expected to be more vulnerable to WDR exposure. Moreover, masonry façades are exposed to different rain and wind events in the long term, resulting in high moisture levels, erosion of mortar joints, and leakage, whereas exposing masonry façades to real WDR events in the laboratory is not achievable.

Additionally, specimens tested in this study were built without any known cracks and deficiencies, whereas many existing masonry façades contain cracks either on bricks or mortar joints. Further, because of the difficulty of preparing specimens with eroded mortar joints, specimens with a raked joint profile were chosen as a representative of eroded joints. However, erosion of mortar joints happens after long-term exposure to WDR, wind abrasion, and freezing-thawing, leading to higher porosity and change of mortar properties.

1.4 Outline of the thesis

The thesis is divided into seven chapters. Chapter 1 introduces the background, objectives of the research, and limitations of the current work. At the beginning of Chapter 2, repointing as a maintenance technique to diminish WDR related issues is introduced, and motivations to make a decision on repointing are discussed. Subsequently, two categories of wind-driven rain studies in relation to building research are discussed. Eventually, as moisture is one of the leading causes of the damage on building façades, moisture transport mechanisms within porous media like masonry are described. Chapter 3 presents a newly developed test setup used to study the exposure of masonry to WDR. Relevant properties of materials and preparation of masonry specimens are described. Chapter 4 focuses on the experimental results, including water absorption and penetration in clay brick masonry. A summary of the appended papers is provided in Chapter 5. The thesis is concluded with a conclusion in Chapter 6, and finally, suggestions for future research are proposed in Chapter 7.

2 Theoretical Framework

In this chapter, repointing as a maintenance technique that is supposed to diminish WDR related problems is introduced, and motivations to make a decision on repointing are discussed. Subsequently, two categories of WDR studies concerning building research are discussed. Different methods to quantify WDR deposition are further introduced, and a well-known and frequently used model, the ISO Standard, to quantify WDR deposition on building façades is presented in detail. The presented model is then applied to study WDR deposition for different locations in Sweden. The obtained results can provide a rational basis for designing the experimental studies and being applied in the test setups. Eventually, since moisture is one of the leading causes of damage on building façades, moisture transport mechanisms within porous media like masonry are presented.

2.1 Repointing

Maintenance due to inevitable deterioration caused by climate actions is needed to ensure the durability performance of a clay brick masonry façade during its expected service lifespan, which often exceeds a hundred years. Climate agents relevant to Nordic countries, including WDR and freeze-thaw cycles, are a significant cause of spalling, delamination, or cracking of bricks and the erosion and cracking of mortar joints. Prior to performing any maintenance, a preliminary assessment including visual inspection with reviewing existing documentation is highly recommended to determine the source and the severity of probable existing damages/problems. Besides, performing tests (non-destructive or destructive) might add valuable information to the state assessment of the façade. Rational decisions can then be made based on the analysis of the information at hand through a cost-benefit analysis. Several recommendations on practical tools to assess the state of the façade and relevant maintenance techniques are reported in Paper I.

One maintenance technique often carried out nowadays in order to tackle problems raised by eroded/cracked mortar joints is repointing. Repointing is the process of raking out existing mortar joints to a certain depth, usually 25 mm, and then replacing them with new mortar that should be compatible with the existing mortar and bricks. Figure 1 illustrates a clay brick masonry façade before, during, and after repointing.

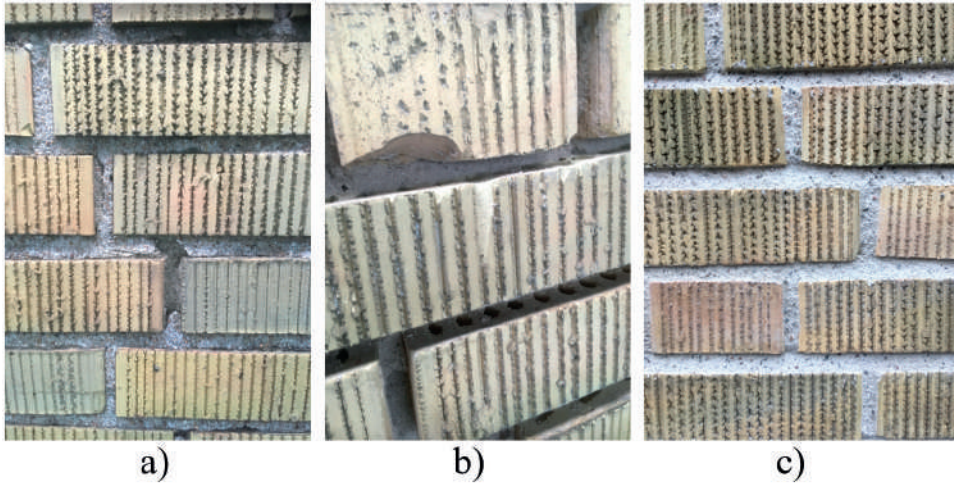


Figure 1. A clay brick masonry façade, before and after repointing a) the initial state where mortar joints were eroded; b) mortar joints were raked out up to the depth of 25 mm; c) new mortar was pointed.

A common argument for repointing is that the erosion of mortar joints facilitates water uptake in façades exposed to WDR [23]. Further, erosion of mortar joints is regarded as unfavorable from an aesthetic point of view, at least in the Nordic countries, since it creates, seen superficially, the impression of building damages. According to the present practice in the Nordic countries, repointing shall be carried out as part of a regular maintenance scheme, after 40-50 years from erection or when limited façade parts with more or less eroded mortar joints are observed [24, 25]. Normally, no further investigations (e.g., concerning factual water up-take) nor alternative measures (e.g., partial repointing of eroded parts) are considered. In light of the presented practices, it can be objected that decision concerning the repointing of clay brick façades is usually not based entirely on rational grounds.

Although repointing is expected to reduce water ingress from WDR [26], repointing to improve only the aesthetics of the façade or, in the case of minor signs of erosion, regardless of its laborious task, may imply unnecessary costs [27, 28]. Since natural sands were used in the mortar mix of many old masonry façades, in the case of repointing, sand made from crushed stones is normally used because of the limited source of natural sands; under this circumstance, repointing will not improve aesthetics. Improper selection and application of repointing mortars can further result in permanent damage to older masonry walls [29, 30]. Specific problems include incompatibility between the new mortar and existing mortar [31] or between the new mortar and bricks (i.e., the weak bond between new mortar and existing bricks) [32, 33], as well as poor workmanship. Thus, in the case of unnecessary repointing, there is a higher risk of aesthetic matters and durability problems in the form of frost damage and spalling of the façade [34]. Figure 2 exemplifies the

adverse effects of selecting improper mortar and poor workmanship during repointing.

Accordingly, there is a need for a systematic approach to decide when repointing is needed and how it should be carried out. Recommended steps to reach a rational decision on repointing are further discussed in Paper I.



Figure 2. An example of adverse effects of selecting unsuitable mortar and shoddy workmanship on repointing

Qualitative and quantitative criteria concerning the need for repointing have been proposed by several researchers, e.g. [24, 26, 35-37], recommending repointing when a) the surface of the mortar joints contains hairline cracks, b) eroded mortar joints to a certain depth [a quarter of an inch, i.e., 6.4 mm] have been observed, c) crack widths larger than 2 mm have been measured, d) the rate of water absorption is more than 4.5 l/m²/h or e) presence of voids has been detected. According to the proposed criteria, it should be investigated to what extent high moisture content and water absorption/penetration are related to the outer part of the mortar joints and whether repointing can make a difference in reducing water absorption/penetration [29, 32]. It should be noted that only 25 mm of the outer part of the cracked/eroded mortar joints or 2.5 times of the mortar joint thickness is normally raked out and replaced with a new mortar in repointing. In this context, the relation between the depth of erosion of the mortar joints and the possible increase in water absorption and penetration from WDR should be examined. Furthermore, the rationality of some of the proposed criteria can be questioned and needs to be investigated, e.g., concerning acceptable crack width, since it has been shown that water ingress in cementitious materials increases exponentially when the crack width exceeds 0.2 mm [38, 39].

2.2 Wind-driven rain

WDR is one of the most important moisture sources affecting the performance of building façades and resulting in the erosion of mortar joints. Therefore, the study of WDR in order to quantify WDR intensity on building façades is essential for hygrothermal and durability analyses. Further, a framework is required to understand frequent WDR events in regions with moderate WDR events, which then can be a rational basis for test conditions in experimental studies.

2.2.1 Measurements and calculations

Generally, studies of WDR consist of two categories; i) the first one mainly deals with quantifying WDR deposition on building façades, and ii) the second category studies the response of buildings to WDR impingement and its effect on building façades. In order to assess the hygrothermal performance of a building envelope, the appropriate estimation of the amount of rainwater striking the building's façade, the first category of WDR studies, is required.

Three different methods, namely, a) experimental, b) semi-empirical, and c) numerical, are used to quantify WDR deposition on building façades. The WDR intensity depends on several factors such as rain intensity, raindrop size, wind speed and its direction, building geometry, and topography.

In experimental methods, rain gauges are used to measure WDR on building façades, and since there is no standardized rain gauge [40], there can be a significant difference in the measurements. Although experimental measurements are still needed to validate semi-empirical and numerical models [40, 41], they are time-consuming and costly, as they should be continued for more extended periods.

Therefore, semi-empirical relationships were established to obtain WDR exposure of building façades based on standard weather data, including wind speed, wind direction, and horizontal rainfall. In order to improve the accuracy of semi-empirical equations, two main modifications are taken into account in different models; a) factors such as building geometry, local topography, and presence of obstruction are considered; b) hourly rainfall and wind speed data are normally used to estimate WDR deposition. Nevertheless, semi-empirical methods are generally accurate only for stand-alone buildings in simple configurations or for preliminary analyses. These methods will not give accurate results in cases where complex flows around buildings due to the influence of the surrounding buildings are observed [40].

Because of the shortcomings in the measurement of WDR in both experimental and semi-empirical methods, numerical methods based on computational fluid dynamics (CFD) can be used to account for building geometry by simulating wind-flow

patterns and trajectories of raindrops. However, the method is far complicated, computationally expensive, and time-consuming.

The second category of WDR studies investigates phenomena such as splashing, bouncing, spreading, and absorption of raindrops, water film and its absorption, moisture accumulation and water content in walls, rain penetration, and runoff [42]. In this regard, Erkal et al. [43] and Abuku et al. [44] have studied splashing, bouncing, spreading, and absorption of raindrops when hitting masonry façades. Further, several studies on the rain absorption and the rainwater runoff, which are responsible for water leakage in building façades and the appearance of surface soiling patterns on façades, have been conducted by Carmeliet and Blocken [45], Robinson and Baker [46], and Newman et al. [47].

By considering the same size for all raindrops and a uniform and steady wind, the general equation for WDR intensity, i.e., water drops passing through an imaginary vertical plane, is expressed as [48, 49]:

$$R_{wdr} = R_h \cdot \frac{U}{V_t} \quad (1)$$

where R_h is the horizontal rain intensity (mm/h), U is the wind speed (m/s), and V_t is the terminal velocity of raindrops (m/s).

In Eq. (1), wind direction is considered perpendicular to the vertical surface, and the assumption is that there is no deflection of wind and raindrops by the vertical surface. Lacy [49] proposed a similar relationship (Eq.(2)) for WDR intensity by considering various results from observations, as presented below:

$$R_{wdr} = 0.222 \cdot U \cdot R_h^{0.88} \quad (2)$$

where 0.222 (s/m) is the WDR coefficient.

The model by Lacy [49] considers the WDR coefficient resulting from the adopted empirical relationships. The associated WDR coefficient of 0.222 s/m was derived for free-field conditions (i.e., free driving rain) and corresponds to a raindrop diameter of 1.2 mm, a realistic value for rain events of light to moderate intensity [50].

To determine the WDR coefficient on a building façade more accurately, several parameters, including building geometry and topography, should be considered. Accordingly, the semi-empirical models proposed by Straube and Burnett (SB) [51] and ISO Standard [52], and the numerical model developed by Choi [53] attempt to quantify the WDR coefficient and WDR intensity by taking into account several parameters such as building geometry, position on façade, environment topography, mean wind speed, and wind direction [54].

In order to take into account disturbed wind-flow patterns around the building, which results in a considerable difference between the WDR intensity in free-field conditions and the WDR intensity on a building façade, an adapted WDR coefficient, α , was introduced. Hence, the WDR relationship can be written as follows:

$$R_{wdr} = \alpha \cdot U \cdot R_h^{0.88} \cdot \cos \theta \quad (3)$$

where α is the WDR coefficient (s/m), and θ is the angle between the wind direction and the normal to the façade.

The ISO Standard of 2009 [52] is mainly established according to the BS 8104 [55] code, based on a long series of WDR measurements within the UK. It should be noted that the model primarily applies to climates similar to the UK. Four main parameters are used in the ISO model to convert the amount of rain that would be collected by a free-standing rain gauge in a flat open field into the amount of rain that would impact a façade. Thus, the WDR coefficient in the ISO model is calculated as follows.

$$\alpha = \frac{2}{9} \cdot C_R \cdot C_T \cdot O \cdot W \quad (4)$$

where C_R is the terrain roughness coefficient, C_T is the topography coefficient, O is the obstruction factor, and W is the wall factor.

The roughness coefficient, C_R , takes into account the variability of mean wind velocity at the site due to the height above the ground and the roughness of the terrain. The ISO model defines four different terrain categories and their relevant parameters to determine the roughness coefficient, C_R at height z , which is calculated as follows.

$$C_R(z) = K_R \cdot \ln\left(\frac{z}{z_0}\right) \text{ for } z \geq z_{\min} \quad (5)$$

$$C_R(z) = C_R(z_{\min}) \text{ for } z < z_{\min} \quad (6)$$

where z is the height above ground [m]; K_R is the terrain factor [-]; z_0 is the roughness length [m], and z_{\min} is the minimum height [m].

In order to account for the increase in mean wind speed over hills and escarpments, the topography coefficient, C_T is introduced, depending on the upwind slope. The obstruction factor, O , takes into account the horizontal distance between the exposed wall and the nearest obstacle, which is at least as high as the wall. Thus, depending on the distance to the nearest obstacle, the obstruction factor varies in the range of 0.2 and 1.0. The wall factor, W , considers wall types, overhangs, and the orientation of bricks affecting the amount of rain incident on a wall. Hence, the wall factor is

considered to be between 0.2 and 0.5 and varies along with the height of the wall. Despite many WDR measurements indicating that the WDR intensity increases from the middle of the façade to the sides [40], the ISO Standard assumes the same wall factor across the width of the wall.

2.2.2 WDR intensities at four sites in Sweden

In this study, ISO Standard [52], one of the most frequently used models, has been used to provide general information about WDR intensity in Sweden, which can be used as a rational basis for test conditions. In doing so, four locations, namely, Malmö, Gothenburg, Uppsala, and Hörby, located in different regions of Sweden, are studied to analyze WDR intensities. It should be mentioned that the hourly rain intensities and wind velocities in Malmö, Gothenburg, Uppsala, and Hörby for the period 1995 – 2020 are used. The climate data is taken from the Swedish Meteorological Hydrological Institute (SMHI) [56].

To have a better picture of WDR intensities that impacted a building façade during 1995 – 2020, a low-rise building with a 15-m height is considered. It is assumed that the wind direction is perpendicular to the façade ($\theta = 0^\circ$) and the building neighbors to farmlands, thus belonging to terrain category II, according to the ISO model. Values of K_R , z_0 , and z_{\min} as a function of the terrain category are given in the ISO model, in which $K_R = 0.19$, $z_0 = 0.05$ m, and $z_{\min} = 4$ m for terrain category II. Thus, the roughness coefficient C_R is equal to 1.084. Additionally, the building is considered to be located in a flat terrain without any obstruction in its surrounding. Hence, the topography coefficient, C_T , and obstruction factor, O , are equal to one. The wall factor, W , for a multi-story building without any overhang and protection, is equal to 0.5 for the upper part of the façade. Therefore, for the considered building, the WDR coefficient, α , is equal to 0.12 s/m.

Figure 3 illustrates the cumulative time-frequency distribution of WDR intensities for the particular building located in Malmö, Gothenburg, Uppsala, and Hörby for the time period between 1995 and 2020. As can be seen, the majority of WDR events occurred with an intensity of less than 1 mm/h. Nevertheless, the highest WDR intensity varies between 8.5 and 36 mm/h for the studied locations during 1995 – 2020.

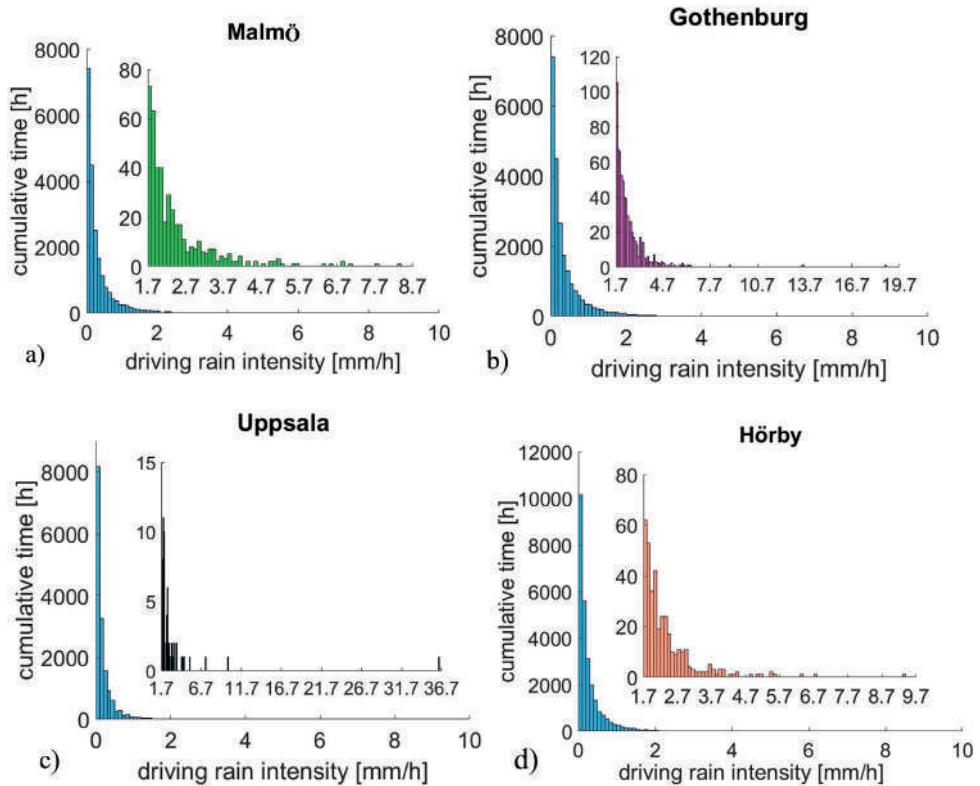


Figure 3. Driving rain intensities from 1995 to 2020 for the considered building located in a) Malmö, b) Gothenburg, c) Uppsala, and d) Hörby

Furthermore, the duration of each WDR event with an intensity of at least 0.1 mm/h for each location is shown in Figure 4. The figure indicates that the majority of WDR events lasted around 1 h to 4 h, though the maximum duration of WDR events was between 23 h and 33 h for the studied locations.

Additionally, the average hourly wind speed at 10 m above ground during WDR spells with an intensity of at least 0.1 mm/h was between 2.7 m/s and 4.2 m/s for the studied locations. Therefore, the mentioned wind speeds impose a pressure difference of less than 10 Pa across the building envelope. Moreover, during the period of 1995 to 2020, the maximum registered wind speed during rainfall events for the studied locations varied between 9.2 m/s and 18.5 m/s, corresponding to an air pressure difference of around 55 Pa – 220 Pa.

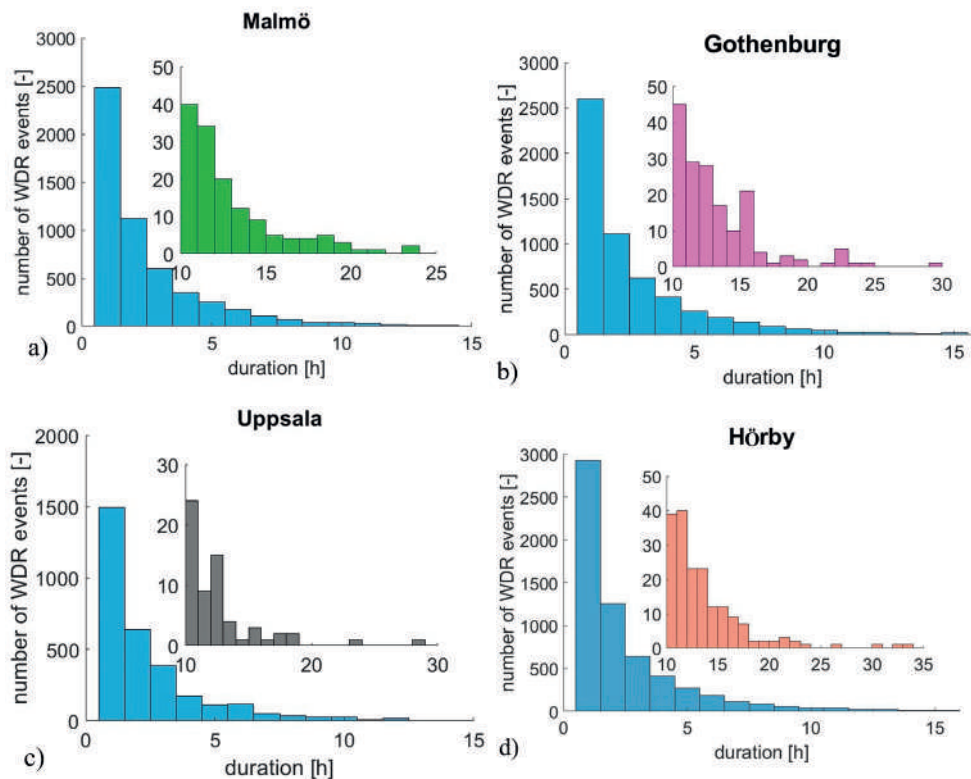


Figure 4. Number and duration of WDR events from 1995 to 2020 for the considered building located in a) Malmö, b) Gothenburg, c) Uppsala, and d) Hörby

2.2.3 Input to test design

The analysis in Section 2.2.2 indicates that water application rates of 72–138 l/m²/h in the current standards [3, 7, 8] represent non-frequent WDR events in Sweden; probably realistic for high-rise buildings and may occur in a short period of time (i.e., not in the hourly scale). Thus, there is a need for a test setup capable of producing a more realistic range of WDR intensities encountered in Sweden to have a better understanding of masonry façade resistance to WDR. It is also clear that differential air pressure levels of 400–1000 Pa, applied in the test standards [3, 11, 12], are quite unlikely to act across the envelope in conjunction with rain.

Moreover, three WDR events taking around 21 h were recorded for Hörby during 1995 – 2020. Figure 5 shows the hourly WDR intensity for these three events, happening during 21 h of consecutive rainfall. The average WDR intensity for Hörby during these events is equal to 0.43 mm/h, 0.52 mm/h, and 0.68 mm/h. Additionally, the maximum hourly WDR intensity for each event is equal to 1.05 mm/h, 1.2 mm/h, and 2.25 mm/h. Therefore, based on the available results,

rain penetration tests of 46 hours and 90 hours with the water spray rate of $72 \text{ l/m}^2/\text{h}$ and $120 \text{ l/m}^2/\text{h}$ in accordance with NBI method 29/1983 [8] and NEN 2778 [7] represent extreme and non-frequent WDR events encountered in Sweden.

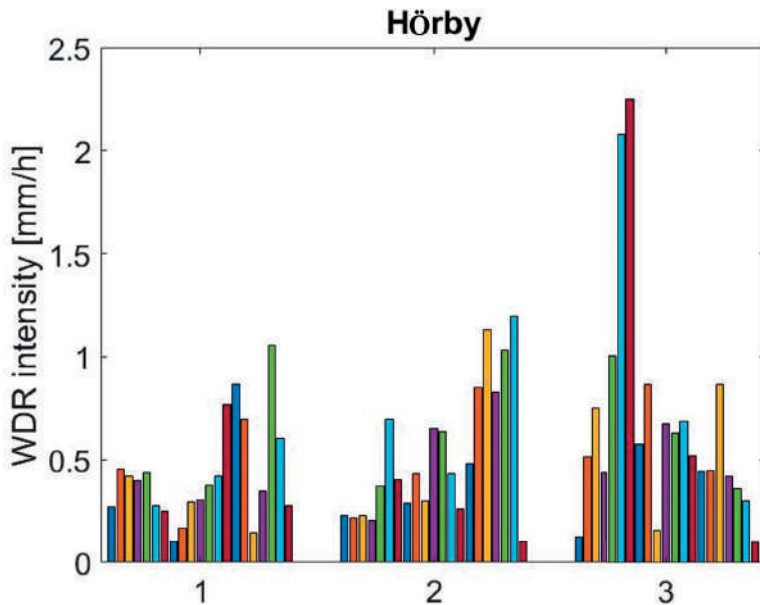


Figure 5. WDR intensity during three rainfall events with the duration of 21 h in Hörby during 1955-2020

2.3 Moisture transport

As moisture is one of the primary agents of damage and deterioration of façades, knowledge about moisture transport in building materials is of great importance. As in any porous material, free (liquid) water and vapor might co-exist in masonry. However, different phases of water are subjected to different mechanisms for transport through the material.

Many building materials, such as bricks and mortars, are hygroscopic, meaning they absorb or release moisture to the environment until equilibrium conditions are reached [59]. The relationship between moisture content and equilibrium relative humidity of building materials can be displayed in the form of so-called sorption-isotherms [60]. Figure 6 shows the absorption and desorption isotherms of typical clay brick and cement-based mortar. The steep slope at about 95% relative humidity can be referred to as the over-hygroscopic region of the sorption isotherm. In this region, water is absorbed mainly through capillary condensation. The moisture

content in bricks in the hygroscopic region is limited, normally below 10 kg/m^3 , whereas it usually is several times higher in mortar.

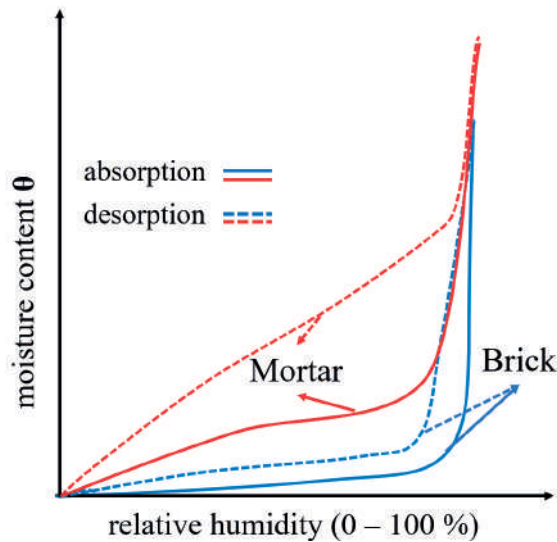


Figure 6. Sorption isotherms of typical clay brick and cement-based mortar

Although clay brick masonry façades absorb and release moisture to reach equilibrium with their ambient condition, the moisture content in this state is limited. Therefore, more attention is paid to moisture transport above the hygroscopic region, where capillary absorption dominates.

The transport mechanism of moisture depends on the phase of water and, as aforementioned, several phases of water co-exist in the pore system. The transport of water vapor is governed by diffusion and convection, whereas the transport of free water can be divided into unsaturated (capillary absorption) and saturated flow (permeation). While several transport mechanisms may occur simultaneously, the transport of free water becomes increasingly dominant as the material enters the over-hygroscopic region. It should be noted that masonry walls exposed to WDR generally do not attain full saturation throughout their depth. Transport of liquid water is thus, under normal circumstances, primarily governed by unsaturated flow through capillary absorption [57, 58].

2.3.1 Unsaturated flow

Since this study focuses on the resistance of masonry to driving rain, moisture transport in the liquid phase is in focus. Liquid transport in a single material, such as bricks or hardened mortar, is well understood and explained with capillary transport theory. Capillary absorption within capillary pores is mainly controlled by

the capillary pressure and can be analyzed by the so-called extended Darcy's equation, which can be written as follows:

$$u = -K(\vartheta) \times \nabla\varphi \quad (7)$$

where u is the flow rate within porous medium [m/s] and $K(\vartheta)$ is the liquid conductivity, also known as unsaturated permeability [m/s], a function of the normalized water content ϑ . The driving force, $\nabla\varphi$, is the gradient of the total hydraulic potential [-]. The hydraulic potential includes not only the capillary potential, Ψ [-], but also other external driving forces (such as external pressure and gravity). ϑ denotes the normalized water content [-] and can be calculated as follows [57, 58]:

$$\vartheta = \frac{\theta - \theta_r}{\theta_s - \theta_r} \quad \& \quad 0 \leq \vartheta \leq 1 \quad (8)$$

where θ is the volumetric water content [m³], θ_r is the residual water content [m³], and θ_s is the saturated water content [m³].

A useful result that follows from Eq. (7) is an equation defining the advance of a water content profile as water is absorbed into an initially dry porous solid. When water is absorbed horizontally into an initially dry porous solid, all points on the water front advance as a function of the square root of time, $t^{1/2}$. In addition, the absorbed mass of water is proportional to the square root of time and can be written as follows.

$$m = \rho_w S A t^{1/2} \quad (9)$$

where m is the absorbed mass [kg], ρ_w is the density of water [kg/m³], S is the sorptivity [m/s^{1/2}], and A is the cross-sectional area [m²]. The sorptivity is an inherent property that describes the material's ability to absorb and transmit water by capillarity. Following Eq. (9), it is possible to determine how far the capillary front reaches as a function of time. The time, t [s], for the capillary front to reach a certain distance, z [m], in a porous medium may be calculated as follows:

$$t = \mu z^2 \quad \text{where} \quad \mu = \left(\frac{p}{S}\right)^2 \quad (10)$$

where μ is the capillary resistance number [s/m²], and p is the porosity [-].

While Eq. (10) is useful for describing the progression of a moisture front in a single material, masonry is made of both brick and mortar. Two materials that are in contact can transfer water through capillary action. In addition, an imperfect bond between brick and mortar can lead to reduced resistance to water along with the brick-mortar interface. Figure 7 illustrates, conceptually, the distribution of water in

clay brick masonry exposed to one-sided wetting under two different assumptions: a) full contact and b) water transport through the brick-mortar interface where it is assumed that the interface acts as a gap. Considering higher sorptivity for the brick in comparison with the mortar, it takes more time for the capillary front to reach a certain depth in the mortar than in the brick. In practice, water will be transported from the brick to mortar (Figure 7.a). Finally, if the capillary resistance of the interfacial zone is lower than that of brick and mortar, then the moisture distribution may conceptually be illustrated as shown in Figure 7.b.

It should be noted that in most instances of rain penetration in brick masonry walls, leakage occurs close to the brick-mortar interface, yet rain can pass through the bricks or the mortar joints under more unusual circumstances.

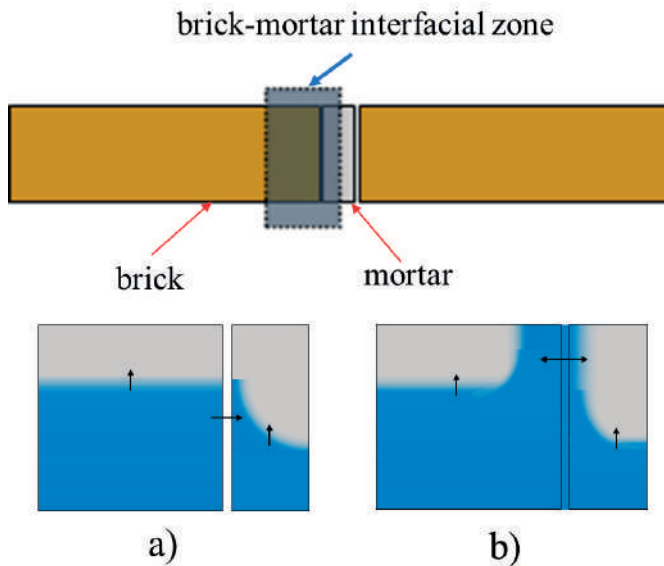


Figure 7. Moisture transport through a brick-mortar interfacial zone; a) full contact and b) lower capillary resistance

2.3.2 Saturated flow

The mathematical description for permeation of liquids through porous materials is based on Darcy's law, which can be written as follows [57, 62]:

$$Q = \frac{k \times A \times \Delta p}{\mu \times \Delta x} \quad (11)$$

Where Q is the volumetric flow rate [m^3/s], k is the permeability [m^2], A is the cross-sectional area [m^2], Δp is the pressure gradient, i.e., the hydrostatic pressure

difference across the studied length, [Pa], μ is the dynamic viscosity [Pa.s], and Δx is the length [m] (Figure 8).

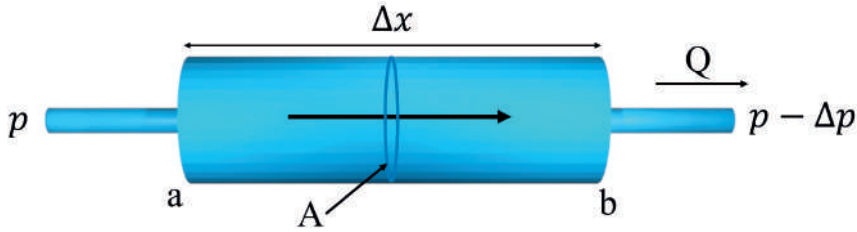


Figure 8. Simple Darcy flow through a liquid-saturated homogeneous medium under the action of a pressure gradient

By considering the hydraulic gradient applied between point a and b, $\nabla p = \Delta p / \Delta x$, Darcy's law is commonly written in terms of the flow rate or Darcy velocity, u [m/s], [57]:

$$u = \frac{Q}{A} = \frac{k \times \nabla p}{\mu} \text{ [m/s]} \quad (12)$$

The hydrostatic pressure is expressed as $p = \rho \cdot g \cdot h$; thus, Darcy's law can be written as follows:

$$u = \frac{k \times \rho \times g \times \partial h}{\mu \times \partial x} = \frac{K_s \times \partial h}{\partial x} \quad (13)$$

where ρ is the liquid density [kg/m³] and g is the gravity [m/s²]. The permeability coefficient, the saturated permeability of the material, K_s , is then described with the following equation [57, 63]:

$$K_s = \frac{k \times \rho \times g}{\mu} \left[\frac{m}{s} \right] \quad (14)$$

Permeation of liquid through porous materials is mainly relevant for studying moisture transport in cracked masonry, particularly in the head joints. It should be noticed that the pressure gradient to drive moisture into the brick masonry in this phase can be the hydrostatic pressure due to gravitational forces and wind imposing a differential air pressure.

2.3.3 Rain penetration of brick masonry façades

During WDR events, a thin water film may form on the exposed surface of the façades depending on the water absorption properties of masonry and WDR intensity. For rain penetration to occur, openings to permit rain penetration and

forces to drive or draw moisture inwards are required. It is clear that there are quite numerous openings on the face of a building in the form of pores, cracks, poorly bonded interfaces, and eroded mortar joints. Eventually, the main driving forces can be the capillary forces, gravity, and air pressure differences, leading to water penetration.

Birkeland [64] claims that water penetration occurs when cracks with 0.1 mm to 5 mm width exist; Grimm [65] categorizes existing interfacial cracks generally ranging between 0.1 and 1 mm. As mentioned above, the driving force for water to penetrate can be the air pressure difference induced by wind pressure, hydrostatic pressure due to gravity, and capillary suction in which for openings smaller than 0.5 mm, the capillary suction seems to be important. Considering that the surface tension of water is approximately 0.075 N/m, the capillary suction pressure for cracks in the range of 0.1 mm to 1 mm wide will be in the order of 75 to 750 Pa. It seems that even in the case of no air pressure difference between the exposed and protected surface, such considerable capillary suction pressures are sufficient to force water into the brickwork, i.e., no applied pressure (either hydrostatic or air) is required [66]. Additionally, significant hydrostatic pressure due to gravity can be built up in the existing interfacial cracks between the brick and mortar interface at the head joints, which may result in leakage [67]. The hydrostatic pressure of around 600 Pa may result from an interfacial crack between the brick and mortar over a typical brick with a height of 60 mm. Therefore, it seems that air pressure difference is not the primary cause of water penetration in brick masonry walls [68]. Further, water penetration in brick masonry specimens without any air pressure difference occurred in the experimental study presented in Paper III.

3 Methods and materials

Repointing of clay brick façades with eroded mortar joints is often motivated by higher water absorption and increased risk for water penetration from WDR. Nevertheless, knowledge concerning to what extent eroded mortar joints cause increased water absorption and penetration from WDR is limited. In this regard, a new test setup was developed to study the resistance of masonry to WDR, providing knowledge that can be applied to make a rational decision on repointing. As previously discussed in Section 2.2.3, the test conditions in the current standards represent extreme WDR conditions. Thus, the test conditions in the test setup presented in this study were adjusted to be more representative of frequently encountered WDR events in Sweden. Subsequently, the bricks and mortars used to prepare masonry specimens were characterized to determine water absorption properties, including the initial rate of absorption (IRA) and water absorption coefficient. Eventually, different types of masonry specimens built with different brick types and mortar joint profile finishes were considered.

3.1 Test setup

As WDR is a substantial source of moisture and a leading cause of mortar joints erosion, there is a need to study the resistance of clay brick masonry façade exposed to WDR. For water penetration to happen, driving forces can be one of the following forces: the kinetic force of raindrops, capillary forces, gravity, air pressure differences, and surface tension. Capillary forces and surface tension are a function of material properties, whereas kinetic forces and differential pressure are a function of the water application, which can be controlled in the test setups [69]. Several test setups are available in the literature [15, 70], aiming to study qualitatively or quantitatively water penetration in masonry walls. A comparative study reviewing the effectiveness of existing water penetration and leakage tests, conducted by Driscoll and Gates [15], identifies a need for a simple test method to complement existing ones since little attention has been given to the correlation between tests and the factors that contribute to water penetration.

Accordingly, a new test setup was developed to study a more realistic behavior of masonry exposure to WDR events. The test setup is able to produce a uniform water spray covering the exposed surface of masonry specimens. A uniform and well-

distributed water spraying pattern was achieved using a low flow, full cone BETE WL nozzle (WL – 1/4, Full Cone, and 90° Spray Angle). It is possible to apply a wide range of water spray rates and air pressure levels, simulating different driving rain intensities. The test setup is equipped with two water pressure regulators and a water flow meter to control the water spray rate. Additionally, two digital scales are employed to measure water absorption and water penetration continuously. A digital camera mounted on the tripod traces the appearance and spread of damp patches. Figure 9 shows the schematic of the test setup.

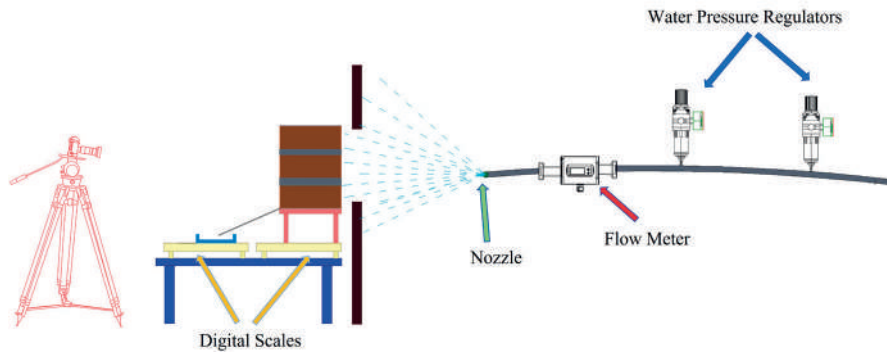


Figure 9. Schematic of the test setup

The following aspects were taken into account to develop the presented test setup:

- a) a nozzle producing low water flow with a full cone spray pattern was used, and
- b) the distance between the surface of the specimens and the nozzle was adjusted to assure a uniform coverage of the exposed surface. The droplet size of the water spray concerning quality and uniformity was examined visually using a paper towel placed in the frame opening and exposed to the water spray for 1-2 seconds, as shown in Figure 10. A more detailed description of the test setup is presented in Paper II and III.



Figure 10. Wet dots on a paper sheet exposed to water spray for 1–2 seconds.

Two improvements in the developed test setup were achieved in comparison with the currently existing test setups. First and foremost, the continuous measurement of the water absorption (mass gain) provides adequate knowledge concerning moisture content of masonry and a basis for analyzing the hygrothermal performance of a building envelope. Secondly, the exposed surface of the specimen is uniformly covered with water drops, unlike other test methods in which the surface of the masonry is kept covered with a thin layer of water film from a pipe/nozzle placed close to the upper part of the specimen. The high water spray rates and differential air pressure used in many standards are to assure that a water film is formed from the beginning of the exposure, allowing water penetration to take place before saturation of the masonry. This means that the influence of the water absorption capacity of the specimen is neglected [67]. Neglecting buffering capacity of masonry gives a misleading picture of clay brick masonry response to WDR exposure.

3.2 Test conditions

It can be observed in the literature that the ASTM E514 [3] standard is one of the most frequently used test methods in studies to investigate water penetration through masonry walls. However, the test conditions of ASTM E514 [3] standard represent extreme driving rain conditions that can only occur at specific locations, with very low probabilities, as analyzed by Fishburn et al. [71] and Cornick and Lacasse [72]. Furthermore, Ribar [6] suggests that current test standards need to be revised to incorporate a realistic exposure condition approach. Additionally, the range of WDR events in Sweden, as shown in Figure 3, indicates that the water application rate of $138 \text{ l/m}^2/\text{h}$ and differential air pressure of 500 Pa is extreme for the Swedish climate. Moreover, according to the field measurements and literature review done by Straube and Burnett [66], driving rain deposition rates of more than $5 - 10 \text{ l/m}^2/\text{h}$ are only very rarely encountered, even on tall buildings. Eventually, Sandin [73] recorded a maximum WDR intensity of about $6 \text{ l/m}^2/\text{h}$ during an observation period lasting 26 months in Gothenburg, Sweden.

Consequently, the primary considered criterion to develop the test setup was lowering the water spray rate compared with the test conditions of ASTM E514 [8] to represent a more realistic range of WDR events. In doing so, in the first experimental campaign, presented in Section 3.3.3, the tests were conducted at zero differential air pressure, at water spray rates varying between 1.7 and $3.8 \text{ l/m}^2/\text{h}$, representing WDR intensities frequently encountered in Sweden (see Figure 3) and approximately 95% lower than the water application rate specified in current standards [3, 7, 8]. In order to obtain the targeted low water spray rates, different combinations of water pressure and nozzle-to-specimen distances were tested. To arrive at the water spray range used in the first campaign, a pressure of 0.55 bar and

a nozzle-to-specimen distance of 55 cm were eventually chosen. Retrospectively, choosing a water pressure of 0.55 bar was not optimal since the recommended operating range of the nozzle is between 0.7 – 20 bars. The flow and thus the water spray became more sensitive to changes in the water pressure.

In the second experimental campaign, presented in Section 3.3.3, to minimize water flow variations and better control the water spray rate, water pressure was adjusted to nearly 1.05 bar, and nozzle-to-specimen distance decreased to roughly 50 cm. Thus, the tests were performed in this campaign with a water spray rate of $6.3 \text{ l/m}^2/\text{h} \pm 5 \%$ and zero differential air pressure. A water spray rate ranging between 5 and $10 \text{ l/m}^2/\text{h}$ was considered by Straube and Brunett [67] as representative for more realistic WDR events.

In both experimental campaigns, triplet masonry specimens were tested over a period of 23 hours, including six consecutive cycles; each cycle consisted of 210 min of water spraying and 20 min of drying. It should be mentioned that the tests were carried out with zero differential air pressure because high wind speeds usually occur only for a small percentage of rain duration, whereas in this study, the specimens were subjected to water spraying for 21 h.

3.3 Materials

3.3.1 Bricks

Three different types of commonly used solid clay bricks on the Swedish construction market, supplied by Wienerberger AB, were considered in this study, named bricks type I, II, and III. Twenty bricks from each type were tested to characterize the initial rate of absorption (IRA) and 24-h water absorption properties; tests were carried out as described in the ASTM C67 standard [74]. The IRA represents the surface absorption rate when the brick just contacts water, whereas the 24-h water absorption represents the amount of water that a brick can absorb when fully immersed in water, expressed as the ratio between the absorbed water and the initial weight. The average IRA of bricks type I, II, and III is equal to 1.95 kg/m^2 , 1.81 kg/m^2 , and 0.71 kg/m^2 , respectively, whereas 24-h water absorption property amounts to 16.0 %, 8.6 %, and 4.0 %, respectively. According to the results of the IRA test, bricks type I and II can be classified as medium suction bricks [I] and [II], while bricks type III are considered low suction bricks. Table 1 summarizes the properties of bricks, including density, IRA, and 24-h water absorption.

Table 1. Material properties of bricks and mortars including density, IRA, 24-h water absorption, and water absorption coefficient (A_w)

Materials	Dimensions (mm × mm × mm)	Density ρ (kg/m ³)	Average IRA (kg/m ² /min)	CoV (%)	Average 24-h water absorption (%)	CoV (%)	Average A_w (kg/(m ² .s ^{0.5}))	CoV (%)
Brick type I	250×120×62	1800	1.95	2.3	16.0	1.6	0.193	0.8
Brick type II	250×120×62	1990	1.81	5.1	8.6	14.5	0.133	16.1
Brick type III	240×115×62	2235	0.71	13.7	4.0	38.6	0.042	22.8
Mortar M 2.5	100×100×100	1869	0.30	15.8	-	-	0.022	8.7
Mortar NHL 3.5	100×100×100	1715	0.80	20.4	-	-	0.159	9.2
Mortar NHL 5	100×100×100	1733	1.10	15.6	-	-	0.236	15.3

Moreover, tests to determine the water absorption coefficient of bricks, A_w , were done on ten bricks from each type according to the ASTM C1403 – 15 standard [75]. The water absorption coefficient, A_w , expresses the rate of capillarity action in a certain time. Bricks were immersed in water at a depth of 3-5 mm from the bed face, and the weight was measured at different time intervals. The increase in mass as a result of water absorption was registered after 1, 5, 10, 20, 30, 60, 120, 180, 240, 300, 360, 1440, and 4320 minutes. The amount of absorbed water per unit area of the brick Q [kg/m²] is defined as the ratio between the difference of increased weight (w_i [kg]) and initial weight (w_0 [kg]) and the cross-sectional area of the brick A [m²] (Eq. (15)).

$$Q = \frac{w_i - w_0}{A} \quad [\text{kg/m}^2] \quad (15)$$

To present the results of the tests, Q [kg/m²] is plotted against the square root of time [s^{1/2}] (Figure 11.a). Eventually, the water absorption coefficient, A_w [kg/(m².s^{0.5})], is mathematically defined as the tangent to the initial, linear branch of the $Q - t^{1/2}$ function (Figure 11.b). The average water absorption coefficient for each type of brick is presented in Table 1.

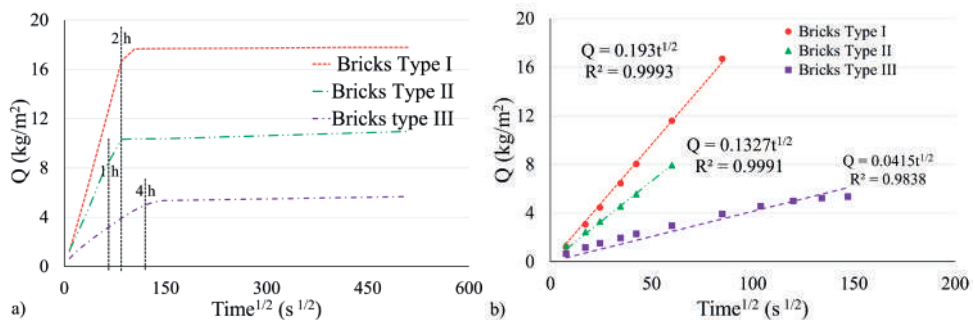


Figure 11. Plot of the average water absorption per unit area against the square root of time for ten masonry brick units from each type (bricks type I, II, & III): a) up to 72 h; and b) during the initial stage of the test.

3.3.2 Mortars

Mortar M 2.5, widely used in masonry façades, was supplied by Weber Saint-Gobain AB; Natural hydraulic lime (NHL) 3.5 and 5 mortars, commonly used for repointing of clay brick façades, were supplied by Målar kalk AB. The recommendation was to use NHL 3.5 with high and medium suction bricks, whereas NHL 5 mortar is recommended to be used with low suction bricks. Eighteen 100 mm cubic side mortar specimens, including 12 M 2.5, 3 NHL 3.5, and 3 NHL 5, were cast to characterize the water absorption properties of mortars. The water absorption coefficient of the mortars was determined according to the ASTM C1403 – 15 standard [75]. Figure 12 shows the water absorption rate of the mortars over the square root of time, and Table 1 summarizes the average IRA and water absorption coefficients of three different types of mortar.

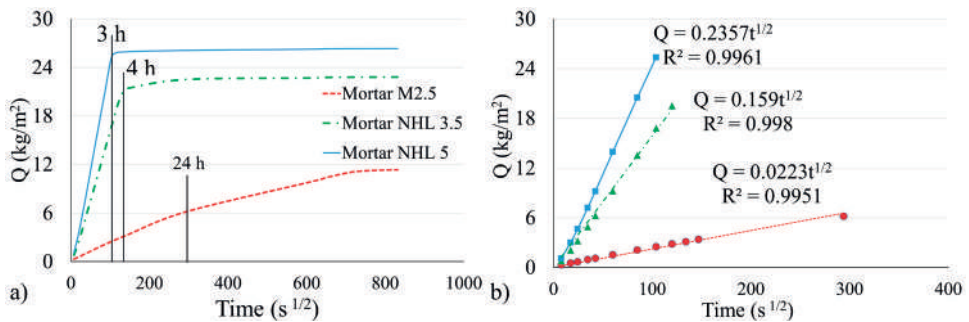


Figure 12. Average water absorption of mortar M 2.5, NHL 3.5, NHL 5: a) up to 8 days; and b) during the initial stage of the test

3.3.3 Masonry specimens

Three different types of bricks with different water absorption properties and two different mortar joint profiles, namely flush and raked, were considered. Flush profiles were subdivided into standard and after-pointed. After-pointing is a common technique in Nordic countries in which the joints are filled with mortar; then, prior to hardening of the mortar, the outer part is removed; and a couple of hours later, the remained part is finally filled with repointing mortar and tooled. Raked specimens can be a reasonable representative of eroded mortar joints. Comparing water absorption and penetration of flush and raked specimens can facilitate understanding how the erosion of the mortar joints might affect WDR-related water absorption and penetration.

The tests were carried out on triplet masonry specimens with the length, height, and depth of 250 ± 5 mm, 215 ± 3 mm, and 120 ± 2 mm, respectively, see Figure 13. The specimens were intended to be representative of a masonry veneer wall. The

specimen size was limited to three bricks in order to facilitate manual handling without damaging either the specimens or the operator. A similar choice was made by Ritchie [13], who studied water penetration in brick masonry by using specimens consisting of five bricks, yet without any head joints.

As summarized in Table 2, in the first campaign (A), 39 triplet masonry specimens were prepared with medium suction bricks type [I] and [II], with three types of joint profile finish: flush, raked, and after-pointed. In the second campaign (B), 36 masonry specimens, built with three different types of bricks, including medium suction bricks type [I] and [II], and low suction bricks, type III, and three different types of joint profile finishes, including flush, raked, and after-pointed were studied. All specimens in the two campaigns were prepared at the same time.

Specimens built with medium suction bricks [I] belong to Series I, whereas Series II consists of specimens prepared with medium suction bricks [II]. Series III includes specimens built with low suction bricks, type III. Each Series is then divided into three groups based on the joint profile finish. Group G1 includes specimens built with mortar M 2.5 with a tooled flush joint profile, whereas group G2 consists of specimens built with mortar M 2.5, with a raked joint profile. Group G3 is also made up of specimens built with mortar M 2.5, but compared with G1, the outer 6 mm of the mortar joint was pointed one day after bricklaying with mortar NHL 3.5 or NHL 5, with a tooled flush joint profile. It should be mentioned that mortar NHL 3.5 was used in the pointing of Series I and II specimens, whereas NHL 5 was used in combination with the specimens of Series III, low suction bricks.

Following the recommendations of the supplier, the bricks were not wetted before bricklaying. These recommendations are in line with those given in [76] concerning the need for pre-wetting bricks as a function of the IRA. To eliminate uncertainties regarding workmanship, a single craftsman built all the specimens. Extra effort went into ensuring that the same amount of water was added to each batch of mortar mix, i.e., eliminating the effect of mortar flow on water penetration. Specimens of group G1, with mortar M 2.5, were tooled with a wooden stick to have a flush profile. For specimens with the raked joint profile, group G2, a 5 mm screw was used to remove extra mortar to reach the depth of 5 mm. For specimens prepared with the after-pointing technique, the excess mortar was removed using a 6 mm screw, and the following day, the 6 mm gap was filled with either NHL 3.5 or NHL 5 and tooled to have a flush joint profile (Figure 13). The workmanship technique used for bricklaying in this study was the so-called pushing of the head joints. Figure 13.c shows the backside of the representative specimens.

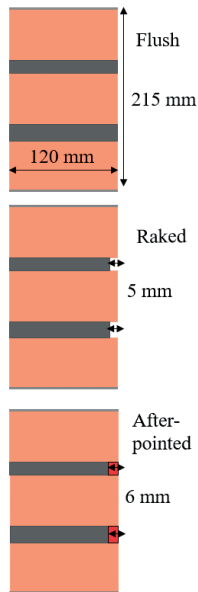


Figure 13. a) Representative specimens from each group and Series after sealing; b) Schematic of the mortar joint profile finishes, and c) Backside of representative specimens

Prior to the testing, all sides except the exposed surface and backside of the specimens were sealed using a two-component sealant (ARDEX P2D and ARDEX S1-K), producing a flexible waterproof coating. The sealing was done to avoid any undesirable water absorption in any other sides except the exposed surface.

The specimens were named following the designation W-X-T-C, where W stands for the experimental campaign (A is the first campaign, B is the second campaign),

X represents the Series (I is the first Series, II is the second Series, III is the third Series), T corresponds to the mortar joint profile finish (F = flush, R = raked, AF = after-pointed), and C refers to the specimen number. For example, specimen A-II-R-2 is one of the specimens tested in the 1st experimental campaign, was built with medium suction bricks type [II], with a raked joint profile, and it is the second specimen of group G2.

Table 2. Specimen designation and configurations

Experimental campaign	Series	Group	Brick	Mortar	Joint profile finish	Ave water spray rate (l/m ² /h)	No. of specimen
First campaign A	Series I	G1	Medium suction type [I]	M 2.5	Flush	3.6	5
		G2	Medium suction type [I]	M 2.5	Raked	3.6	5
		G3	Medium suction type [I]	M 2.5 / NHL 3.5	After-pointed	3.4	5
	Series II	G1-a	Medium suction type [II]	M 2.5	Flush	3.2	5
		G1-b	Medium suction type [II]	M 2.5	Flush	2.0	3
		G2	Medium suction type [II]	M 2.5	Raked	2.3	8
		G3	Medium suction type [II]	M 2.5 / NHL 3.5	After-pointed	2.0	8
Second campaign B	Series I	G1	Medium suction type [I]	M 2.5	Flush	6.3	4
		G2	Medium suction type [I]	M 2.5	Raked	6.3	4
		G3	Medium suction type [I]	M 2.5 / NHL 3.5	After-pointed	6.3	4
	Series II	G1	Medium suction type [II]	M 2.5	Flush	6.3	4
		G2	Medium suction type [II]	M 2.5	Raked	6.3	4
		G3	Medium suction type [II]	M 2.5 / NHL 3.5	After-pointed	6.3	4
	Series III	G1	Low suction	M 2.5	Flush	6.3	4
		G2	Low suction	M 2.5	Raked	6.3	4
		G3	Low suction	M 2.5 / NHL 5	After-pointed	6.3	4

In the first campaign (A), the specimens in groups G1, G2, and G3 of Series I were exposed to an average water spraying rate of 3.6, 3.6, and 3.4 l/m²/h. Specimens of group G1 of Series II are divided into two groups, G1-a and G1-b, based on the average water application rate. In this regard, the average water spraying rate for groups G1-a, G1-b, G2, and G3 of Series II was 3.2, 2.0, 2.3, and 2.0 l/m²/h, respectively (Table 2). However, in the second campaign (B), all specimens were exposed to a uniform and constant water spray rate of 6.3 l/m²/h ± 5% (Table 2). It should be noted that the first campaign includes only Series I and II specimens, whereas the second campaign consists of all specimens of Series I, II, and III.

4 Experimental results

This chapter presents the results of two experimental campaigns and is divided into four subsections: general observations, water absorption, damp patches, and water penetration. In the first part, observations and qualitative results regarding the response of specimens exposed to water spray, observed during testing, are presented. Section 4.2 summarizes the experimental test results regarding the water accumulation and moisture content of the specimens. Section 4.3 provides information about the appearance and spread of damp patches on the backside of the specimens. Section 4.4 indicates the amount of water that was collected from the backside of specimens due to leakage.

4.1 General observations

This part presents the obtained qualitative results, including water absorption behavior, surface saturation, the appearance of damp patches, and water penetration observed during the testing of the specimens. Firstly, the specimens were exposed to a water spray, with a rate controlled by two water pressure regulators. At the beginning of the test, the specimens absorbed most of the sprayed water, whereas the rest of the water drops bounced off.

Afterward, runoff started on the exposed surface of the specimens, indicating that surface saturation was attained. The time to attain surface saturation varied between different specimens, depending on the water spray rate and the water absorption coefficient of the bricks. Subsequently, the first visible damp patches usually appeared on the backside of the specimens in the vicinity of the head joint. It should be noted that for a few specimens of Series III, the first dampness was observed soon after starting the test. Subsequently, the dampness spread on the entire second course, including the head joint. Then, the bottommost course became damp. The dampness eventually spread to the uppermost course until the entire protected side of the specimen became damp. However, the backside of a few specimens within Series III did not get fully damp.

The absorption then continued until the specimens reached full saturation, depending on the water spray rate, the water absorption coefficient of bricks, and the water absorption capacity of masonry. However, several specimens did not reach

full saturation, mostly because of the low water spray rate and low water absorption properties of masonry. In the first experimental campaign (A), due to the low water spray rate, the amount of water collected from the backside of the specimens, the water penetration, was limited. Thus, water penetration was only registered in the second campaign (B), where the water spray rate increased compared to the first campaign (A). In most specimens, water penetration started when the specimens were close to saturation. Water penetration mainly occurred through the brick-mortar interface, particularly the bed joint between the first and the second course.

4.2 Water absorption

As the developed test setup was equipped with a scale capable of measuring the amount of absorbed water continuously during the test, in this section, the results of water absorption in specimens tested in the first (A) and second (B) experimental campaigns are presented.

4.2.1 First campaign (A)

It should be mentioned that individual specimens in campaign A were exposed to water spray rates varying between 1.7 and 3.8 l/m²/h. The water absorption, Q [kg/m²], herein is defined as the amount of absorbed water [kg] per unit area of the masonry specimen [m²]. Figure 14 shows the absorption behavior of masonry specimens during 23 h of testing, tested in the first experimental campaign (A). Since the water spray rate of Series II group G1-a is similar to those of Series I, they are plotted in the same graph (see Figure 14.a). It should further be kept in mind that the specimens in Series I and Series II Group G1-a were exposed to a more intensive spray rate (3.2 – 3.6 l/m²/h) than the specimens in Series II group G1-b, G2, and G3 (2.0 – 2.3 l/m²/h).

It is clear that during the 1st cycle (3.5 h), the absorption behavior is linear, indicating that most of the sprayed water was absorbed within the specimens. Accordingly, the absorption behavior of Series II group G1-a during the first cycle is similar to those of Series I specimens, yet with different absorption properties of the bricks. Hence, it can be seen that the absorption during the first cycle, prior to surface saturation, is strongly dependent on the water spray rate. Similarly, the absorption behavior of Series II group G1-b, G2, and G3 during the first cycle is similar to each other (Figure 14.b), indicating that the water spray rate is the governing agent influencing the amount of absorbed water. The slight difference in the amount of absorption after the 1st cycle is related to the difference in the water spray rate; the greatest absorption was recorded in group G2 exposed to an average spray rate of 2.3 l/m²/h,

in comparison with group G1-b and G3 exposed to the average water spray rate of $2.0 \text{ l/m}^2/\text{h}$.

It was mentioned that a large portion of the sprayed water during the first cycle was absorbed within specimens. Since the absorption behavior is linear during the first cycle, i.e., surface saturation is not attained yet, the difference between the amount of sprayed water and absorbed water can be considered as bounce-off. Therefore, around 8 – 23 % of the sprayed water is considered to have bounced off from the specimens' surface.

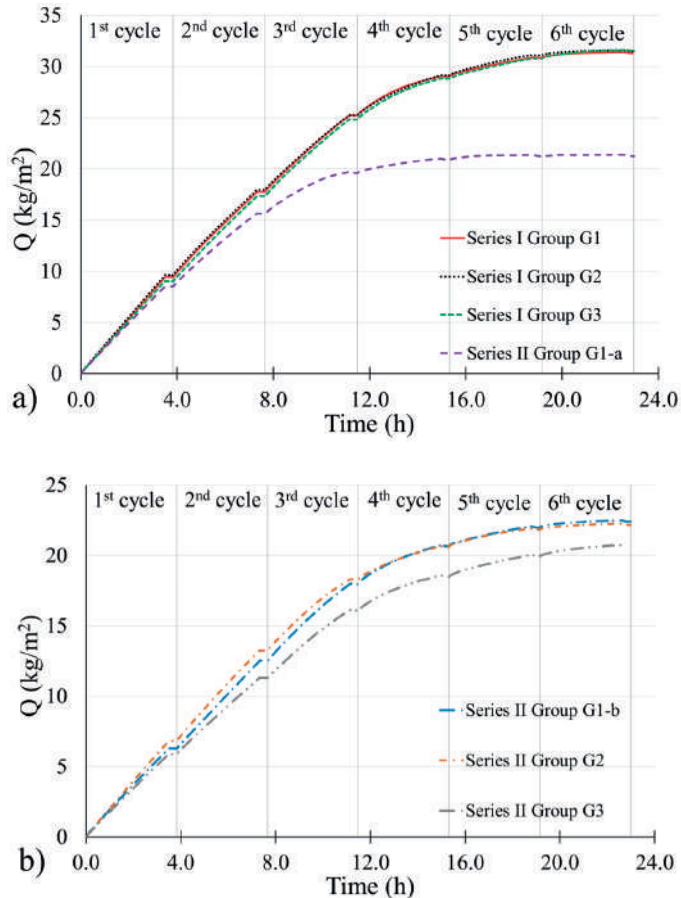


Figure 14. Average water absorption vs. time response of a) Series I and Series II group G1-a; b) Series II group G1-b, G2, and G3 in the first experimental campaign (A)

As the test progressed, the absorption behavior became nonlinear, indicating saturation of the exposed surface. The time to attain surface saturation is dependent on the water spray rate and water absorption coefficient of the masonry. Accordingly, surface saturation was attained later for Series I in comparison with

Series II group G1-a, indicating that a higher water absorption coefficient allows rapid moisture transport and postpones saturation of the exposed masonry surface layer, as stated by Van Den Bossche et al. [17] and further discussed in Paper II. Surface saturation was attained at the end of the 3rd cycle for all groups of Series I and II, except Series II group G1-a in which the absorption curve becomes nonlinear at the end of the 2nd cycle. Once the surface saturation was attained, a water film was formed on the exposed surface of the masonry, and the absorption behavior became more dependent on the water absorption coefficient and water absorption capacity of the masonry.

Eventually, as can be seen, the absorption continues until the middle of the 6th cycle for Series I, showing the specimens are close to fully saturated. However, for Series II groups G1-b, G2, and G3, the absorption continues until the end of the test, mainly attributed to the relatively low water spray rate. In contrast, the absorption ends during the 5th cycle for Series II group G1-a, indicated by the slope of the $Q - t$ curve becoming close to zero (i.e., nearly no water accumulation in the specimens) during the remainder of the test.

4.2.2 Second campaign (B)

Figure 15 shows the average amount of water absorption, Q [kg/m^2], during 23 h of testing in all groups within Series I, II, and III tested in the second experimental campaign (B). It should be noted that all specimens were exposed to a uniform and constant water spray rate of $6.3 \text{ l}/\text{m}^2/\text{h} \pm 5\%$. During the initial 10 minutes to 2 hours of tests, depending on the Series, most sprayed water was absorbed, indicating that surface saturation was not attained yet. The bounce-off varied between 7 % and 14 %.

Surface saturation for Series I and II were attained after around 1 h and 2 h, respectively. In contrast, the occurrence of surface saturation took only 10 minutes for Series III, as shown in Figure 15.b. Once the surface saturation was attained, which can be seen from the deviation from a linear slope of the absorption curve, the absorption response becomes nonlinear. The time to reach surface saturation varied between each Series depending on the water absorption coefficient of the bricks. It can be observed that surface saturation was attained during the 1st cycle for all groups, G1, G2, and G3, within each Series, though it took more time for Series I, specimens prepared with bricks with the absorption coefficient of $0.193 \text{ kg}/(\text{m}^2 \cdot \text{s}^{0.5})$, in comparison with Series II and III, built with bricks with the absorption coefficient of $0.133 \text{ kg}/(\text{m}^2 \cdot \text{s}^{0.5})$ and $0.042 \text{ kg}/(\text{m}^2 \cdot \text{s}^{0.5})$, respectively.

After the attainment of surface saturation in specimens of Series I and II, the absorption behavior becomes nonlinear, and the slope of the curve decreases until the point where it becomes close to zero, i.e., nearly no water accumulation in the specimens. The absorption ends during the 4th cycle for Series I and II, specimens

prepared with medium suction bricks type I and II. In contrast, once the surface saturation was attained at the beginning of the 1st cycle for Series III, the absorption behavior became nonlinear and continued until the end of the test. Based on the obtained results, the water absorption rate in masonry specimens during 23 h of the test depends on the water absorption coefficient of the bricks and water spray rate, whereas the total amount of water absorption is mostly correlated to the absorption capacity of the masonry.

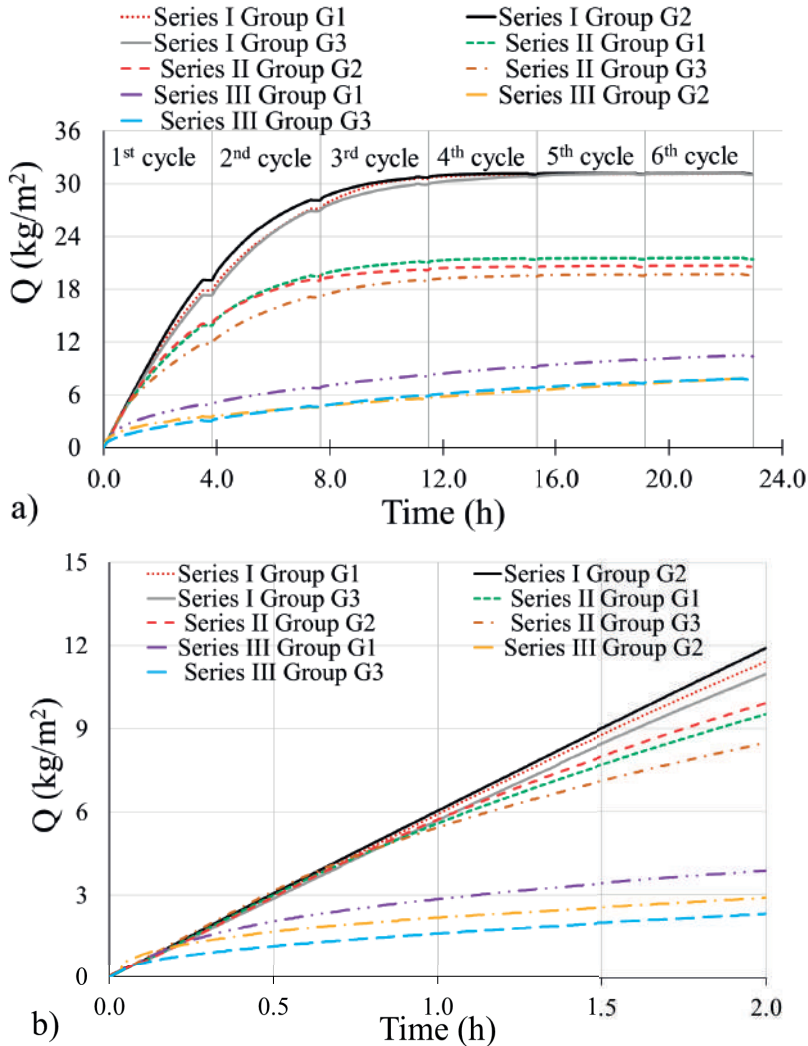


Figure 15. Average water absorption vs. time response of Series I, Series II, and Series III in the second experimental campaign (B), a) during 23 h of testing and b) during the first two hours after starting the test

Table 3 summarizes the average amount of water absorption, Q [kg/m^2], within each group after performing the first and sixth cycles. Based on the obtained results in campaign A, the water absorption in the first cycle is dependent on the water spray rate. For instance, in Series II, the lowest average water absorption, amounting to $5.9 \text{ kg}/\text{m}^2$, is exhibited by group G3, exposed to the lowest average water application rate of $2.0 \text{ l}/\text{m}^2/\text{h}$. Similarly, group G1-a, which was exposed to the highest average water application rate of $3.2 \text{ l}/\text{m}^2/\text{h}$, has the highest average water absorption of $8.5 \text{ kg}/\text{m}^2$ in Series II. However, in campaign B, as specimens were exposed to the same water spray rate, $6.3 \text{ l}/\text{m}^2/\text{h}$, the slight difference in the amount of water absorption after the 1st cycle for each group within each Series might be related to the; a) variability in brick absorption properties, b) effect of mortar joint profile finish, and c) variation in the applied spray rate, taking into account a mentioned tolerance of 5 % in the spray rate.

Table 3. The average water absorption and time to the appearance of the first visible damp patch on the backside of each group within each Series in Campaign A and B after the first and the sixth cycle

		Ave water spray rate ($\text{l}/\text{m}^2/\text{h}$)	Ave 1st cycle Absorption (kg/m^2)	Ave Total Absorption (kg/m^2)	CoV %	Time to the 1st dampness (h)
Campaign A	Series I group G1	3.6	9.4	31.3	0.6	7.9
	Series I group G2	3.6	9.6	31.5	0.3	7.8
	Series I group G3	3.4	9.0	31.5	0.2	8.0
	Series II group G1-a	3.2	8.5	21.2	10.4	4.8
	Series II group G1-b	2.0	6.3	22.4	6.3	6.3
	Series II group G2	2.3	6.8	22.2	6.0	5.9
	Series II group G3	2.0	5.9	20.6	5.6	6.4
Campaign B	Series I group G1	6.3	17.8	30.9	0.9	2.5
	Series I group G2	6.3	19.0	30.9	0.5	2.6
	Series I group G3	6.3	17.3	31.0	0.7	3.7
	Series II group G1	6.3	13.8	21.4	10.0	2.0
	Series II group G2	6.3	14.0	20.5	10.4	1.5
	Series II group G3	6.3	11.8	19.6	2.7	3.1
	Series III group G1	6.3	4.8	10.4	19.3	1.0
	Series III group G2	6.3	3.5	7.7	10.1	6.9
	Series III group G3	6.3	3.1	7.7	30.3	3.6

It can be seen that the average total absorption in specimens of Series I, tested in the first (A) and the second (B) experimental campaigns, is nearly equal to 31.0 kg/m^2 , highlighting a negligible difference in the average water absorption between groups G1, G2, and G3. In contrast, the average water absorption for groups G1, G2, and G3 of Series II varied between 20.6 kg/m^2 and 22.4 kg/m^2 in campaign A and between 19.6 kg/m^2 and 21.4 kg/m^2 in campaign B. The obtained results indicate a strong correlation between the total amount of absorption and the absorption capacity of the masonry. The difference in the results of average water absorption between each group in Series III is mainly attributed to the high variability in the water absorption capacity of the bricks ($\text{CoV} = 38.6 \%$).

According to the obtained results, water absorption is not dependent on the joint profile finishes, suggesting that the impact of eroded mortar joints on water absorption from WDR is inconsiderable. In contrast, water absorption in clay brick masonry is a function of the water absorption properties of masonry, especially that of the bricks, and the water spray rate. The obtained results from specimens prepared with raked joint profiles as representative of eroded mortar joints may provide the basis for the decision-makers concerning repointing. Eroded mortar joints may not lead to a significant increase in water absorption in masonry façades built with solid clay bricks.

4.3 Damp patches

A digital camera was mounted behind the specimens in the presented test setup, providing the opportunity to obtain the location of the first visible dampness and the relative damp area over time. Figure 16 shows the location of the first visible damp patch on the backside of the specimens tested in the first campaign (A). It can be seen that the first dampness appeared close to the brick-mortar interface, indicating that the interfacial zone between brick and mortar is the primary path for water penetration.

Figure 16 and Table 3 summarize the time to the appearance of the first damp patch on the backside of the specimens. In the first campaign (A), the average time to the appearance of the first dampness for all groups of Series I is around 8 h, highlighting the insignificant effect of joint profile finish. In Series II, the dampness appeared after 4.8 h on the backside of group G1-a specimens with the water spray rate of $3.2 \text{ l/m}^2/\text{h}$, whereas it took nearly 6.4 h for group G1-b and G3 specimens exposed to the water spray rate of $2.0 \text{ l/m}^2/\text{h}$, suggesting the considerable effect of water spray rate on the appearance of the first damp patch. Moreover, comparing the time to the appearance of the first damp patch between all groups of Series I and group G1-a Series II, though specimens were exposed to a similar water spray rate, the obtained

results indicate the impact of brick absorption capacity on time to the appearance of the first dampness.

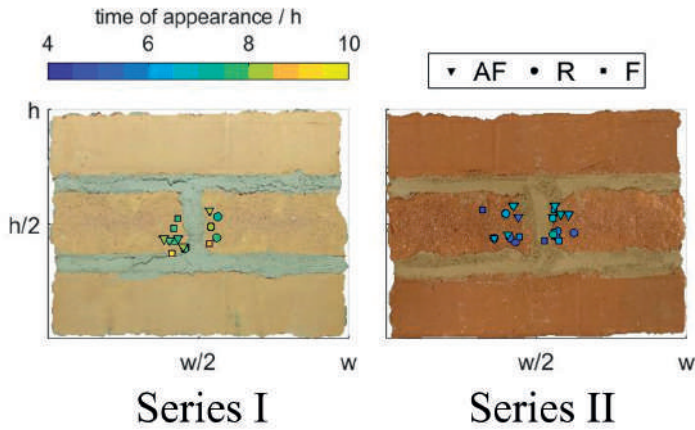


Figure 16. Location and time to the appearance of the first damp patch on the backside of specimens in campaign A

Figure 17 shows the time and location of the first visible dampness that appeared on the backside of specimens tested in the second campaign (B). Similar to the first campaign (A), with some exceptions, the first visible dampness appeared close to the brick-mortar interface in the vicinity of the head joint. Additionally, for those specimens where the dampness did not appear in the vicinity of the head joint, the time to the appearance of the first damp patch is significantly postponed. Accordingly, the obtained results indicate the importance of the resistance of the brick-mortar interface, particularly the head joint, to WDR.

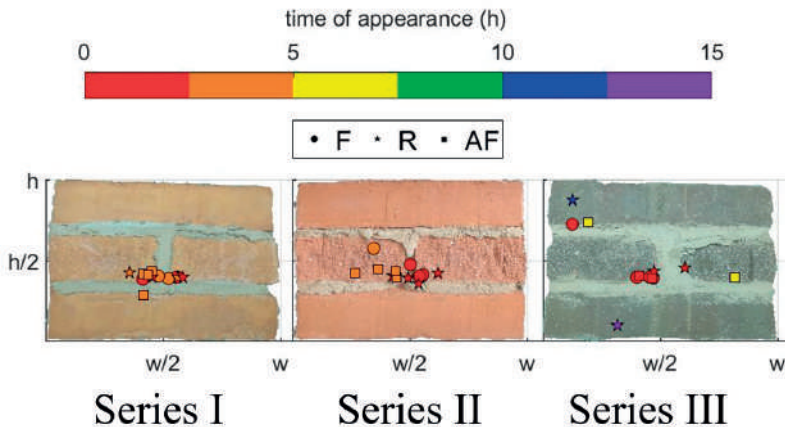


Figure 17. Where and when the first damp patch appeared on the backside of specimens in campaign B

Once the first damp patch appeared, mainly in the vicinity of the head joint, then typically it spread on the entire second course, including the head joint. Subsequently, the bottommost course became damp. The dampness eventually spread to the uppermost course until the entire protected side of the specimen became damp, as shown in Figure 18. However, it was observed that the backside of several specimens within Series III, specimens prepared with low suction bricks, did not reach even 50 % dampness after 21 h of water spray exposure.

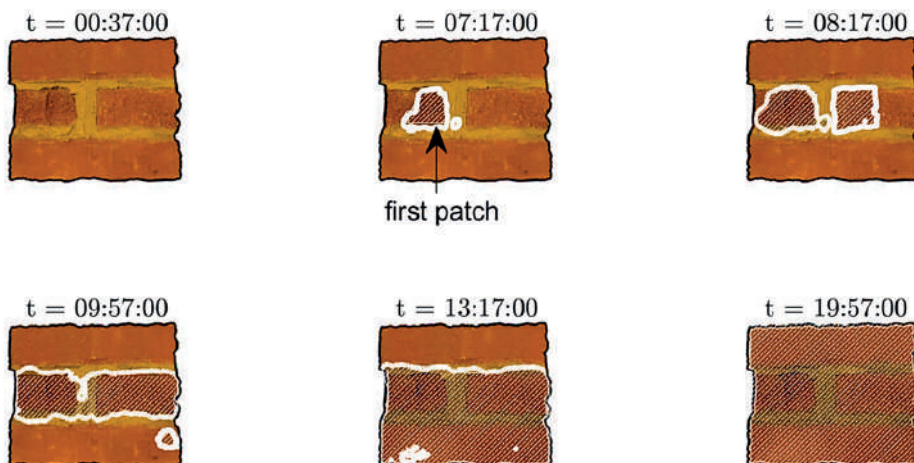


Figure 18. Appearance and growth of dampness on the backside of specimen A-II-F-6 at different time intervals.

The obtained results highlight the importance of the workmanship and a well-established contact between brick and mortar, as it may increase the time to the appearance of the first dampness and change its location. Additionally, the results reveal the low resistance of head joints to WDR, which might be related to the difficulty of the workmanship in filling the head joints and low compaction in comparison with bed joints [82]. Further, the effect of joint profile finishes on the time and location of the first visible dampness is negligible, whereas water spray rate and water absorption properties of bricks may strongly influence the time to the appearance of the first damp patch.

4.4 Water penetration

As no considerable amount of water leakage that could be collected from the backside of the specimens was observed in the first experimental campaign (A), this section only presents the results of water penetration in specimens tested in the second experimental campaign (B).

In the test setups of current standards and research studies, high water spray rate and air differential pressure are applied to rapidly form a water film on the exposed surface of the specimens and force the water in without gaining the benefit from the storage capacity of masonry [67]. In contrast, in the first campaign (A) conducted in this study, because of the low water spray rate and zero differential air pressure, no considerable amount of water penetration could be collected, indicating that the specimens could absorb most of the sprayed water. The limited leakage is probably due to the fact that specimens in campaign A got saturated at the end of the test. Thus, gravity is the probable driving force, see Section 2.3.3.

The average amount of water penetration [kg/m^2] for each group within each Series during 23 h of testing is shown in Figure 19 and Table 4. It can be seen that water penetration in all groups within Series I and II started at the end of the second cycle or the beginning of the third cycle, indicating that it started when the masonry specimens were nearly close to saturation, as already noted by Straube and Burnett [67]. Further, it is observed that for Series III, specimens prepared with low suction bricks, a lower value of water penetration was recorded in comparison with Series I and II. In this regard, the average amount of penetrated water of groups G1, G2, and G3 of Series I and II are in the range of $2.0 \text{ kg}/\text{m}^2 - 4.4 \text{ kg}/\text{m}^2$. In contrast, there is no considerable water penetration for specimens of Series III, except specimen B-III-F-1, B-III-AF-2, and B-III-AF-3.

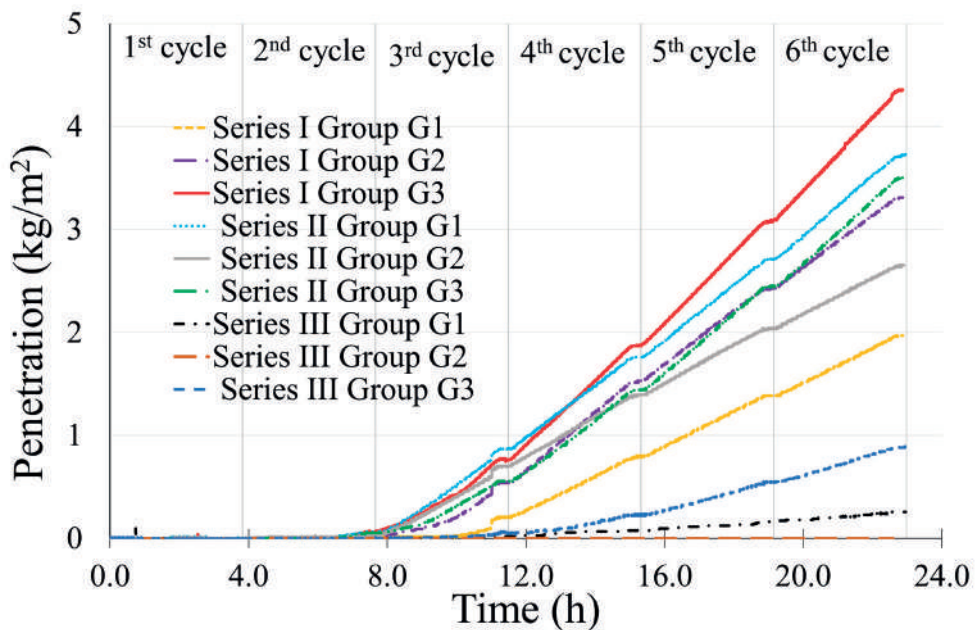


Figure 19. Average water penetration vs. time response of all Series in the second experimental campaign (B)

Table 4. Water penetration in terms of time to leakage, the amount of penetration, and leakage percentage for individual specimens of campaign B

	Specimens	Time to leakage (h)	Ave time to leakage (h)	Penetration (kg/m ²)	Ave Penetration (kg/m ²)	Leak in the 6 th cycle (%)	Ave (%)	Tot leak (%)	Ave (%)
Campaign B	Series I group G1	B-I-F-1	11.0	10.4	1.1	2.0	1.3	2.6	0.8
		B-I-F-2	9.9		2.2		3.0		1.7
		B-I-F-3	10.1		2.7		3.6		2.1
		B-I-F-4	10.4		1.9		2.6		1.4
	Series I group G2	B-I-R-1	8.4	8.8	3.5	3.3	4.6	4.0	2.6
		B-I-R-2	6.9		2.8		3.3		2.2
		B-I-R-3	9.4		6.3		7.8		4.8
		B-I-R-4	10.4		0.6		0.2		0.4
	Series I group G3	B-I-AF-1	8.5	8.2	3.5	4.4	5.3	5.8	2.7
		B-I-AF-2	9.4		5.9		8.8		4.4
		B-I-AF-3	6.6		8.0		8.9		6.1
		B-I-AF-4	-		0.0		0.0		0.0
	Series II group G1	B-II-F-1	8.1	9.4	3.5	3.7	4.3	4.6	2.7
		B-II-F-2	15.0		0.5		1.3		0.4
		B-II-F-3	6.3		4.6		5.6		3.4
		B-II-F-4	8.0		6.3		7.1		4.8
	Series II group G2	B-II-R-1	7.8	8.6	3.9	2.7	4.5	2.8	3.0
		B-II-R-2	8.2		2.8		2.6		2.1
		B-II-R-3	11.0		0.3		0.2		0.2
		B-II-R-4	7.5		3.6		3.8		2.7
Series II group G3	B-II-AF-1	11.1	9.0	2.6	3.5	4.3	4.8	2.0	
	B-II-AF-2	6.6		3.7		3.6		2.8	
	B-II-AF-3	9.0		4.5		6.8		3.4	
	B-II-AF-4	9.1		3.3		4.5		2.5	
Series III group G1	B-III-F-1	10.8	-	0.9	0.2	1.4	0.4	0.7	
	B-III-F-2	-		0		0		0	
	B-III-F-3	-		0		0		0	
	B-III-F-4	-		0		0		0	
Series III group G2	B-III-R-1	-	-	0	0	0	0	0	
	B-III-R-2	-		0		0		0	
	B-III-R-3	-		0		0		0	
	B-III-R-4	-		0		0		0	
Series III group G3	B-III-AF-1	-	-	0.0	0.9	0	1.4	0	
	B-III-AF-2	10.9		1.3		2.4		1.0	
	B-III-AF-3	8.6		2.2		3.1		1.6	
	B-III-AF-4	-		0.0		0		0	

It was previously mentioned that water mainly penetrated through the brick-mortar interface, particularly from the bed joint between the first and the second course. Although no differential air pressure was applied in the second experimental campaign (B), the driving potentials forcing water to penetrate might be gravity and kinetic energy of water drops, as stated by Straube and Burnett [67].

The obtained results suggest that water penetration is highly dependent on the water content of specimens (saturation level), brick absorption properties, and the water spray rate. However, it can be seen that the effect of joint profile finish on water penetration is insignificant since the highest amount of leakage in Series I was recorded for group G3 whereas, in Series II, specimens of group G1 had the greatest amount of water penetration.

Table 4 summarizes the results of water penetration for each specimen tested in the second campaign. Also, the approximate time when water penetration started is presented in Table 4. The average time for water to start penetrating varied between 8 and 10 hours for all groups within Series I and II. All specimens in Series I and II experienced water leakage, except specimen B-I-AF-4. Interestingly, the greatest amount of water penetration, 8.0 kg/m^2 , was recorded for Specimen B-I-AF-3, whereas no penetrated water was observed for specimen B-I-AF-4. For Series III, no penetration was registered, except B-III-F-1, B-III-AF-2, and B-III-AF-3. Moreover, no water penetration was observed for Series III group G2, specimens prepared with low suction bricks and raked joint profile, which might depend on the fact that the specimens were not saturated, see Figure 15.a.

It should be mentioned that the penetrated water mainly passed through the brick-mortar interface, indicating the importance of the interfacial zone on masonry's resistance to WDR. For instance, in nine out of twelve specimens in Series III, the amount of water penetration was nearly equal to 0 kg/m^2 . Compared to Series I and II, the sharp contrast is attributed to continuous contact in the brick-mortar interface and the absence of known defects. However, in specimens B-III-F-1, B-III-AF-2, and B-III-AF-3, a water penetration of 0.9 kg/m^2 , 1.3 kg/m^2 , and 2.2 kg/m^2 , respectively, were registered, indicating that the quality of the workmanship might not have been as high as the other specimens of Series III. It should be further observed that the amount of penetrated water varied within a considerable range also in Series I and II, between $0 - 8 \text{ kg/m}^2$ and $0.3 - 6.3 \text{ kg/m}^2$, respectively. Figure 20 shows the significant variability in the results of water penetration in the individual specimens of Series I group G2. Accordingly, several factors might contribute to the large scatter in the results of water penetration by comparing individual specimens even with similar brick and joint profile; a) the quality of the workmanship to completely fill the joints might differ between specimens, b) the bond, i.e., the adequate contact between brick and mortar might not be achieved in some specimens, and c) there is a large variability in the absorption properties of bricks and mortar.

The obtained results highlight the impact of water absorption properties of bricks on the leakage through specimens, as water penetration in specimens prepared with low suction bricks was considerably lower than those prepared with medium suction bricks type I and II, as already noted by Ritchie and Plewes [77]. Moreover, comparing water penetration of each group within each Series shows that the effect of mortar joint profile on water penetration is negligible.

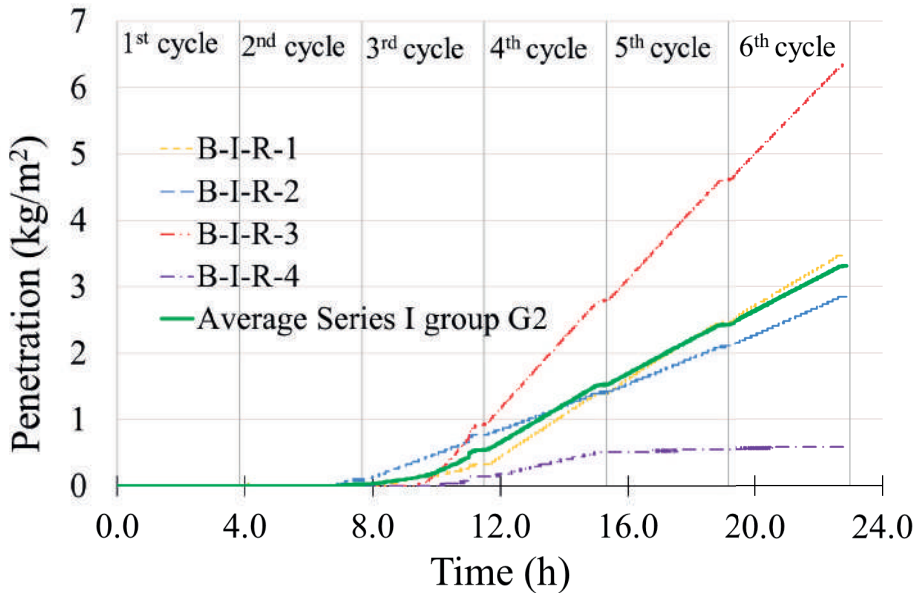


Figure 20. Water penetration in the individual specimens of Series II group G2 within campaign B

The results of total leakage and leakage during the sixth cycle are summarized in Table 4. Leakage herein is defined as the ratio between the amount of sprayed water and the amount of penetrated water. According to guidelines presented in the ASHRAE Standard 160:2009, a one percent leakage of WDR is normally assumed during heat, air, and moisture (HAM) simulations. In the light of the present results, WDR events with an intensity below $3.8 \text{ l/m}^2/\text{h}$ might not result in significant, if any, water leakage through a clay brick masonry veneer with a thickness of 120 mm. Yet, a water spray rate of $6.3 \text{ l/m}^2/\text{h}$ during 21 h might lead to a leakage of up to 8.9 % of the sprayed water.

The amount of leakage highly depends on the absorption properties of bricks and generally occurs once the masonry is close to saturation. It should be further noticed that leakage might happen in masonry specimens after around 8 h – 10 h of exposure to WDR with an intensity of $6.3 \text{ l/m}^2/\text{h}$, depending on the sorptivity and water absorption capacity of masonry. As mentioned in Section 2.1, most WDR events in Sweden take around 1 h to 4 h with an intensity of less than 1 mm/h , indicating the low probability of a WDR event with the duration of 21 h and an intensity of $6.3 \text{ l/m}^2/\text{h}$.

The importance of filling the head joints to control water penetration in masonry walls is noteworthy, as it is considered one of the most important factors influencing water penetration [5, 70, 71, 78]. The common workmanship techniques to fill the head joints are known as “pushing the head joint” and “buttering”, as illustrated in

Figure 21, buttering being recommended as the better one [5]. However, as mentioned in Section 3.3.3, the workmanship technique employed in this study was the so-called pushing of the head joint.

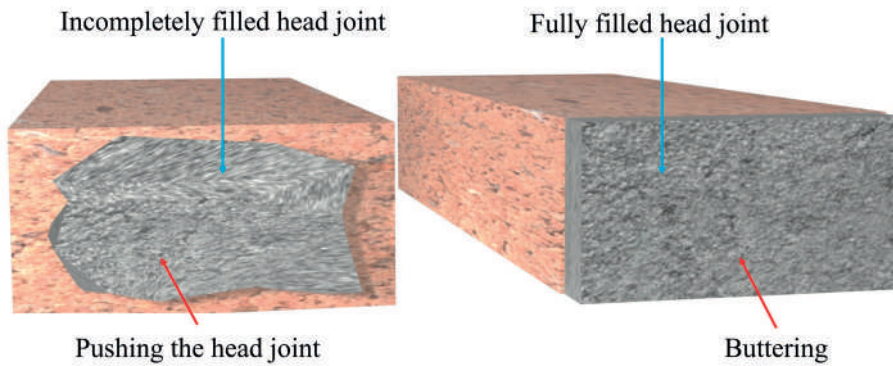


Figure 21. Common workmanship methods for filling the head joints

5 Summary of the appended papers

Paper I

Repointing is a maintenance technique with the potential of reducing the WDR-related issues of eroded mortar joints though the criteria to make a rational decision on repointing are not well established. Several criteria exist to facilitate the decision on whether repointing is needed or not, yet some proposed criteria can be questioned. A review providing the results of a state-of-the-art study concerning field and laboratory methods to assess water content and water uptake caused by WDR is presented. Using the information on water content and water uptake to rationally analyze whether repointing can improve the technical condition of clay brick façades in relation to WDR action is discussed. Accordingly, destructive and non-destructive test methods to measure moisture content and water absorption in masonry façades are reviewed. It is recommended that the visual inspection, if not conclusive, be accompanied by one of the presented test methods to assess the state of the façade, leading to a more rational decision on repointing. Further, alternative maintenance techniques which may postpone the need for costlier maintenance and reveal potential defects or problems are presented.

Paper II

Brick masonry façades are widely used because of their long-term performance and high durability, yet climate agents including WDR and freezing-thawing result in inevitable deterioration and erosion of masonry façades. The test conditions of the majority of existing standards and research studies are representative of extreme WDR events, and there is a need for a simple test setup to study the resistance of masonry to WDR. Accordingly, an experimental study was conducted to study the behavior of masonry in terms of water absorption and penetration exposed to water spraying by developing a new test setup. The appearance of damp patches and their spread on the backside of the specimens was recorded using a digital camera mounted behind the specimens. Several parameters, including the brick absorption properties and different mortar joint profiles, were considered. Triplet masonry specimens were built with three different types of brick and two different types of joint profile finishes, namely flush and raked. Raked specimens were considered representative of eroded mortar joints. The specimens were exposed to a uniform water spray rate of 1.7 – 3.8 l/m²/h, simulating more realistic WDR events encountered in Sweden. The obtained results indicate that water absorption is

mainly dependent on the water absorption properties of bricks, including the water absorption coefficient and water absorption capacity. In contrast, the effect of mortar joint profile on water absorption in masonry is not considerable. The first visible damp patch on the backside of the specimens appeared close to the brick-mortar interfacial zone, indicating the lower resistance of the head joints to WDR, mainly attributed to lower compaction and difficulty of workmanship to fill in joints completely.

Paper III

An experimental campaign was designed to study water absorption and penetration in triplet masonry specimens exposed to uniform water spray. The specimens were exposed to a water spray rate of 6.3 l/m²/h and zero differential air pressure. The presented setup was equipped with two digital scales providing the opportunity to measure water absorption and penetration continuously during 23 h of testing. The results highlight the effect of brick absorption properties on water absorption and penetration. However, the impact of joint profile on water absorption and penetration was negligible. Masonry specimens prepared with low suction bricks and low absorption capacity showed better resistance to WDR than those prepared with medium suction bricks and higher absorption capacity. Further, the first dampness appeared close to the brick-mortar interface in most specimens, indicating the brick-mortar interfacial zone as the primary path for water penetration.

6 Conclusions

The response of clay brick masonry exposed to a uniform water spray was studied by employing a newly developed test setup. Two main experimental campaigns were performed, and different parameters, including water spray rate, water absorption properties of bricks, and mortar joint profile, were considered. The specimens in this study were exposed to water spray rates varying between 1.7 and 6.3 l/m²/h, a reduction of approximately 90% in comparison with the water application rate specified in current standards and many studies. Based on the obtained results, the following conclusions can be drawn:

- The moisture absorption response of the masonry specimens was mainly dependent on the water absorption properties of the bricks.
- Prior to the surface saturation, the water absorption in masonry specimens was highly dependent on the water spray rate and water absorption coefficient of bricks. Once the surface saturation was attained, the behavior was dependent on both the water absorption coefficient of bricks and the water absorption capacity of the bricks.
- The effect of mortar joint profile on water absorption and penetration was not considerable.
- Water penetration started when the masonry specimens were nearly close to saturation, highlighting that the gained benefit from the storage capacity of masonry could postpone the occurrence of water penetration.
- The time to the appearance of the first visible damp patch on the backside of specimens was also affected by the water spray rate and absorption properties of bricks.
- The first dampness appeared close to the brick-mortar interface in the vicinity of the head joint, indicating the lower resistance of head joints to WDR. Further, the adequate filling of the head joint might affect the location and the time to the appearance of the first visible damp patch.
- For specimens exposed to a water spray rate of around 3.5 l/m²/h, it took nearly 16 h to get a completely wet masonry specimen (i.e., reach entire dampness on the backside of masonry). Additionally, for specimens

prepared with low water absorption properties, the backside did not reach full dampness, even after 21 h of water spraying with the rate of 6.3 l/m²/h.

- The newly developed test setup might facilitate the verification of moisture simulations as it enables continuous water absorption and penetration measurements combined with tracing of damp areas on the backside of masonry specimens.

7 Future Research

The current work provided an insight into the resistance of clay brick masonry façades to WDR. It is widely accepted among both researchers and practitioners that differential air pressure induced by wind is the governing agent that influences water penetration in masonry. The focus of the current study was to produce low water spray rates, which are uniform and representative of WDR in Sweden, while the effect of pressure stemming from wind has so far not been considered. However, the developed test setup presented in this study is capable of producing different levels of air pressure. An important point for future research is to study masonry exposure to WDR with different levels of differential air pressure.

The masonry specimens in the present project were prepared in laboratory conditions and built without any known defects such as cracks. Based on the present as well as previous research, it is believed that the brick-mortar interface provides a path of least resistance for water penetration. Further, many of the existing masonry façades are cracked and eroded due to differential movements, reinforcement corrosion, and harsh weather conditions. These imperfections can provide other similar pathways for water to penetrate through the masonry. Thus, to better understand the effect of cracks and other imperfections, there is a need to study water absorption and penetration in such masonry specimens both in laboratory and field.

Imperfections may also be caused by workmanship, and the current work revealed the importance of workmanship in filling the joints and brick-mortar interface on the resistance of masonry to WDR. Another critical step is comparing the effect of different workmanship methods on the resistance of masonry to driving rain.

The masonry specimens in the present project were prepared with solid bricks. Yet, many clay brick masonry façades in Sweden have been constructed with perforated bricks. Thus, studying water absorption and water penetration in masonry with perforated bricks might generate useful knowledge.

In the absence of differential air pressure, the expected driving force to push water through masonry seems to be the gravitational force. In the current study, water penetration could be detected in the absence of a pressure difference. Thus, there is a need to shed light on the effect of hydrostatic pressure due to gravitational forces on leakage.

Simulations of moisture accumulation in masonry walls with other configurations than studied in the present project might be a possible way to extend the validity of the present results. This is especially interesting in the case of thick masonry walls, in which experimental studies might be much more difficult to be carried out in practice.

Simulations could further be used to analyze moisture safety in external walls with the external leaf consisting of clay brick masonry, especially in the light of the indications that gravity might be an important driving force for water penetration in walls exposed to WDR.

Techniques that are used to apply new mortar during repointing may affect water absorption and penetration into clay brick masonry. Compared to the traditional method to fill the raked joints with a trowel by hand, machine-driven equipment to apply new mortar is often used. The mortar used for machinery equipment usually has higher water content, resulting in difficulties in compacting the mortar. Consequently, filling mortar joints with machine-driven equipment may result in lower strength, air voids, and poor contact between bricks and mortar. Thus, the effects of different methods to fill the raked joints should be investigated.

Eventually, there is a need to develop a solid knowledge to make rational decisions on repointing and address the following questions:

- a) The tools and methods that can be employed to rake out the mortar.
- b) The depth to which the existing mortar should be raked out.
- c) The compatibility of the repointing mortar with the existing units and mortar.

References

- [1] M. Abuku, H. Janssen, and S. Roels, "Impact of wind-driven rain on historic brick wall buildings in a moderately cold and humid climate: Numerical analyses of mould growth risk, indoor climate and energy consumption," *Energy and Buildings*, vol. 41, no. 1, pp. 101-110, 2009/01/01/ 2009, doi: <https://doi.org/10.1016/j.enbuild.2008.07.011>.
- [2] S. Shahreza, M. Molnár, J. Niklewski, I. Björnsson, and T. Gustavsson, "Making decision on repointing of clay brick facades on the basis of moisture content and water absorption tests results—a review of assessment methods," in *Brick and Block Masonry-From Historical to Sustainable Masonry*: CRC Press, 2020, pp. 617-623.
- [3] *ASTM E514 / E514M-14a, Standard Test Method for Water Penetration and Leakage Through Masonry*, A. International, West Conshohocken, PA, 2014.
- [4] R. Cacciotti, "Brick masonry response to wind driven rain," *Engineering Structures*, vol. 204, p. 110080, 2020.
- [5] F. Slapø, T. Kvande, N. Bakken, M. Haugen, and J. Lohne, "Masonry's Resistance to Driving Rain: Mortar Water Content and Impregnation," *Buildings*, vol. 7, no. 3, p. 70, 2017.
- [6] J. Ribar, "Water permeance of masonry: a laboratory study," in *Masonry: Materials, Properties, and Performance*: ASTM International, 1982.
- [7] *NEN 2778:2015 nl. Vochtwering in gebouwen (Moisture control in buildings)*, Nederlands, 2015.
- [8] *NBI 29/1983 Mørtler. Tetthet mot slagregn (Mortars. Resistance to driving rain)*, Norges byggforskningsinstitutt: Oslo, Norway, 1983.
- [9] C. Groot and J. Gunneweg, "The influence of materials characteristics and workmanship on rain penetration in historic fired clay brick masonry," *Heron*, 55 (2), 2010.
- [10] R. R. Vilató, "WATER PENETRATION TEST ON CONCRETE BLOCK MASONRY," in *the 15th International Brick and Block Masonry Conference*, Florianópolis – Brazil, 2012.
- [11] J. C. Z. Piaia, M. Cheriaf, J. C. Rocha, and N. L. Mustelier, "Measurements of water penetration and leakage in masonry wall: Experimental results and numerical simulation," *Build. Environ.*, vol. 61, pp. 18-26, 2013.
- [12] K. B. Anand, V. Vasudevan, and K. Ramamurthy, "Water permeability assessment of alternative masonry systems," *Build. Environ.*, vol. 38, no. 7, pp. 947-957, 2003/07/01/ 2003, doi: [https://doi.org/10.1016/S0360-1323\(03\)00060-X](https://doi.org/10.1016/S0360-1323(03)00060-X).

- [13] T. Ritchie, "Small-panel method for investigating moisture penetration of brick masonry," in "Internal Report (National Research Council of Canada. Division of Building Research); no. DBR-IR-160," National Research Council of Canada, 1958/09/01 1958.
- [14] S. Van Goethem, N. Van Den Bossche, and A. Janssens, "Watertightness Assessment of Blown-in Retrofit Cavity Wall Insulation," *Energy Procedia*, vol. 78, pp. 883-888, 2015/11/01/ 2015, doi: <https://doi.org/10.1016/j.egypro.2015.11.012>.
- [15] M. E. Driscoll and R. E. Gates, "A Comparative Review of Various Test Methods for Evaluating the Water Penetration Resistance of Concrete Masonry Wall Units," in *Masonry: Design and Construction, Problems and Repair*: ASTM International, 1993.
- [16] L. R. Baker and F. W. Heintjes, "Water leakage through masonry walls," *Architectural Science Review*, Article vol. 33, no. 1, pp. 17-23, 1990, doi: 10.1080/00038628.1990.9696662.
- [17] N. Van Den Bossche, M. Lacasse, and A. Janssens, "Watertightness of masonry walls: an overview," in *12th International conference on Durability of Building Materials and Components (XII DBMC-2011)*, 2011, vol. 1: FEUP Edições, pp. 49-56.
- [18] S. Kahangi Shahreza, J. Niklewski, and M. Molnár, "Experimental investigation of water absorption and penetration in clay brick masonry under simulated uniform water spray exposure," *Journal of Building Engineering*, vol. 43, p. 102583, 2021/11/01/ 2021, doi: <https://doi.org/10.1016/j.jobbe.2021.102583>.
- [19] R. Forghani, Y. Totoev, S. Kanjanabootra, and A. Davison, "Experimental investigation of water penetration through semi-interlocking masonry walls," *Journal of Architectural Engineering*, vol. 23, no. 1, p. 04016017, 2017.
- [20] M. Lacasse, T. O'Connor, S. Nunes, and P. Beaulieu, "Report from Task 6 of MEWS project: Experimental assessment of water penetration and entry into wood-frame wall specimens-final report," *Institute for Research in Construction, RR-133, Feb*, 2003.
- [21] A. Rathbone, *Rain and air penetration performance of concrete blockwork*. Cement and Concrete Association, 1982.
- [22] H. Hens, S. Roels, and W. Desadeleer, "Rain leakage through veneer walls, built with concrete blocks," in *CIB W40 meeting in Glasgow*, 2004.
- [23] A. Fried, A. Tovey, and J. Roberts, *Concrete masonry designer's handbook*. CRC Press, 2014.
- [24] S. M. Tindall, "Repointing Masonry—Why Repoint?," *Old-House Journal*, pp. 24-31, January/February 1987.
- [25] B. Brief, "Maintenance of Brick Masonry," *Brick Industry Association, Technical Notes on Brick Construction*, vol. 46, pp. 1-11, December 2017.
- [26] J. G. Stockbridge, "Repointing masonry walls," *APT bulletin*, vol. 21, no. 1, pp. 10-12, 1989.
- [27] S. Johnson, "The neglected craft of repointing—an architect's view," ed: Crown copyright NSW Heritage Office & the author, 2000.

- [28] P. Maurenbrecher and J. E. Lindqvist, "RILEM TC 203-RHM: Repair mortars for historic masonry : Requirements for repointing mortars for historic masonry," (in eng), *Materials and Structures*, article vol. 45, no. 9, pp. 1303-1309, 2012 2012. [Online]. Available: <http://urn.kb.se/resolve?urn=urn:nbn:se:ri:diva-2706>.
- [29] A. H. P. Maurenbrecher, K. Trischuk, M. Z. Rousseau, and M. I. Subercaseaux, "Repointing mortars for older masonry buildings: design considerations," (in eng), *Construction Technology Update*; no. 67, 2008/03/01 2008, Art no. 6 p., doi: 10.4224/21274782.
- [30] P. M. C. L. Paul Jeffs, "Repointing Masonry Walls – Matching the Techniques for Success or Failure," ed. Technical Workshop Restoration, Reconstruction and Maintenance of Masonry Structures, Dalhousie University Continuing Technical Education: Conservation of Heritage Structures & Older Buildings.
- [31] R. Veiga and F. Carvalho, "Some performance characteristics of lime mortars for rendering and repointing ancient buildings," in *Proc. Br. Masonry Soc. No. 8*, 1998, pp. 353-356.
- [32] D. Young, "Repointing mortar joints: some important points," in *Australia ICOMOS Conference*, Adelaide Australia, 5-8 November 2015.
- [33] C. W. Westermann, Heinrich and Schulz, Jens-Uwe, "Increased Durability of Repointing In Historical Masonry – Engineering Model and Sensitivity Analysis," presented at the 13th Canadian Masonry Symposium, Halifax, Canada, 4-7 June, 2017.
- [34] A. Maurenbrecher, K. Trischuk, M. Rousseau, and M. Subercaseaux, "Key Considerations for Repointing Mortars for the Conservation of Older Masonry (IRC-RR-225)," *Canada: Institute for Research in Construction, National Research Council of Canada, Ottawa*, 2007.
- [35] I. M. Griffin, "Deterioration mechanisms of historic cement renders and concrete," Doctoral dissertation, University of Edinburgh, 2013.
- [36] M. Holland, *Practical Guide to Diagnosing Structural Movement in Buildings*. John Wiley & Sons, 2012.
- [37] B. Brief, "Repointing (Tuckpointing) Brick Masonry," *Brick Industry Association*, July 2005.
- [38] K. Wang, D. C. Jansen, S. P. Shah, and A. F. Karr, "Permeability study of cracked concrete," *Cement and concrete research*, vol. 27, no. 3, pp. 381-393, 1997.
- [39] C.-M. Aldea, S. P. Shah, and A. Karr, "Permeability of cracked concrete," *Materials and structures*, vol. 32, no. 5, pp. 370-376, 1999.
- [40] B. Blocken and J. Carmeliet, "A review of wind-driven rain research in building science," *Journal of Wind Engineering and Industrial Aerodynamics*, vol. 92, no. 13, pp. 1079-1130, 2004/11/01/ 2004, doi: <https://doi.org/10.1016/j.jweia.2004.06.003>.
- [41] E. Cho, C. Yoo, M. Kang, S.-u. Song, and S. Kim, "Experiment of wind-driven-rain measurement on building walls and its in-situ validation," *Build. Environ.*, vol. 185, p. 107269, 2020/11/01/ 2020, doi: <https://doi.org/10.1016/j.buildenv.2020.107269>.
- [42] B. Blocken, D. Derome, and J. Carmeliet, "Rainwater runoff from building facades: A review," *Build. Environ.*, vol. 60, pp. 339-361, 2013/02/01/ 2013, doi: <https://doi.org/10.1016/j.buildenv.2012.10.008>.

- [43] A. Erkal, D. D' Ayala, and L. Sequeira, "Assessment of wind-driven rain impact, related surface erosion and surface strength reduction of historic building materials," *Build. Environ.*, vol. 57, pp. 336-348, 2012.
- [44] M. Abuku, H. Janssen, J. Poesen, and S. Roels, "Impact, absorption and evaporation of raindrops on building facades," *Build. Environ.*, vol. 44, no. 1, pp. 113-124, 2009/01/01/ 2009, doi: <https://doi.org/10.1016/j.buildenv.2008.02.001>.
- [45] J. Carmeliet and B. Blocken, "Driving rain, rain absorption and rainwater runoff for evaluating water leakage risks in building envelopes," in *9th International Conference on Performance of Exterior Envelopes of Whole Buildings (Buildings IX)*, 2004.
- [46] G. Robinson and M. C. Baker, "Wind-driven rain and buildings," in "Technical Paper (National Research Council of Canada. Division of Building Research); no. DBR-TP-445," National Research Council of Canada, 1975/07 1975.
- [47] A. J. Newman, D. Whiteside, and P. B. Kloss, "Full-scale water penetration tests on twelve cavity fills—Part II. Three built-in fills," *Build. Environ.*, vol. 17, no. 3, pp. 193-207, 1982/01/01/ 1982, doi: [https://doi.org/10.1016/0360-1323\(82\)90039-7](https://doi.org/10.1016/0360-1323(82)90039-7).
- [48] V. Korsgaard and T. L. Madsen, *CORRELATION BETWEEN MEASURED DRIVING RAIN AND COMPUTED DRIVING RAIN*. TECHN. UNIV. DENMARK, HEAT INSULATION LABOR., 1962.
- [49] R. E. Lacy, "Driving rain maps and the onslaught of rain on buildings," in *Proc. of CIB/RILEM Symposium on Moisture Problems in Buildings, Helsinki, 1965*, 1965.
- [50] A. Best, "The size distribution of raindrops," *Quarterly Journal of the Royal Meteorological Society*, vol. 76, no. 327, pp. 16-36, 1950.
- [51] J. Straube and E. Burnett, "Simplified prediction of driving rain on buildings," in *Proceedings of the international building physics conference, 2000: Eindhoven University of Technology Eindhoven, the Netherlands*, pp. 375-382.
- [52] *EN ISO 15927-3, Hygrothermal performance of buildings—Calculation and presentation of climatic data. Part 3: calculation of a driving rain index for vertical surfaces from hourly wind and rain data*, 2009.
- [53] E. Choi, "Determination of wind-driven-rain intensity on building faces," *Journal of Wind Engineering and Industrial Aerodynamics*, vol. 51, no. 1, pp. 55-69, 1994.
- [54] B. Blocken and J. Carmeliet, "Overview of three state-of-the-art wind-driven rain assessment models and comparison based on model theory," *Build. Environ.*, vol. 45, no. 3, pp. 691-703, 2010/03/01/ 2010, doi: <https://doi.org/10.1016/j.buildenv.2009.08.007>.
- [55] B. S. Institution, *Code of Practice for Assessing Exposure of Walls to Wind-driven Rain*. British Standards Institution, 1992.
- [56] "<https://www.smhi.se/data>." SMHI, "SMHI Öppna data". (accessed September 2020).
- [57] C. Hall and W. D. Hoff, *Water transport in brick, stone and concrete*, 2nd Edition ed. CRC Press, 2011.
- [58] Z. Liu, P. Zhang, J. Bao, and Y. Hu, "Numerical Simulation of Water Transport in Unsaturated Recycled Aggregate Concrete," (in English), *Frontiers in Materials*,

Original Research vol. 7, no. 314, 2020-September-21 2020, doi:
10.3389/fmats.2020.560621.

- [59] M. Karoglou, A. Moropoulou, Z. Maroulis, and M. Krokida, "Water sorption isotherms of some building materials," *Drying technology*, vol. 23, no. 1-2, pp. 289-303, 2005.
- [60] H. M. Künzel, "Simultaneous heat and moisture transport in building components," *One-and two-dimensional calculation using simple parameters. IRB-Verlag Stuttgart*, vol. 65, 1995.
- [61] L. Mengel, H.-W. Krauss, and D. Lowke, "Water transport through cracks in plain and reinforced concrete—Influencing factors and open questions," *Construction and Building Materials*, vol. 254, p. 118990, 2020.
- [62] P. K. Mehta and P. J. Monteiro, *Concrete: microstructure, properties, and materials*. McGraw-Hill Education, 2014.
- [63] P. A. Claisse, *Transport properties of concrete: Measurements and applications*. Elsevier, 2014.
- [64] Ø. Birkeland and S. Svendsen, "Norwegian test methods for rain penetration through masonry walls," in *Symposium on Masonry Testing*, 1963: ASTM International.
- [65] C. T. Grimm, "Masonry cracks: a review of the literature," *Masonry: materials, design, construction, and maintenance*, 1988.
- [66] J. F. Straube and E. F. Burnett, "Driving rain and masonry veneer," in *Water leakage through building facades*: ASTM International, 1998.
- [67] J. Straube and E. Burnett, "Rain control and screened wall systems," in *Proc. 7th Conf. on Building Science and Technology. Durability of Buildings. Design, Maintenance, Codes and Practices*. Toronto, 1997, pp. 20-21.
- [68] J. F. Straube, "The Performance of Wall Systems Screened with Brick Veneer," University of Waterloo, 1994.
- [69] C. L. Galitz and A. R. Whitlock, "The application of local weather data to the simulation of wind-driven rain," in *Water Leakage Through Building Facades*: ASTM International, 1998.
- [70] C. T. Grimm, "Water permeance of masonry walls: a review of the literature," in *Masonry: Materials, Properties, and Performance*: ASTM International, 1982.
- [71] C. C. Fishburn, D. Watstein, and D. E. Parsons, *Water permeability of masonry walls*. US Department of Commerce, National Bureau of Standards, 1938.
- [72] S. Cornick and M. Lacasse, "An Investigation of Climate Loads on Building Façades for Selected Locations in the United States," *Journal of ASTM International*, vol. 6, no. 2, pp. 1-22, 2009.
- [73] K. Sandin, "Fuktillstånd i autoklaverade lättbetongväggar : fältmätning av slagregnets och ytskiktets inverkan (Rapport TVBM; Vol. 3026)," Avd Byggnadsmaterial, Lunds tekniska högskola, 1987.
- [74] ASTM C67 / C67M-20, *Standard Test Methods for Sampling and Testing Brick and Structural Clay Tile*, A. International, West Conshohocken, PA, 2020.
- [75] *ASTM C1403 - 15, Standard Test Method for Rate of Water Absorption of Masonry Mortars*, A. International, West Conshohocken, PA, 2015.

- [76] T. Ritchie and J. I. Davison, "Factors affecting bond strength and resistance to moisture penetration of brick masonry," (in eng), *ASTM Special Technical Publication*, no. 320, pp. 16-30, 1963/07/01 1963.
- [77] T. Ritchie and W. G. Plewes, "A review of literature on rain penetration of unit masonry," (in eng), *Technical Paper (National Research Council of Canada. Division of Building Research)*, 1957/05 1957, Art no. iii, 72 p., doi: 10.4224/40001176.
- [78] C. C. Fishburn, *Water permeability of walls built of masonry units*. US Department of Commerce, National Bureau of Standards, 1942.

Paper I



Making decision on repointing of clay brick facades on the basis of moisture content and water absorption tests results – a review of assessment methods

S.K. Shahreza, M. Molnár, J. Niklewski & I. Björnsson

Department of Building and Environmental Technology, Division of Structural Engineering, Lund University, Lund, Sweden

T. Gustavsson

Tomas Gustavsson konstruktioner AB, Lund, Sweden

ABSTRACT: Use of clay brick masonry in façades is often motivated by its aesthetic values and durability. Yet, mortar joints exposed to climate agents erode over time, expected to cause elevated moisture content and water absorption. Thus, it is often recommended that 40- to 50-year-old façades should be repointed – a measure which is intrusive and costly. Decision is in many cases taken without a clear evidence that repointing will diminish water absorption and moisture content in the renovated walls. This paper presents the results of a state-of-the-art study on field and laboratory methods to measure moisture content and water absorption in clay brick masonry. For common buildings, use of low cost and time efficient measurement methods is feasible. However, prior to measurements, analysis of technical and climate data combined with a visual inspection might give a rational basis for decision on repointing or other alternative maintenance measures.

1 INTRODUCTION

Clay brick masonry is one of the most common building materials in the façades of residential buildings in the Nordic countries. The ubiquitous use of clay brick masonry as façade material is due to its aesthetic values, good durability and low maintenance needs. Although the expected technical life time of a clay brick façade is more than hundred years, maintenance can still be needed due to inevitable deterioration caused by climate and ambient actions. Important climate actions in a Nordic climate include wind-driven rain (WDR) and freeze-thaw-cycles – actions that individually or in conjunction can cause spalling, delamination or cracking of bricks and erosion and cracking of mortar joints.

The focus in this paper is on the repointing of mortar joints, since it is an intrusive and costly maintenance measure. A common argument for repointing is that the erosion of mortar joints facilitates water up-take in façades exposed to WDR (Fried et al., 2014). Further, erosion of mortar joints is, at least in the Nordic countries, regarded as detrimental from an aesthetic point of view, since it creates, seen superficially, the impression of poor technical condition of the building. Understanding that aging of clay brick façades can be perceived as an aesthetic value, e.g. through exposure of fossil shells in the surface of the mortar joints, is generally poor (Tägil et al., 2011).

According to the present practice in the Nordic countries, repointing shall be carried out as part of a regular maintenance scheme, after 40-50 years from erection or when limited façade parties with more or less eroded mortar joints are observed (Tindall, 1987, Brief, 2017). No further investigations, e.g. concerning factual water up-take, are usually carried out. Nor are alternative measures, such as partial repointing of eroded façade parties, considered - full repointing is regularly carried out without a more in-depth analysis of the possible technical, economic or aesthetic implications of this measure. In the light of the presented practices it can be objected that decision concerning repointing of clay brick façades usually is not based on rational grounds.

In the present paper the results of a state-of-the-art study concerning field and laboratory methods to assess water content and water up-take caused by WDR are presented. Using information on water content and water up-take to rationally analyse whether repointing can improve the technical condition of clay brick façades in relation to WDR action is discussed and research and development needs are identified.

2 RESEARCH APPROACH

A literature review concerning repointing of clay brick façades has been carried out with keywords

including repointing, masonry, clay brick façade, masonry façade, brick masonry, mortar joints, mortar, environmental factors, wind-driven rain, impingement, water up-take, water penetration, moisture content, durability, erosion and deterioration. Other search terms include destructive and non-destructive tests, study of WDR, field, laboratory, etc. Main literature sources and databases include Lund University Library, National Library of Sweden including the libraries of all Swedish universities, ASCE Library, Engineering Village (Elsevier), Wiley Online Library. In addition to library searches, meetings with Swedish and German researchers and industry representatives provided additional sources of information.

3 RESULTS

3.1 Tests measuring moisture content

A number of non-destructive and destructive experimental procedures for assessing moisture conditions of brick facades have been reviewed based on previous research studies (Emerisda, 2014, Bison et al., 2011, Litti et al., 2015, Hola, 2017, Larsen, 2012). Experimental procedures can be categorized into three groups based on their destructiveness and their type of output. The groups are described as follows: *group A* - destructive tests (DT) measuring moisture content quantitatively; *group B* non-destructive tests (NDT) measuring moisture content quantitatively; and *group C* - NDT indicating moisture content qualitatively. The potential for making on-site measurements using each experimental procedure is also assessed.

Tests belonging to *group A* include, among others, gravimetric tests, the calcium carbide test and the chemical method (Karl Fisher). Although destructive tests are generally seldom carried out on historical buildings, there is no consensus whether or not they are appropriate for residential buildings.

Gravimetric testing involves sampling by core drilling, after which the samples are dried in an oven at a specified temperature. Finally, the actual moisture content (MC) is generally derived from the difference in weight of the sample before and after drying (Camuffo and Bertolin, 2012, EN, 1993). Gravimetric testing is considered being a precise and reliable method to measure moisture content in masonry walls; however, sampling by core drilling is perceived as a drawback.

The calcium carbide test involves grinding a sample from the masonry wall and mixing the powder with a certain amount of calcium carbide (Blystone et al., 1962, ASTM, 2011, Camuffo and Bertolin, 2012). Subsequently, the moisture content can be derived from the pressure of the gas released during the reaction between calcium carbide and water, by the use of a calibration curve (Binda et al.,

1996). While the test is appropriate for on-site measurements, it is less reliable than the gravimetric test.

The chemical method, invented by Karl Fisher, is based on the reaction between iodine and water, producing a non-conductive chemical substance. It is possible to carry out titration on site to determine trace amounts of water in a sample. The capabilities of this test are measuring accurately small amounts of moisture and determining the water content level from low values till saturation (Schöffski, 2006, Bruttel and Schlink, 2003). However, it is stated that the chemical method would be helpful for small samples and not reliable for masonry walls (Hola et al., 2012).

Among tests belonging to *group B*, nuclear magnetic resonance (NMR) and neutron radiography are of special interest. *Nuclear magnetic resonance* (NMR) is a non-contacting, fast, accurate, and reliable technology to measure the water content in masonry walls and to evaluate the distribution of moisture content along the wall surface (Pel et al., 1996, Wolter and Krus, 2005, Litti et al., 2015). *Neutron radiography* records the radiation passing through an object by a position sensitive detector. Although both methods quantitatively and non-destructively measure the water content in walls, their high cost and limited availability (Hola, 2017) make their applicability to common buildings rather limited. They could, however, be employed under certain circumstances, such as for buildings with great cultural or economic values.

Tests in *group C* include, among others, the paper indicator method, infrared thermography (IRT), holographic radar and the dielectric and microwave methods. The *paper indicator* method is a simple and inexpensive method to qualitatively evaluate the moisture content in a masonry wall. In this test, contact between chemical papers and the moist surface of a facade provides indications of the moisture content based on the subsequent change in colour of the paper; similar to the litmus paper test for evaluating acidity (Hola, 2017).

IRT uses thermal imagery to map the location of damp areas and the existence of voids (Griffin, 2013), yet without the possibility of quantitative evaluation of the moisture content. This non-destructive test is carried out in-situ with at a relatively low cost. The time when the test can be performed is critical and limits its use, since it is strongly affected by environmental conditions [high relative humidity and low temperature] (Emerisda, 2014, Bison et al., 2011).

Holographic radar has the capability to detect moisture in the range of 50 to 200 mm beneath the surface as a function of continuous wave frequency (Litti et al., 2015, Bison et al., 2011). Also, detection of voids is possible. In contrast with IRT, the holographic radar technique is not influenced by relative humidity or air temperature (Litti et al., 2015).

The *dielectric* method works on the principle of variation of the dielectric constant of a material in the presence of water. The dielectric constant increases with increasing moisture content, making differences in moisture content detectable. This test is commonly employed by surveyors to determine the moisture distribution along the height of masonry walls. The method is, however, limited to depths of 50 to 100 mm (Hola, 2017). The *microwave* method is another non-destructive method which works on the principle of reduction of the radiation intensity as microwaves pass through a damp material (Hola, 2017). Thus, the more water the specimen contains, the bigger the energy loss. This method is procedurally similar to the dielectric one, however the microwave method can be used to depths up to 300 mm (Hola, 2017). The advantages of these two techniques are low cost of the equipment and ease of use (Emerisda, 2014, Hola, 2017).

The main features of the test methods described in this section are, together with methods to be described in section 3.2, summarized in Table 1.

3.2 Tests measuring water absorption

There are several quantitative methods available for measuring the amount of water being absorbed through a brick masonry wall. They are divided into two groups - *group D* comprising low-intrusive methods, while *group E* including NDT methods. Again, the potential for making on-site measurements using each experimental procedure is also assessed.

A newly developed, *group D* technique to measure water absorption is named Wasseraufnahme Messgerät – WAM (*Instrument for measurement of water up-take* – the author’s translation), which measures water absorption in the absence of wind pressure

(Möller and Stelzmann, 2013, Stelzmann et al., 2015). The apparatus includes a scale, a storage tank and a pipe with nozzles. The apparatus is attached to a section of the wall with the edges and sealed in order to create a closed system (Figure 1a). The apparatus then projects a water film on the entire section. Run-off water that is not absorbed is collected. The rate of absorption can be calculated and monitored in real time by continuously weighing the amount of moisture in the closed system. The apparatus is portable and can easily be used in-situ. If attached to the lower end of a wall, the apparatus can rest on the ground or alternatively on a small support. In order to test the upper parts of a wall, the apparatus needs to be attached by 8 screws, making it semi-intrusive (*group D*).

Among NDT methods (*group E*), the RILEM tube test, the Franke plate and the Stockbridge method are reviewed here. The *RILEM tube test* is widely used to quantify water absorption during a specified period of time through an up-take tube, with possible application in laboratory and on site (RILEM, 1978, Crissinger, 2005). The uptake tube is first sealed to the substrate with a putty and then filled with water. The amount of absorbed water is recorded during specified time intervals. This simple NDT test is helpful for assessing the water absorption rate before and after repointing. However, it only provides results for a small area of masonry wall and results are not precise when the tube is applied on mortar joints. In order to speed up the procedure, it is suggested to use several tubes in different locations (Figure 1.b).

The Franke-Platte method consists of a plate (25 cm × 8.1 cm absorption area) and a tube like the RILEM tube (Figure 1.c). The procedure is similar to the RILEM tube test with the exception that rather than attaching a tube to a small area, a plate is attached to an area including bricks and mortar

Table 1. Summary of test method features.

Test	Group	Destructiveness ¹	Output ²	Application	On site
Gravimetric	A	De	QN	moisture content and its distribution	-
Calcium carbide	A	De	QN	moisture content	✓
Chemical method (Karl Fisher)	A	De	QN	moisture content indirectly	✓
Nuclear magnetic resonance (NMR)	B	N	QN	surface (flat) moisture content	✓
Neutron radiography	B	N	QN	moisture content	✓
Paper indicator method	C	N	QL	moisture content level	✓
Infrared thermography (IRT)	C	N	QL	surface moisture content	✓
Holographic radar	C	N	QL	moisture content (flat surface)	✓
Dielectric method	C	N	QL	moisture content	✓
Microwave method	C	N	QL	moisture content	✓
Wasseraufnahme Messgerät (WAM)	D	L	QN	water penetration	✓
RILEM tube test	E	N	QN	water penetration	✓
Franke-Platte	E	N	QN	water penetration	✓
Stockbridge (Stockbridge, 1989)	E	N	QN	water penetration	✓

1. De – destructive, N – non-destructive, and L – low intrusive

2. QL – qualitative and QN – quantitative

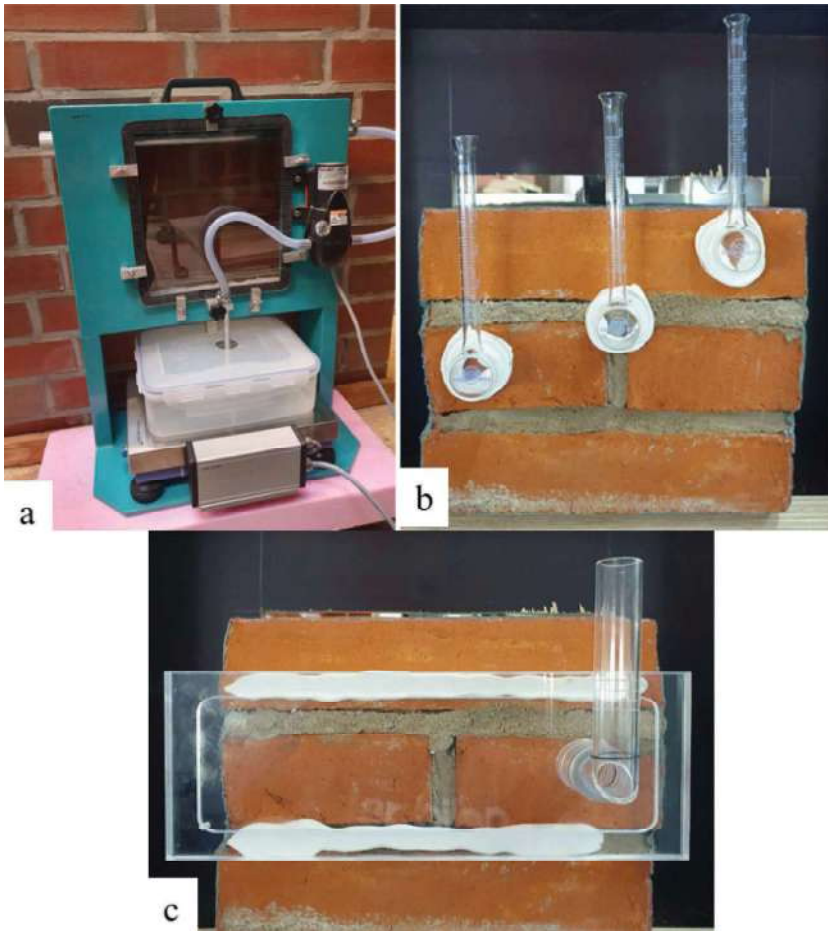


Figure 1. Apparatus and set-up of test methods measuring water absorption; (a) WAM Device, (b) RILEM tube test, (c) Franke Platte.

joints (Franke and Bentrup, 1991, Neumann et al., 2014, Stelzmann et al., 2015).

Stockbridge developed a watertight frame (91×122 cm area of the wall) to be attached to a masonry façade while measuring the water absorption (Stockbridge, 1989, ASTM, 2014), without refilling the absorbed water. It is recommended that if the rate of absorption is less than one litre per hour, no repointing is needed. Further, it is stated that if the absorption rate is larger than five litres per hour, repointing will result in a substantial decrease in water absorption. Unfortunately, it is not shown how these criteria have been established.

4 DISCUSSION AND STRATEGIES

The results presented in the previous section show that there are a couple of methods to assess moisture content and water absorption in clay brick facades. Each method is associated with costs related to investment in equipment and operation. Qualitative or quantitative information possible to obtain must be valued in relation to its usefulness. In the following sections a brief analysis and discussion are presented concerning circumstances when decision on repointing can be more rational by using information obtained by the presented methods.

4.1 Preliminary investigations

Prior to carrying out potentially costly and time-consuming experimental studies, either in laboratory or on-site, gathering basic information concerning the building, local climate and weather history can provide useful information such as:

- Age of the building; previous façade maintenance measures; type and/or brand of the bricks and of the mortar;
- Occupants' or building owners' reports on problems with dampness of external walls; dampness or discoloration of façades;
- Local climate data indicating temperature, precipitation, wind intensity and direction; current, reliable weather records.

Based on the above information, previous experience and knowledge of the performance of similar façades, a competent inspector might conclude whether increased dampness of façades and external walls depends on moisture and water absorption characteristics of the bricks and mortar, seasonal increase in WDR or recent heavy driving rain events. Further investigations might not be needed nor repointing.

A visual inspection can further shed light on the general condition of the façade, including moisture and moisture related aspects, by registering incidence of:

- Eroded mortar joints with respect to erosion depth and cracks;
- Damaged bricks with respect to spalling and cracks;
- Efflorescence, discoloration and microbiological growth.

Presence of eroded mortar joints indicate that climate actions have a tangible impact on the façade, a hypothesis that can be further underpinned if the incidence and degree of erosion is correlated with the exposure of the façade to WDR. Efflorescence, discolorations and microbiological growth concentrated to façade parties with eroded mortar joints might indicate that the erosion of the mortar joints constitute the root cause of these phenomena, making repointing, especially of the eroded parties, justifiable. Yet, there is a lack of knowledge concerning to what extent water absorption from WDR can be diminished by repointing.

4.2 On-site and laboratory testing

When preliminary examinations are considered inconclusive, on-site and laboratory testing of moisture content and water absorption might be justifiable. By taking into consideration benefits and drawbacks, one or more suitable test methods among those presented in *section 3* might be chosen.

Despite their high accuracy, the usability of Group A tests is somewhat limited, since they

damage the examined buildings. Similarly, although the nuclear magnetic resonance (NMR) method can provide accurate results concerning moisture content, its high cost will limit its usage when it comes to common residential buildings. Thus, in most residential projects, NDT methods determining moisture content qualitatively (Group C) are recommended, though their accuracy is lower than that of other methods'.

Although high moisture content is not necessarily an indicator that repointing is needed, alteration of moisture content over time might indicate erosion of both mortar joints and of bricks. Thus, recurring measurements or continuous monitoring over time of moisture content of brick façades of high cultural or economic value might, in spite of high costs, be justifiable.

Methods measuring water absorption, named group D and E in this paper, can indicate the degree of erosion of different façade parties, since both larger, protrusive cracks and surfaces with micro-cracks are expected to absorb more water. Clay brick façades with eroded and recessed joints are further believed to absorb more water, yet, to the knowledge of the authors, no quantitative models have been established.

4.3 Criteria for decision on repointing

Qualitative and quantitative criteria concerning the need for repointing have been proposed by e.g. (Griffin, 2013, Tindall, 1987, Holland, 2012, Brief, 2005, Stockbridge, 1989), recommending repointing when a) the surface of the mortar joints contain hairline cracks, b) eroded mortar joints to a certain depth [a quarter of an inch, i.e. 6.4 mm] have been observed, c) high suction/retention mortar has been used, d) crack widths larger than 2 mm have been measured, e) the rate of water absorption is more than 4.5 litre/hour/m², or f) presence of voids has been detected, e.g. by means of the IRT test.

Considering the suitability of the mentioned criteria and that during repointing joints are generally raked out to approximately 25 mm or 2.5 times of the mortar joint thickness (Maurenbrecher et al., 2008, Young, 2015), it should be investigated to what extent high moisture content and water absorption are related to the condition of the outer part of the mortar joints and whether a repointing can make a difference. In this context, the relation between the depth of erosion of the mortar joints and the possible increase in water absorption from WDR should be quantified.

Furthermore, the rationality of some of the proposed criteria can be questioned, e.g. concerning acceptable crack width, since it has been shown that water ingress in cementitious materials increases exponentially when the crack width exceeds 0.2 mm (Wang et al., 1997, Aldea et al., 1999).

Eventually, possible benefits and drawbacks of other maintenance techniques rather than repointing

to restore the appearance and technical condition of a facade should be considered as well.

4.4 Alternative maintenance techniques

Cleaning and plant removal techniques can be used to postpone the need of costlier maintenance actions. Furthermore, their implementation may uncover potential hidden defects or problems.

Cleaning techniques can be categorized into three different groups: abrasive cleaning, chemical cleaning and water cleaning. Cleaning dirt, soil, stains and paints is not only a way to restore aesthetics of a facade; it is also a method to maintain the structure and postpone repointing (Mack and Grimmer, 2000). However, if inappropriate cleaning techniques are adopted, damage to the masonry facade may result. Generally, washing gently with low pressure water is a lenient cleaning technique. Application of mechanical or chemical cleaning is not recommended, particularly not in the case of historic façades, since it might damage the masonry surface.

Plant removal can even be considered as an alternative technique to repointing. The presence of biological growths like ivy, lichens, and mosses affect water penetration, water evaporation and drying process. As such, removing these growths will result in a reduced moisture content and potentially eliminate the need for repointing.

Superficial hairline cracks in mortar joints can be repaired by surface grouting. Texture, colour, and properties of the repair grout must be chosen to match the existing mortar. Bricks with larger cracks can be replaced.

High water content in combination with freeze-thaw cycles over the service life of the facade may cause spalling (with the brick face flaking and crumbling) due to the volume increase of water when it is freezing. Damaged bricks should be with new units with similar properties. However, to limit future damages, the root cause of high-water content has to be identified and dealt with appropriately, if possible.

Water-repellent (WR) coating has been considered as a technique to reduce water penetration (Brown, 1982, Coney and Stockbridge, 1988), although there is a debate about its efficiency. In some cases it has been argued that applying water repellents cannot protect the brick-mortar interfacial zone from water ingress (Slapø and AL, 2017).

5 CONCLUSIONS

To reach a rational decision concerning repointing, different methods to measure moisture content and water absorption in clay brick façades were discussed. A systematic review of the available techniques, as presented in this paper, might contribute to improve current recommendations with respect to maintenance of clay brick masonry facades. To sum

up, a rational strategy including following steps can reveal the real need for repointing:

- Preliminary studies prior to conducting costly and time-consuming measurements might clarify whether repointing is needed.
- Measurements of moisture content and water absorption can deliver data for deeper analyses. In selecting the most appropriate measuring technique, the stakeholder should consider the purpose of the measurements and the value of the data.
- Non-destructive, qualitative and inexpensive measurement techniques such as the RILEM tube or the dielectric method may therefore be favourable over more complex ones.
- Criteria available in the literature, can be used, with due engineering judgement, to reach a rational decision on repointing.
- Other maintenance techniques such as removal of microbiological growth or cleaning by water, have the potential to reduce moisture content and water absorption into brick façades, and thus to postpone the need of more fundamental maintenance measures such as repointing.

ACKNOWLEDGMENTS

The authors gratefully acknowledge financial support from SBUF - The Development Fond of the Swedish Construction Trade (grant 13576) and TMPB - The Masonry and Render Construction Association.

REFERENCES

- Aldea, C.-M., Shah, S. P. & Karr, A. 1999. Permeability of cracked concrete. *Materials and structures*, 32, 370–376.
- ASTM 2011. Standard Test Method for Field Determination of Water (Moisture) Content of Soil by the Calcium Carbide Gas Pressure Tester, D4944-18. West Conshohocken, Pennsylvania: American Society for Testing and Materials.
- ASTM 2014. Standard test method for field determination of water penetration of masonry wall surfaces, C1601-14a. West Conshohocken, PA: ASTM International.
- Binda, L., Squarcina, T. & Van Hees, R. 1996. Determination of moisture content in masonry materials. Calibration of some direct methods.
- Bison, P., Cadelano, G., Capineri, L., Capitani, D., Casellato, U., Faroldi, P., Grinzato, P., Ludwig, N., Olmi, R., Priori, S., Proietti, N., Rosina, E., Ruggeri, R., Sansonetti, A., Soroldoni, L. & Valentini, M. 2011. Limits and Advantages of Different Techniques for Testing Moisture Content in Masonry. *Materials Evaluation*, 69, 111–116.
- Blystone, J., Pelzner, A. & Steffens, G. 1962. Moisture content determination by the calcium carbide gas pressure method. *Highway Research Board Bulletin*.
- Brief, B. 2005. Repointing (Tuckpointing) Brick Masonry. *Brick Industry Association*.

- Brief, B. 2017. Maintenance of Brick Masonry. *Brick Industry Association, Technical Notes on Brick Construction*, 46, 1–11.
- Brown, R. H. 1982. Initial effects of clear coatings on water permeance of masonry. *Masonry: Materials, Properties, and Performance*. ASTM International.
- Bruttel, P. & Schlink, R. 2003. Water determination by Karl Fischer titration. *Metrohm monograph*, 8, 50003.
- Camuffo, D. & Bertolin, C. 2012. Towards standardisation of moisture content measurement in cultural heritage materials. *E-Preserv. Sci*, 9, 23–35.
- Coney, W. B. & Stockbridge, J. G. 1988. The effectiveness of waterproofing coatings, surface grouting, and tuck-pointing on a specific project. *Masonry: Materials, Design, Construction, and Maintenance*. ASTM International.
- Crissing, J. 2005. Measuring moisture resistance to wind-driven rain using a RILEM tube. Tech. Rep.
- EMERISDA 2014. Summary report on existing techniques, procedures and criteria for assessment of effectiveness of interventions. TU Delft: Emerisda.
- EN 1993. Wood-based panels – Determination of moisture content, 322. Brussels: European Committee for Standardisation (CEN TC 346).
- Franke, L. & Benstrup, H. 1991. Einfluss von Rissen auf die Schlagregensicherheit von hydrophobiertem Mauerwerk und Prüfung der Hydrophobierbarkeit, Teil 2. *Baustenschutz Bausanierung*, 14, (117–121).
- Fried, A., Tovey, A. & Roberts, J. 2014. *Concrete masonry designer's handbook*, CRC Press.
- Griffin, I. M. 2013. *Deterioration mechanisms of historic cement renders and concrete*. Doctoral dissertation, University of Edinburgh.
- Hola, A. Measuring of the moisture content in brick walls of historical buildings—the overview of methods. IOP Conference Series: Materials Science and Engineering, 2017. IOP Publishing, 012067.
- Hola, J., Matkowski, Z., Schabowicz, K., Sikora, J., Nita, K. & Wójtowicz, S. 2012. Identification of moisture content in brick walls by means of impedance tomography. *COMPTEL: Int J for Computation and Maths. in Electrical and Electronic Eng.*, 31.
- Holland, M. 2012. *Practical Guide to Diagnosing Structural Movement in Buildings*, John Wiley & Sons.
- Larsen, P. K. 2012. Determination of Water Content in Brick Masonry Walls using a Dielectric Probe. *Journal of Architectural Conservation*, 18, 47–62.
- Litti, G., Khoshdel, S., Audenaert, A. & Braet, J. 2015. Hygrothermal performance evaluation of traditional brick masonry in historic buildings. *Energy and Buildings*, 105, 393–411.
- Mack, R. C. & Grimmer, A. E. 2000. Assessing cleaning and water-repellent treatments for historic masonry buildings. *Preservation Update*.
- Maurenbrecher, A. H. P., Trischuk, K., Rousseau, M. Z. & Subercaseaux, M. I. 2008. Repointing mortars for older masonry buildings: design considerations. *Construction Technology Update*; no. 67.
- Möller, U. & Stelzmann, M. 2013. Neue Messmethode zur Bewertung der kapillaren Wasseraufnahme von Fassaden. *wksb*, 69, 62–65.
- Neumann, H.-H., Niermann, M. & Steiger, M. 2014. *Methodenentwicklung zur zerstörungsfreien Prüfung des Wassertransportes für die Planung und zum Bautenschutz in historischem Ziegelmauerwerk bei dem Einsatz von Innenraumdämmungen: Abschlussbericht zu dem DBU-geförderten Vorhaben, Förderkennzeichen: 28751-45*, Universität Hamburg, Fachbereich Chemie, Anorganische und Angewandte Chemie.
- Pel, L., Kopinga, K. & Brocken, H. 1996. Moisture transport in porous building materials. *Heron*, 41, 95–105.
- RILEM, D. Protection of Stone Monuments. Experimental Methods. Test No. II. 4. Water absorption under low pressure (pipe method). International Symposium UNESCO-RILEM Paris, 1978.
- Schöffski, K. S., D. 2006. Karl Fischer Moisture Determination. *Encyclopedia of Analytical Chemistry*.
- Slapo, F. & Al, E. 2017. Masonry's Resistance to Driving Rain: Mortar Water Content and Impregnation. *Buildings*, 7, 70.
- Stelzmann, M., Möller, U. & Plagge, R. 2015. Waterabsorption-measurement instrument for masonry façades. *ETNDT6, Emerging Technologies in Non-Destructive Testing*, 6, 27–29.
- Stockbridge, J. G. 1989. Repointing masonry walls. *APT bulletin*, 21, 10–12.
- Tägil, T., Gustavsson, T., Bergkvist, K. & Staaf, B. M. 2011. *Modernismens tegelfasader (The clay brick facades of the Modernism) in Swedish*, Arkus Publication.
- Tindall, S. M. 1987. Repointing Masonry—Why Repoint? *Old-House Journal*, 24–31.
- Wang, K., Jansen, D. C., Shah, S. P. & Karr, A. F. 1997. Permeability study of cracked concrete. *Cement and concrete research*, 27, 381–393.
- Wolter, B. & Krus, M. 2005. Moisture Measuring with Nuclear Magnetic Resonance (NMR). In: KUPFER, K. (ed.) *Electromagnetic Aquametry: Electromagnetic Wave Interaction with Water and Moist Substances*. Berlin, Heidelberg: Springer Berlin Heidelberg.
- Young, D. Repointing mortar joints: some important points. Australia ICOMOS Conference, 5-8 November 2015 Adelaide Australia.

Paper II





Experimental investigation of water absorption and penetration in clay brick masonry under simulated uniform water spray exposure

Seyedmohammad Kahangi Shahreza^{*}, Jonas Niklewski, Miklós Molnár

Division of Structural Engineering, Department of Building and Environmental Technology, Lund University, John Ericssons Väg 1, SE-223 63, Lund, Sweden

ARTICLE INFO

Keywords:

Clay brick masonry
Wind-driven rain
Water absorption
Dampness
Water penetration
Mortar joint profile

ABSTRACT

In this study, we performed an experimental investigation of water absorption and penetration in clay brick masonry exposed to cyclic water spraying by employing a newly developed test setup. Several parameters, including brick absorption properties and different mortar joint profiles, were investigated. The specimens were exposed to a uniform water spray rate ranging between 1.7 and 3.8 l/m²/h, and water absorption and dampness patches on the non-exposed backside (the protected side) of the specimens monitored continuously. The results indicate that the amount of absorbed water is highly dependent on the water absorption coefficient and absorption capacity of the bricks, whereas the mortar joint profiles do not influence water absorption. The first dampness patches on the specimens' backside appeared in the vicinity of the head joint, and the time until the first patch appeared correlated well with water content levels. Accordingly, the first visible dampness patches appeared on the specimens' backside at water content levels corresponding to 50%–60% of full saturation level. Additionally, the specimens' backside reached 90% dampness at water content levels corresponding to 95% of full saturation level. As a feature attributed to the absence of known defects and zero differential air pressure, no measurable amounts of penetrated water could be collected at the specimens' backside. The newly developed test setup might facilitate verification of moisture simulations and provide a basis for rational decision-making concerning clay brick masonry design and maintenance.

1. Introduction

Clay brick masonry façades are widely used in Nordic countries because of their durability and a lowered need for costly maintenance. Nevertheless, exposure to wind-driven rain (WDR) may cause moisture accumulation and water penetration [1–3], that is, conditions that have the potential to deteriorate both the masonry itself and other wall components in exterior walls [4–6]. WDR might further cause erosion of the joints in clay brick masonry [7,8], thus impairing the aesthetics of façades. Currently, there is a widespread perception among practitioners that eroded mortar joints cause increased water uptake from WDR, a perception that is used as motivation for repointing. Yet, there is a divergence in experts' views on this question [9,10]. Accordingly, studying water absorption and water penetration in clay brick masonry with mortar joint profiles resembling eroded mortar joints might create rational decision support concerning repointing.

Generally, WDR studies can be divided into two categories: i) quantification of WDR deposition on façades, with rain intensity, rain-drop size, wind speed, building geometry, and the topography of the

surrounding terrain as important parameters [11–14]; and ii) the response of façades to WDR impingement in relation to, for example, splashing, bouncing, runoff, differential air pressure, material properties, and presence of cracks and voids [15,16].

During WDR events, the outer surface of masonry façades absorbs parts of the incident rainwater, dependent on the capillary absorption properties of units and mortar, until capillary saturation is attained. Once the exposed surface is saturated, a water film is formed on the exposed surface. When cracks and voids are present, large amounts of water may penetrate through the masonry [17–19]; in such instances, wind pressure is a significant agent that promotes water penetration.

Formation of a water film on the façade surface and subsequent water penetration due to wind pressure is the basis for many established test setups used in experimental studies of WDR penetration in walls [17,20–22]. In the test setups of the earliest studies on water penetration in brick masonry [17,20,22–24], which then became the basis of many of the current testing standards, water was sprayed with the aid of a pipe placed near the upper edge of specimens and the surface of specimens kept covered with a water film. Although various test setups for

^{*} Corresponding author.

E-mail addresses: mohammad.kahangi@kstr.lth.se (S. Kahangi Shahreza), jonas.niklewski@kstr.lth.se (J. Niklewski), miklos.molnar@kstr.lth.se (M. Molnár).

<https://doi.org/10.1016/j.jobe.2021.102583>

Received 10 December 2020; Received in revised form 14 April 2021; Accepted 17 April 2021

Available online 24 April 2021

2352-7102/© 2021 The Author(s). Published by Elsevier Ltd. This is an open access article under the CC BY license (<http://creativecommons.org/licenses/by/4.0/>).

exploring water penetration in masonry have been proposed in different standards and research studies, the applied water spray and air pressure rates represent rather extreme WDR conditions [20,25–34]. For instance, water application rates of 72–138 l/m²/h [25–27,29,31–33,35–37] in combination with differential air pressure levels of 400–1000 Pa [25–27,31,35,38] represent extreme driving rain conditions [22,23], most probably relevant for tall buildings. Hence, several authors have pointed out the need to develop a simple test setup able to operate at considerably lower water application rates [25,28,39–41].

Accordingly, Forghani et al. [37] adjusted the differential air pressure of 500 Pa in the ASTM E514 [31] to 45 Pa. Further, tests with differential air pressure in the range of 0–750 Pa were carried out in studies conducted by Slapoš et al. [26], Anand et al. [29], and Lacasse et al. [42]. In experimental studies carried out by Rathbone [43] and Hens et al. [44], clay brick masonry walls were subjected to water spray rates between 2.0 and 6.4 l/m²/h. Although Rathbone [43] and Hens et al. [44] reduced the water spray rates by 95% in comparison with the ASTM E514 standard [31], still the method to spray water was similar to the one applied in ASTM E514 [31], i.e. concentrated to a line close to the specimens' top aiming to create a water film on the exposed surface.

To overcome shortcomings highlighted with water penetration methods used in ASTM E514 [31], we have developed a new test method for producing a uniform water spray exposure in this study. The test setup is adapted to simulate exposure to a wide range of WDR intensities. The mass gain—that is, the amount of absorbed water by the test specimens—is measured continuously throughout the test, and water penetration through clay brick masonry specimens is studied by employing a digital camera to record when and where visible dampness patches appear and how they spread on specimens' backside. Thus, the present study diverges from existing studies investigating water penetration and dampness on the backside, the protected side, of masonry walls, exposed to extreme conditions [9,25,26,31], facilitating acquisition of information about the moisture conditions and water accumulation in masonry.

The experimental campaign included two series of clay brick masonry specimens, prepared with two different types of bricks and two different mortar joint profiles, namely raked and flush. Raked specimens were used to gain knowledge on how WDR related water absorption and penetration might be affected in eroded mortar joints. Flush profiles were subdivided into standard and after-pointing. After-pointing is a common technique in Nordic countries in which the joints are filled with mortar; then, prior to hardening of the mortar, the outer part is removed; and the day after bricklaying, the remained part is finally filled with mortar and tooled. The tests were conducted at zero differential air pressure, at water spray rates varying between 1.7 and 3.8 l/m²/h, approximately 95% lower than the water application rate specified in current standards and many studies [25,27,29,31,35,37].

2. Materials and methods

2.1. Test setup

In this study, a test setup was designed to expose brick masonry specimens to water spraying, simulating WDR. A uniform and well-distributed water spraying pattern was achieved using a low flow, full cone BETE WL nozzle (WL – 1/4, Full Cone, and 90° Spray Angle), creating a conical spray pattern with droplets, which was placed 55 cm away from the specimens' surface. The schematic of the test setup is shown in Fig. 1. Moreover, two pressure regulators were mounted in series to minimize fluctuations stemming from pressure variations in the urban water supply. An IFM SM4000 electronic magnetic-inductive water flow meter was also used to continuously monitor the output flow for further corrections. The tests were performed with zero differential air pressure between the specimens' exposed side (the front side) and protected side (the backside) with a water application rate varying between 1.7 and 3.8 l/m²/h, representing WDR intensities frequently encountered in Sweden, see Fig. A.1. Significant efforts have been made to reduce the water application rate to the mentioned interval, which indicates that using larger water application rates poses no difficulties.

The tests were carried out with zero differential air pressure because high wind speeds usually occur only for a small percentage of rain duration, whereas in this study, the specimens were subjected to water spraying for 21 h.

Each test lasted 23 h, divided into six cycles, with each cycle consisting of 210 min of watering and 20 min of pausing. The specimens' front face, the exposed side, was carefully centered within the test apparatus to be uniformly covered by water droplets. To this end, first, a sealing tape was applied on the scale plate to avoid any undesired water accumulation under the specimens, and the specimens were then placed on the sealing tape. A DINI ARGEO digital scale 30 kg/2 g was used for continuous logging of the weight of the specimens. Although the weighing of specimens is usually done before and after the test in other studies [26], the possibility to measure it continuously during the test was considered in the modified test setup. Additionally, a digital camera was placed behind the specimens to take photos every 2 min, resulting in time-lapse videos. Hence, the time and location of the first visible dampness patch appearing on the backside of specimens were recorded as well as the spatial distribution and spread of subsequent patches.

2.1.1. Image processing

A GoPro HERO8 Black digital camera with a 12-megapixel sensor recorded the backside of the specimens every 2 min; its position was fixed, and a ColorChecker was placed next to the masonry specimen. The first recorded image was used as a reference image, and each subsequent image was compared with it to detect dampness patches. The image analysis was performed in MATLAB (R2019a) using the following procedure. As slight changes in illumination occurred, the ColorChecker was used for color correction. Any displacement between the two images—owing to, for example, vibrations causing unintended camera

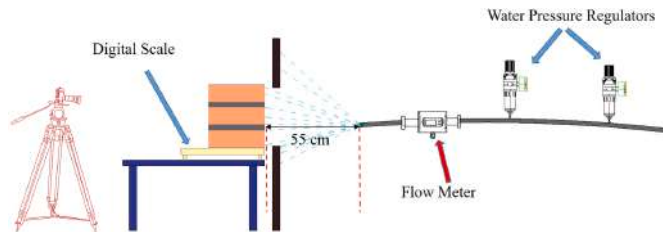


Fig. 1. Schematic of the test setup.

movement—was corrected using image cross-correlation. The difference between each image and the reference image was then calculated as the squared sum of the difference in each color channel (R, G, and B). The resulting image, representing the change in color from the initial state, was then thresholded with a fixed value. Finally, the resulting binary image was subjected to a morphological filter to reduce any residual noise. The relative damp area could then be calculated in each time step as the sum of white pixels divided by the sum of pixels within the area confined by the specimen edges. The algorithm used for the analysis was designed to ignore any patches originating from the specimen boundary, which occurred in some instances.

2.2. Materials

Units and mortars selected in this study are representative of that used in typical Swedish brick masonry façades. Two types of bricks, based on their absorption properties, and two different types of mortars, namely M 2.5 and natural hydraulic lime (NHL) 3.5 mortar, were used in the experimental campaign. The bricks, type Röd Slåt and Röd Marktegel, are Haga red solid clay bricks from Wienerberger AB. Mortar M 2.5 is a cement-based mortar typically used for bricklaying in Northern Europe, whereas NHL 3.5 mortar is recommended for repointing clay brick façades with high and medium suction bricks. Ready-mixed mortars M 2.5 and NHL 3.5 were supplied from Weber Saint-Gobain AB and Målar kalk, respectively.

In the following sections, the water absorption properties of both bricks and mortars are presented.

2.2.1. Bricks

In total, 40 bricks (20 bricks of each kind) were used to determine their initial rate of absorption (IRA) and 24-h water absorption properties. Tests to determine the IRA and water absorption properties of bricks were performed as described in the ASTM C67 standard [45].

The average IRA of type I bricks, amounting to 1.95 kg/m², is 7.7% higher than the average IRA of type II bricks, which amounts to 1.81 kg/m². Therefore, both types of bricks can be classified as medium suction bricks. Nevertheless, the average 24-h water absorption of type I bricks is 86% larger than that of type II bricks (Table 1). The IRA represents the surface absorption rate when the brick just contacts water, whereas the 24-h water absorption represents the amount of water that a brick can absorb when fully immersed in water, here expressed as the ratio between the absorbed water and the initial weight.

Moreover, to determine the water absorption coefficient A_w, 10 bricks from each type were studied. In this regard, the bricks were immersed in water at a depth of 3–5 mm for a specific period of time, as described in the ASTM C1403 – 15 standard [46]. The increase in mass as a result of water absorption was registered after 1, 5, 10, 20, 30, 60, 120, 180, 240, 300, 360, 1440, and 4320 min. The amount of absorbed water per unit area of the brick Q [kg/m²] is defined as the ratio between the difference of increased weight (w_i [kg]) and initial weight (w₀ [kg]) and the cross-sectional area of the brick A [m²] (Eq. (1)).

$$Q = \frac{w_i - w_0}{A} \text{ [kg / m}^2\text{]} \tag{1}$$

Table 1

Density and average water absorption properties, including initial rate of absorption, 24-h absorption, and water absorption coefficient of bricks and mortars.

	Dimensions (mm × mm × mm)	Density ρ (kg/m ³)	Average IRA (kg/m ² /min)	CoV (%)	Average 24-h water absorption (%)	CoV (%)	Average water absorption coefficient A _w (kg/(m ² .s ^{0.5}))	CoV (%)
Bricks I	252 × 120 × 62	1800	1.95	2.3	16.0	1.6	0.193	0.8
Bricks II	252 × 120 × 62	1990	1.81	5.1	8.6	14.5	0.133	16.1
M 2.5	100 × 100 × 100	1869	0.30	19.7	–	–	0.022	19.7
NHL 3.5	100 × 100 × 100	1715	0.80	20.4	–	–	0.159	20.4

To present the results of the tests, Q [kg/m²] is plotted against the square root of time [s^{1/2}] (Fig. 2.a). Eventually, the water absorption coefficient A_w [kg/(m².s^{0.5})] is mathematically defined as the tangent to the initial, linear branch of the Q – t^{1/2} function (Fig. 2.b).

The IRA, 24-h cold-water absorption, and water absorption coefficient of bricks type I and II are summarized in Table 1. For simplicity and according to the IRA test values, in the following sections, brick types I and II are considered medium suction brick [I] and [II], respectively. Although both types of bricks were classified as medium suction bricks according to their IRA value, the difference in the 24-h absorption and water absorption coefficient results is notable.

2.2.2. Mortars

A total of 15, 100 mm-side cubic mortar specimens, 12 M 2.5, and 3 NHL 3.5, were cast to determine the water absorption coefficient of the respective mortar types. The same preconditioning and test method used

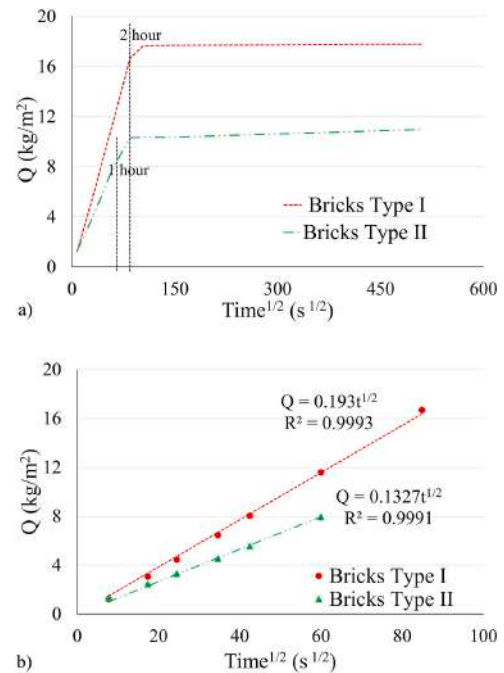


Fig. 2. Plot of water absorption per unit area against the square root of time for 10 masonry brick units from each type (bricks type I & II): a) up to 72 h; and b) during the initial stage of the test.

to determine the water absorption coefficient of the bricks was performed for the cubic mortar specimens, as described in the ASTM C1403 – 15 standard [46]. Fig. 3 shows the water absorption rate of the mortars over the square root of time, and Table 1 summarizes the average results of the IRA and water absorption coefficient properties of two different types of mortar.

2.3. Masonry specimens

This experimental work focused on studying water absorption and penetration in brick masonry specimens as a function of (i) the brick type (medium suction [I], medium suction [II]), and (ii) the mortar joint profile finish (flush, raked, after-pointed). A total of 39 triplet masonry specimens were built from the same batch of brick. The specimens were intended to be representative of a masonry veneer wall. The sample size is limited to three bricks in order to facilitate manual handling without damaging either the specimens or the operator. A similar choice was made by Ritchie [20], who studied water penetration in brick masonry by using specimens consisting of five bricks yet without any head joints. As shown in Fig. 4, the masonry specimens consisted of three courses of brick, with the length of one brick and the depth of half brick. The thickness of the bed joints varied between 13 and 18 mm to achieve a fixed height of 215 ± 3 mm for all specimens. The length and depth of the specimens were 250 ± 5 mm and 120 ± 2 mm, respectively.

The specimens are divided into two series based on the brick types (Table 2). Series I, which included 15 specimens, was built with bricks type I (medium suction bricks [I]), whereas Series II comprised 24 specimens built with bricks type II (medium suction bricks [II]).

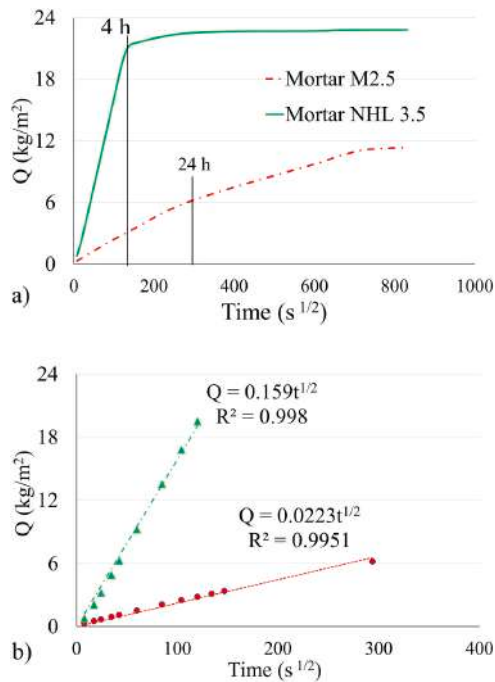


Fig. 3. Average absorption of mortar M 2.5 and NHL 3.5: a) up to 8 days; and b) during the initial stage of the test.

Additionally, specimens within each series were divided into three groups, namely G1, G2, and G3, according to the mortar joint finish (Table 2). Group G1 comprises specimens pointed with mortar M 2.5 and tooled to have a flush joint profile. Specimens with a 5 mm raked joint pointing with mortar M 2.5 belong to group G2. Group G3 is also made up of specimens with mortar M 2.5, but compared with G1, the outer 6 mm of the mortar joint was pointed one day after bricklaying with mortar NHL 3.5 and tooled to flush joint profile. A schematic of the prepared specimens and joint profile finishes is shown in Fig. 4.

The specimens are named according to the notation X-Y-Z, where X, Y, and Z correspond to the brick type (I = medium suction [I], II = medium suction [II]), mortar joint profile finishes (F = flush, R = raked, and AF = after-pointed), and specimen number, respectively. For example, specimen I-R-2 belongs to Series I, was built with medium suction bricks [I], with a 5 mm raked joint, and it is the second specimen of group G2.

Before bricklaying, all bricks were stored for three weeks in a laboratory with a controlled indoor climate ($18\text{--}20$ °C and 30–35% RH). To follow the recommendations of the brick manufacturer, the specimens were prepared without pre-wetting of the bricks before bricklaying. Each mortar mix was prepared with the same amount of water. Specimens of group G1, with mortar M 2.5, were tooled professionally to have a flush profile. For specimens with the raked joint profile, group G2, the specimens were pointed with mortar M 2.5, and then a 5 mm screw was used to remove extra mortar to reach the depth of 5 mm. For specimens prepared with the after-pointing technique, the excess mortar was removed using a 6 mm screw, and the following day, the 6 mm gap was filled with NHL 3.5 and tooled to have a flush joint profile. Finally, all specimens were cured for 28 days by daily wetting and storage under plastic sheets.

Testing took place three months after the bricklaying. Prior to testing, the specimens were stored in a climate room for two months at a temperature of 20 °C and relative humidity of 60%. All sides of the specimens, except front and back sides, were sealed to avoid any undesirable water absorption/evaporation through the top, bottom, and lateral sides. A two-component sealant composed of a base component and activator component, typically used for waterproofing applications, was employed.

2.4. Testing regime

As shown in Table 2, specimens in groups G1, G2, and G3 of Series I were exposed to an average water spraying rate of 3.6, 3.6, and 3.4 $\text{l}/\text{m}^2/\text{h}$, respectively. Specimens of group G1 of Series II are divided into two groups, G1-a and G1-b, based on the average water application rate. In this regard, the average water spraying rate for groups G1-a, G1-b, G2, and G3 of Series II was 3.2, 2.0, 2.3, and 2.0 $\text{l}/\text{m}^2/\text{h}$, respectively.

3. Results

3.1. Water absorption time response

The average amount of absorbed water Q (kg/m^2) for all groups in Series I and II during 23 h of testing is presented in Fig. 5a and Fig. 5b. In order to better compare the water spraying tests and the water absorption tests for bricks and mortars (Figs. 2 and 3), Q is plotted against the square root of time ($t^{1/2}$). It should further be kept in mind that the specimens in Series I and Series II Group G1-a were exposed to a more intensive spray rate (3.0–3.8 $\text{l}/\text{m}^2/\text{h}$) than the specimens in Series II Group G1-b, G2, and G3 (1.7–2.6 $\text{l}/\text{m}^2/\text{h}$).

As shown in Fig. 5a, the absorption behavior of Series II group G1-a is similar to those of Series I during the first cycle, indicating that most of the sprayed water was absorbed, no matter what the absorption properties of bricks were. Similarly, the absorption behavior of group G1-b, G2, G3 during the first cycle is similar to each other (Fig. 5.b), indicating that in this case, the water spray rate is the governing agent influencing

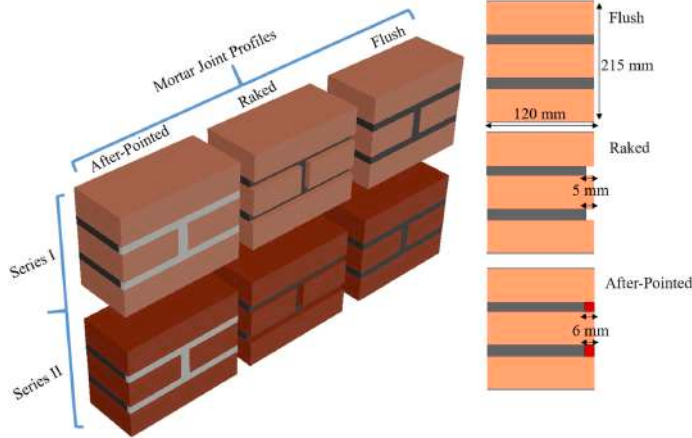


Fig. 4. Schematic of the specimens and mortar joint profile finishes.

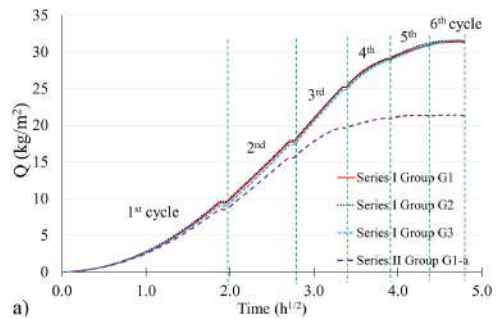
Table 2
Specimen designation and configurations.

Group	Brick	Mortar	Joint profile finishes	No. of specimens	Water spray rate (L/m ² /h)
Series I (250 mm × 215 mm × 120 mm)	G1	Medium	M 2.5 Flush	5	3.6
	G2	Suction	M 2.5 Raked	5	3.6
	G3	Type (I)	M 2.5/ NHL After-pointed	5	3.4
Series II (250 mm × 215 mm × 120 mm)	G1-a	Medium	M 2.5 Flush	5	3.2
	G1-b	Suction	M 2.5 Flush	3	2.0
	G2	Type (II)	M 2.5 Raked	8	2.3
	G3	M 2.5/ NHL After-pointed	8	2.0	

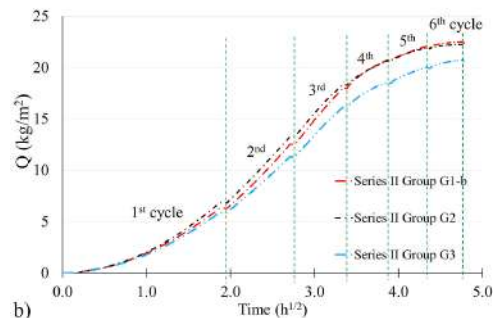
the amount of absorbed water. Accordingly, the slight difference in the amount of absorption after the 1st cycle is due to the difference in the water spray rate; Series II group G2 was exposed to a higher water spray rate in comparison with group G1-b and G3.

After performing the 1st cycle, the absorption response versus the square root of time became linear. The linearity of the $Q - t^{1/2}$ relationship indicates that the capacity of the specimens to absorb water was in balance with the water supplied to the surface. Subsequently, once surface saturation occurred, the absorption behavior against the square root of time became nonlinear. Surface saturation was attained at the end of the 3rd cycle for all groups of Series I and II, except Series II group G1-a in which the absorption curve became nonlinear at the end of the 2nd cycle. It can be seen that surface saturation was attained more quickly in group G1-a of Series II, exposed to a water spray rate close to those of all groups within Series I, indicating that a higher water absorption coefficient allows rapid moisture transport and postpones saturation of the exposed masonry surface layer, as stated by Van Den Bossche et al. [41].

Moreover, it can be seen that for the specimens in Series I, absorption continues until the middle of the sixth cycle. From the middle of the sixth cycle (21 h after starting the test), roughly no water is absorbed in



a)



b)

Fig. 5. Average water absorption vs. square root of time response of a) Series I and Series II group G1-a; b) Series II group G1-b, G2, and G3.

the specimens, indicating that they are close to full saturation. At the same time, for specimens of group G1-a in Series II, saturation took place at the beginning of the fifth cycle, indicated by the slope of the $Q - t^{1/2}$ curve becoming close to zero (i.e., nearly no water accumulation in the

specimens) during the remainder of the test. In contrast, for specimens of groups G1-b, G2, and G3 of Series II, the absorption did not end, indicating that the specimens did not attain full saturation, a fact mainly attributed to the relatively low water spray rate. Since saturation of the mortar used in the joint takes more than 23 h, see Fig. 3.a, it seems reasonable that neither Series I nor Series II achieve full saturation during the 23 h long water spraying tests.

For each specimen, the water application rate and water absorption after the first and the sixth cycle are summarized in Table 3. Results indicate that the water absorption in the first cycle is dependent on the water spray rate. For instance, in Series II, the lowest average water absorption, amounting to 5.9 kg/m², is exhibited by group G3, exposed to the lowest average water application rate of 2.0 l/m²/h. Similarly, group G1-a, which was exposed to the highest average water application rate of 3.2 l/m²/h, has the highest average water absorption of 8.5 kg/m² in Series II. Fig. 6 shows the water absorption in each specimen after the first cycle as a function of the corresponding water application rate V₀ (l/m²/h). As surface saturation was not attained in the first cycle and the specimens absorbed most of the sprayed water, there is a nearly linear relationship between water application rate and water absorption. Furthermore, from Fig. 6 it can be observed that the rate of water absorption decreases with increasing water application rate, which indicates that bounce off increases with increasing water application rates, as already noted by Van Den Bossche et al. [41] and Abuku et al. [47].

Eventually, as the test progressed and the surface of the specimens became saturated, the results indicate that the water absorption was decreasingly influenced by the water application rate. Consequently, the amount of absorbed water at the end of the test is mostly correlated to

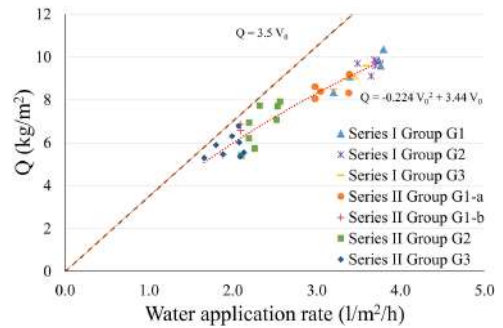


Fig. 6. Water absorption in the first cycle vs. water application rate, V₀.

the absorption capacity of the masonry. Accordingly, for Series I, it can be observed that after the sixth cycle, there is a negligible difference in the average water absorption between groups G1, G2, and G3, as the average water absorption for all three groups is approximately equal to 31.5 kg/m². In contrast, in Series II, the average water absorption varies between 20.6 and 22.4 kg/m², mainly attributed to a higher variability in the water absorption capacity of these bricks, 14.5%, versus 1.6% for Series I bricks.

Fig. 7 shows the average amount of absorbed water after each cycle

Table 3
Water absorption of tested specimens after the first and sixth cycle.

	Specimens	Initial Weight (g)	Water spray rate (l/m ² /h)	Average l/m ² /h	First cycle Absorp. (kg/m ²)	Average (kg/m ²)	Total Absorp. (kg/m ²)	Average (kg/m ²)	CoV (%)
Series I Group G1	I-F-1	11700	3.8	3.6	10.4	9.4	31.6	31.3	0.6
	I-F-2	11722	3.8		9.6		31.1		
	I-F-3	11434	3.7		9.8		31.2		
	I-F-4	11656	3.2		8.4		31.4		
	I-F-5	11694	3.4		9.1		31.3		
Series I Group G2	I-R-1	11672	3.7	3.6	9.6	9.6	31.4	31.5	0.3
	I-R-2	11586	3.7		9.8		31.5		
	I-R-3	11622	3.6		9.1		31.3		
	I-R-4	11588	3.5		9.7		31.7		
	I-R-5	11668	3.7		9.9		31.4		
Series I Group G3	I-AF-1	11756	3.6	3.4	9.6	9.0	31.6	31.5	0.2
	I-AF-2	11598	3.4		9.1		31.6		
	I-AF-3	11552	3.5		9.0		31.4		
	I-AF-4	11634	3.3		9.0		31.5		
	I-AF-5	11738	3.2		8.5		31.5		
Series II Group G1-a	II-F-1	12664	3.4	3.2	9.2	8.5	21.5	21.2	10.4
	II-F-2	12623	3.4		8.3		18.3		
	II-F-3	12591	3.0		8.4		23.2		
	II-F-4	12684	3.0		8.6		24.0		
	II-F-5	12468	3.0		8.1		19.2		
Series II Group G1-b	II-F-6	12684	1.9	2.0	5.4	6.3	21.3	22.4	6.3
	II-F-7	12637	2.1		6.9		24.4		
	II-F-8	12669	2.1		6.6		21.5		
	II-R-1	12762	2.1		5.4		24.0		
	II-R-2	12575	2.5		7.1		20.1		
Series II Group G2	II-R-3	12628	2.5	2.3	7.7	6.8	22.3	22.2	6.0
	II-R-4	12762	2.6		7.9		21.3		
	II-R-5	12624	2.3		7.7		24.0		
	II-R-6	12649	2.2		6.9		22.6		
	II-R-7	12609	2.2		6.2		20.9		
	II-R-8	12665	2.3		5.7		22.3		
	II-AF-1	12598	1.9		5.5		20.6		
	II-AF-2	12995	2.1		5.5		20.4		
Series II Group G3	II-AF-3	12697	2.1	2.0	6.0	5.9	19.6	20.6	5.6
	II-AF-4	12669	2.1		6.8		21.1		
	II-AF-5	12712	2.0		6.3		20.4		
	II-AF-6	12599	2.1		5.4		19.7		
	II-AF-7	12745	1.8		5.9		23.4		
	II-AF-8	12669	1.7		5.3		19.6		

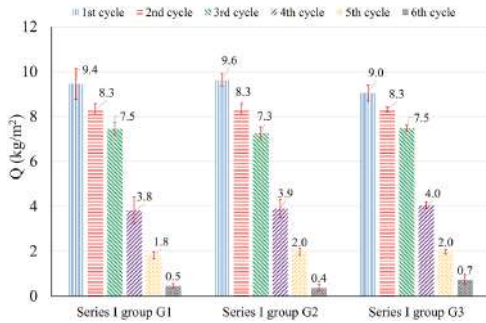


Fig. 7. Effects of the joint finishes (G1, G2, and G3) on the average water absorption in Series I.

for each group of Series I. The average water absorption after each cycle is of similar magnitude, irrespectively, of the mortar profile finish, as shown in Fig. 7. This indicates that mortar joint profile finishes have a negligible effect on water absorption.

3.2. Dampness patches

Since no water runoff that could be collected from the backside of the specimens was observed during the tests, only dampness on the backside of the specimens is reported. As mentioned in Section 2.1.1, a digital camera taking photos every second minute was employed to monitor the specimens' backside. The images were post-processed to identify the time and location of the first dampness patch and used to trace the spread of dampness until the end of the test. Fig. 8 shows the relative location of the first dampness patch in the x and y directions projected on the image of a single specimen to visualize the geometry. The exact geometry and location of the head joint were subject to some variation between specimens, which explains the scatter in the x-direction.

The high concentration of points around the head joint (position $w/2$) shows that the first visible dampness patch consistently appeared on the bricks in the second course, close to the head joint.

The appearance of the first visible dampness patch in the vicinity of

the head joint could be related to the poor compaction of the head joint, difficulty in filling the head joint adequately [17], and open brick-mortar interfaces [25].

The first dampness patch appeared on the bricks in the second course, close to the brick-mortar interface zone, and then typically spread on the entire second course, including the head joint, see Fig. 9. Appearance of the first dampness patches in the vicinity of the head joint indicates that besides capillary transport through the pore system of the bricks, moisture might have also been transported by a system of gaps at the brick-head joint interface [25]. Subsequently, the bottommost course became damp. The dampness eventually spread to the uppermost course until the entire protected side of the specimen became damp.

The time to appearance of the first visible dampness patch on the backside of specimens is summarized in Table 4. The first dampness patch appeared after 7.8–8.0 h in Series I and 4.8–6.4 h in Series II. The time to the appearance of the first visible dampness patch on the backside of the specimens and the corresponding water application rate is shown in Fig. 10.

As shown in Fig. 10, a higher water application rate corresponds to a shorter time to the appearance of the first visible dampness patch on the protected side of the specimens. Furthermore, time to the appearance of the first visible dampness patch is not only dependent on the water application rate but also is influenced by the specimens' water absorption properties. Accordingly, when specimens are exposed to similar water spray rates, the time to the appearance of the first visible dampness patch is longer for specimens with high water absorption capacity (Series I, made of bricks with an average absorption capacity of 16%) than for specimens with medium water absorption capacity (Series II, group G1-a, made of bricks with an average water absorption capacity of 8.6%). Higher water absorption capacity seems to delay the time to appearance of dampness patches on the protected side.

The time to achieving 90% of the specimens' backside covered with dampness patches is reported in Table 4. The average time to reach 90% dampness coverage on the backside of specimens was 16.0, 16.3, and 16.8 h for groups G1, G2, and G3 of Series I, respectively. For groups G1-a, G1-b, G2, and G3 of Series II, it took 12.5, 16.5, 15.3, and 17.2 h, respectively. Thus, the water application rate affected not only the time to the appearance of the first visible dampness patch but also the time to reach 90% of dampness on the specimens' backside.

Besides the water application rate, the appearance of dampness patches is also influenced by the water content in the specimens. As shown in Fig. 11.a, the first dampness patch appeared at a water

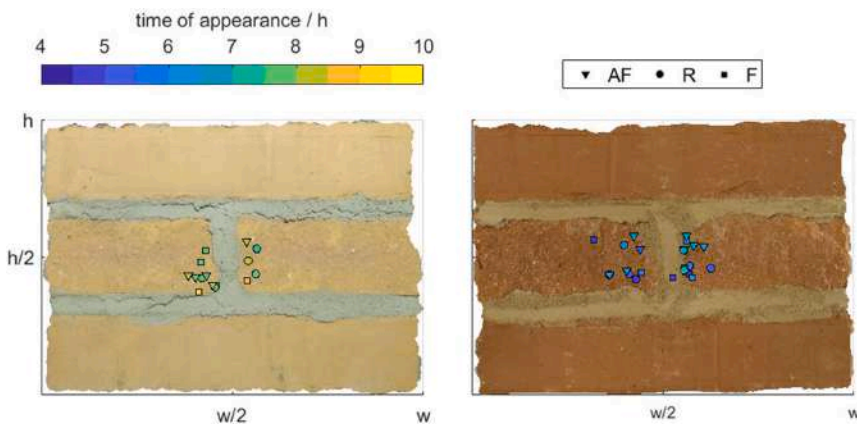


Fig. 8. Location of the first visible dampness patch on the backside of the specimens: a) Series I; and b) Series II.

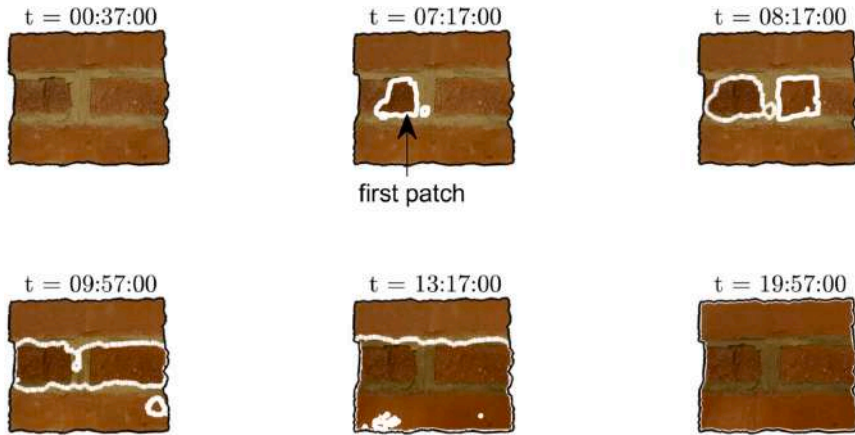


Fig. 9. Dampness appearance and growth on the backside of specimen II-F-6 at different time intervals.

Table 4

Time to the first dampness patch and to 90% of dampness on the backside of specimens and their corresponding water absorption.

	Specimen	time to the 1st (h)	Average (h)	Absorption (kg/m ²)	Average (kg/m ²)	time to reach 90% (h)	Average (h)	Absorption (kg/m ²)	Average (kg/m ²)
Series I Group G1	I-F-1	7.6	7.9	18.6	18.6	15.9	16.0	29.9	29.6
	I-F-2	7.1		17.7		16.5		29.7	
	I-F-3	7.5		18.1		15.7		29.4	
	I-F-4	9.1		20.0		15.5		29.6	
	I-F-5	8.4		18.3		16.5		29.6	
Series I Group G2	I-R-1	7.6	7.8	18.1	18.3	15.8	16.3	29.8	29.9
	I-R-2	7.8		18.4		16.5		30.0	
	I-R-3	7.5		17.6		15.9		29.7	
	I-R-4	8.2		19.0		16.4		30.0	
	I-R-5	7.9		18.3		16.7		29.8	
Series I Group G3	I-AF-1	7.9	8.0	18.7	18.3	15.9	16.9	29.8	30.0
	I-AF-2	8.1		18.4		17.1		30.0	
	I-AF-3	7.9		17.9		16.8		29.9	
	I-AF-4	8.1		18.5		17.1		30.1	
	I-AF-5	8.2		18.2		17.4		30.0	
Series II Group G1-a	II-F-1	4.3	4.8	10.4	10.7	12.4	12.5	20.6	20.2
	II-F-2	4.6		9.9		11.7		17.5	
	II-F-3	4.8		10.6		12.9		21.8	
	II-F-4	5.6		12.7		13.6		22.7	
	II-F-5	4.7		9.8		12.1		18.6	
Series II Group G1-b	II-F-6	6.4	6.3	9.7	10.8	18.4	16.5	20.6	21.1
	II-F-7	6.1		11.3		15.5		22.4	
	II-F-8	6.5		11.3		15.6		20.3	
Series II Group G2	II-R-1	6.7	5.9	10.9	10.7	16.3	15.3	22.6	20.8
	II-R-2	4.5		8.5		14.2		19.0	
	II-R-3	5.4		11.3		14.0		21.2	
	II-R-4	5.5		11.4		14.0		20.0	
	II-R-5	5.7		11.5		15.0		22.1	
	II-R-6	5.5		10.2		14.9		20.8	
	II-R-7	6.3		10.3		16.7		19.5	
	II-R-8	7.2		11.8		17.6		21.0	
Series II Group G3	II-AF-1	6.8	6.4	10.3	10.3	16.5	17.2	19.5	19.8
	II-AF-2	6.7		10.4		17.7		19.2	
	II-AF-3	6.9		11.1		16.4		19.0	
	II-AF-4	5.4		9.7		16.2		20.1	
	II-AF-5	6.6		10.9		17.8		18.8	
	II-AF-6	6.1		9.0		18.9		22.8	
	II-AF-7	6.2		10.7		16.9		19.1	
	II-AF-8	6.7		10.2		17.1		19.6	

absorption of 18.3–18.6 kg/m² and 10.3–10.8 kg/m² in the specimens of Series I and II, respectively. The difference in the amount of absorbed water within the same Series is rather limited, indicating that the mortar

joint finish has a limited effect on the time to the apparition of the first dampness patch.

The registered water absorption levels correspond to 58% and 49%

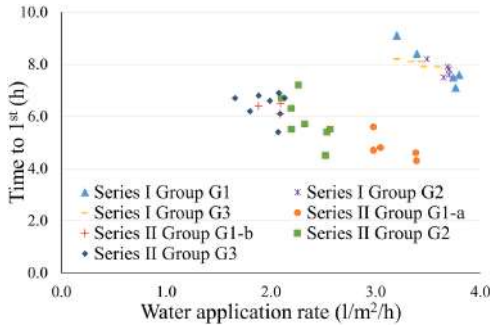


Fig. 10. Water application rate vs. time to the appearance of the first dampness patch.

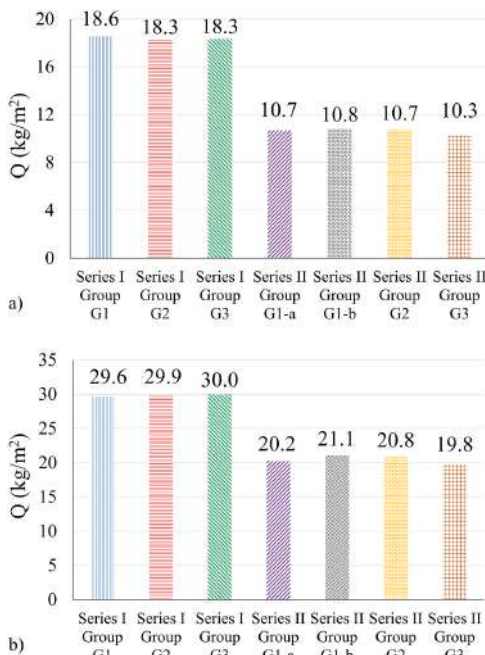


Fig. 11. Corresponding average water absorption: a) when the first dampness appeared on the backside of specimens; and b) when the specimens' backside became 90% damp.

of the final water content of Series I and II, respectively. The registered difference might be related to a more permeable contact zone in the head joints of the specimens prepared with bricks with lower water absorption coefficient and lower water absorption capacity. Similar to the appearance of the first visible dampness patch, the time to reach 90% dampness area on the backside of the specimens was roughly the same within each Series. Accordingly, the corresponding average water absorption was approximately 29.6–30.0 kg/m² for Series I and varied

between 19.8 kg/m² and 21.1 kg/m² for Series II, as shown in Fig. 11. b.

4. Discussion

4.1. Influence of test parameters

4.1.1. Water absorption

Experimental results indicate that a large proportion of the water applied on the surface of the specimens during the first cycle, namely 76%–92%, was absorbed by the specimens. As shown in Fig. 6, in the first cycle, there is a nearly linear relationship between the water application rate and absorption. The remainder of the applied water spray, namely 8%–23%, is considered to have bounced off from the specimens' surface.

This conclusion is supported by visual observations carried out during the test, indicating the absence of runoff during the first test cycles. The plausibility of this conclusion is also underpinned by the fact that the amount of bounce off increased with increasing spraying rate, which can be observed by comparing group G1-a and G1-b of Series II, where the specimens have the same material and mortar joint finish characteristics. The specimens in group G1-a, exposed to a water spray rate of 3.2 l/m²/h, accumulated 8.5 kg/m² water during the first cycle, corresponding to a bounce off of around 24%, see Table 3. In comparison, the specimens in group G1-b, exposed to a water spray rate of 2.0 l/m²/h, accumulated 6.3 kg/m² water during the same cycle, corresponding to a bounce off of nearly 10%. These findings indicate, that increasing WDR intensities increase the percentage of bounce off, a phenomenon described by Van Den Bossche et al. [41] and Abuku et al. [47].

As mentioned in Section 3.1, the linear relationship between the amount of absorbed water and the square root of time during the 2nd and the 3rd cycle indicated that the amount of absorption is in good agreement with the absorption behavior of the bricks. For instance, the slope of the $Q - t^{1/2}$ curve in the 2nd and the 3rd cycle for specimens of Series I is approximately equal to 0.192 kg/(m².s^{0.5}), showing the influence of the water absorption coefficient of the bricks. The mortar joint finish does not seem to have a discernible effect on the absorption behavior of the masonry specimens.

Moreover, based on the available results, first, the impact of joint profile finishes on water absorption of masonry is negligible, particularly after long exposure to driving rain. Second, when surface saturation is attained, the water application rate is less significant.

4.1.2. Dampness patches

As mentioned in Section 3.2, the first visible dampness appeared on the bricks in the second course, in the vicinity of the head joint. This indicates that the primary path for water to penetrate a brick masonry wall is passing through the brick-mortar interfacial zone [25,48]. The location of the first dampness patch in the vicinity of the head joints might be explained by deficient contact between mortar and bricks or the presence of voids, often attributed to practical difficulties during bricklaying. In the present study, the specimens were built by pushing the head joint, while the recommended technique is to butter the end of bricks prior to laying to ensure optimal filling of the head joints [19,26]. Jonell and Moller [17] suggest that it is practically difficult to get the vertical joint completely filled with pushing technique; thus, unfilled joints are the primary path for water penetration in brick walls. Slapø et al. [26] found that buttering the bricks can significantly improve the masonry quality. This highlights the importance of good workmanship to control water penetration in masonry walls [9,17,19,26].

According to Table 4, the first visible dampness patch in the Series I specimens appeared at the end of the second and the beginning of the third exposure cycle. In contrast, for specimens of Series II, group G1-b to G3, the first dampness patch was already observed during the second exposure cycle, that is, approximately 90 min earlier than in the specimens of Series I.

For all groups, except group G1-a of Series II, the dampness area reached 90% on the specimens' backside during the fifth cycle. For group G1 of Series II, 90% of dampness was observed on the specimens' backside during the fourth cycle.

Based on the available results, the impact of joint profile finishes on the appearance of the first dampness patch on the specimens' backside is negligible, particularly after long exposure to driving rain. Hence, the present findings do not support the results presented by Hines and Mehta [9], namely that joint profile finishes substantially influence water penetration in masonry walls. This difference in results might be explained by the fact that, in their study [9], a considerably higher water exposure rate was used in combination with high differential air pressure.

4.2. Time to attain surface saturation

The time to reach surface saturation for a masonry façade when exposed to driving rain is dependent on both the sorptivity of the masonry and the WDR intensity, as shown by Hall and Kalimeris [49]. According to the Sharp Front (SF) model [50], the time to attain surface saturation, t_s [h], is given by Eq. (2)

$$t_s = 0.5 \frac{60 \times S^2}{V_0^2} \tag{2}$$

where S is the sorptivity [mm/min^{0.5}], and V_0 is the driving rain intensity [mm/h]. The sorptivity is calculated as the ratio between the water absorption coefficient, A_w [kg/(m².s^{0.5})], and the density [kg/m³] of water.

In the present study, the average time to reach surface saturation, t_s , for both bricks and mortars are summarized in Table 5. It should be noted that for Series I and Series II group G1-a, around 23% of the applied water is considered to have been bounced off. The corresponding bounced off for Series II, except group G1-a, is considered to be around 11%. It can be seen that the theoretical time to attain surface saturation of bricks, t_s , varied between 8.7 h–9.8 h for Series I, whereas, for Series II, it ranged from 5.2 h to 10.0 h. It must be observed that the average water spray rate varied between 2.0 and 3.6 mm/h. While the time to surface saturation of the bricks generally varies between 5 and 10 h, the time to attain surface saturation for mortar M 2.5 is only

around 0.1 h and 0.3 h. In the case of mortar NHL 3.5, the time to surface saturation varies between 6.6 and 14.4 h, though this calculation is valid only if the joint was fully filled with mortar NHL 3.5, while it is not the case in the specimens of group G3, which were filled with 114 mm of mortar M 2.5 and 6 mm of mortar NHL 3.5. As the surface of the joints manufactured with mortar M 2.5 became saturated earlier, the water running off from the joints was probably absorbed by the bricks. Consequently, the actual time to attain surface saturation for bricks during testing might have happened earlier than indicated by t_s .

Fig. 12 shows the average water absorption versus time response for all groups in Series I and II during 23 h of testing. The linear branch in the first cycles shows that the specimens absorbed a large part of the sprayed water. As the test progressed, the water absorption curve became nonlinear, indicating runoff due to saturation of the exposed surface. Therefore, according to Fig. 12, the time when the absorption curve became nonlinear can be considered as the time to surface saturation. This time is denoted t_{exp} as summarized in Table 5. It can be seen that the absorption behavior became nonlinear roughly at the end of the 3rd cycle for all groups within Series I and II except group G1-a in Series II. For group G1-a in Series II, the absorption curve against time became

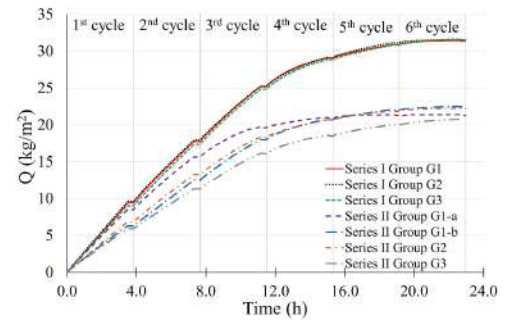


Fig. 12. Average water absorption time response.

Table 5
Average time to attain surface saturation and the corresponding amount of absorbed water. t_s – time calculated with Eq. (2); t_{exp} – time estimated using Fig. 12.

		Sorptivity (mm/min ^{0.5})	Water spray rate (mm/h)	Time to surface saturation t_s (h)	Q_s at the time of surface saturation (kg/m ²)	Q_{exp} at the time of surface saturation t_{exp} (kg/m ²)	Time to surface saturation t_{exp} (h)
Series I Group G1	Brick type I	1.49	3.6	8.7	24.2	21.7	10.0
	Mortar M 2.5	0.17	0.1	0.1	0.3		
Series I Group G2	Brick type I	1.49	3.6	8.7	24.2	21.8	10.0
	Mortar M 2.5	0.17	0.1	0.1	0.3		
Series I Group G3	Brick type I	1.49	3.4	9.8	25.6	23.5	10.0
	Mortar NHL 3.5	1.23	0.3	6.6	–		
Series II Group G1-a	Brick type II	1.03	3.2	5.2	12.9	12.4	6.5
	Mortar M 2.5	0.17	0.1	0.1	0.4		
Series II Group G1-b	Brick type II	1.03	2.0	10.0	17.8	17.4	10.0
	Mortar M 2.5	0.17	0.3	0.3	0.5		
Series II Group G2	Brick type II	1.03	2.3	7.6	15.5	14.3	8.5
	Mortar M 2.5	0.17	0.2	0.2	0.4		
Series II Group G3	Brick type II	1.03	2.0	10.0	17.8	15.7	10.0
	Mortar NHL 3.5	1.23	0.3	14.4	–		

nonlinear at the end of the 2nd cycle.

The amount of absorbed water Q_i (kg/m^2) at the time when the surface saturation was attained is summarized in Table 5. Q_i is defined as the product of the water spray rate and the time to reach surface saturation of the bricks, t_s , taking into account the already mentioned percentage of the bounce off. Q_{exp} represents the amount of absorbed water at t_s taken from Fig. 12. It should be noted that the 20 min pausing between each cycle was deducted and not considered in the calculations of Q_i and Q_{exp} . Comparing Q_i and Q_{exp} (Table 5), corresponding to theoretical and experimental water absorption at the time of attaining surface saturation, respectively, a reasonable accordance can be seen. The differences between theoretically and experimentally determined data might be related to a) bricks might have different sorptivity properties in different directions, mentioned as anisotropy in sorptivity [50, 51]; and b) Q_i has been calculated based on the sorptivity of the bricks, whereas the experimentally determined Q_{exp} represents the amount of water absorbed by the masonry.

4.3. Test setup

In this study, three main criteria were considered to develop the test setup: 1) the sprayed water on the specimens' surface should be distributed uniformly on the exposed surface; 2) the sprayed water should consist of water drops, a representative for rainfall, and not mist or drizzle; and 3) the water application rate should be lowered in comparison with the test conditions of ASTM E514 [31] to be more representative of a wide range of WDR events. To achieve a uniform spray pattern covering the whole area of the exposed face, a full cone nozzle was used. Furthermore, many trials were done to find a suitable water pressure level and distance between the nozzle and the specimen, finally arriving at the test parameters presented in Fig. 1. It must be mentioned that the chosen combination of test parameters is only one out of many possible combinations.

The capability of different nozzle types to produce a water spray consisting of droplets was examined visually and by exposing sheets of paper with high absorption capacity for the water spray during approximately 1–2 s. The result of such a test is shown in Fig. 13, where the wet dots are attributed to water droplets.

To meet the third criterion, different low-flow nozzles have been tested. The largest difficulty consisted in combining low flow levels with a water spray consisting of droplets since this, in many cases, required operation of the nozzles below the pressure range specified by the supplier. When choosing water spray rates to be used in the tests, weather data and WDR intensities for three different locations in Sweden, a region with moderate WDR events, were analyzed; the details are provided in Appendix A.

Notably, continuous water absorption measurement provides



Fig. 13. Wet dots on a paper sheet exposed to water spray for 1–2 s.

valuable information about moisture conditions in the specimens. As during short-duration rainfalls or initial phases of rainfall events similar to the first and second cycles of the performed tests in this study, dampness patches usually do not appear on the backside of masonry walls, monitoring water absorption is a suitable measure to characterize the response of masonry exposed to WDR. Furthermore, results from water absorption measurements, combined with data on water penetration and appearance of dampness areas on the backside of masonry, can be beneficial for subsequent modeling of moisture conditions in masonry.

Nevertheless, the results suggest that for a more realistic investigation of masonry façade's response to WDR exposure, the conditions in the newly developed test setup need to be revised as no water penetration that could be collected from the backside of specimens was observed, in spite of 21 h of exposure of water spraying.

Notably, this study has addressed the question of the effects of mortar joint profile finishes on water absorption and water penetration in masonry exposed to water spraying, yet without any differential air pressure. As the specimens were prepared without known defects, the results of this study cannot be taken as representative of the response of masonry façades with cracks and voids, especially when these are exposed to WDR with high wind pressure. Thus, it is anticipated that the test setup can be developed to encompass studies of the WDR response of specimens with defects exposed to significant differential air pressure.

5. Conclusions

In this study, we investigated the response of clay brick masonry exposed to uniform water spray with application rates of $1.7\text{--}3.81\text{ m}^2/\text{h}$ at zero differential air pressure on triplet specimens, with dimensions 250 mm (length) \times 215 mm (height) \times 120 mm (depth), in laboratory conditions. The mass gain in the specimens was continuously measured, and the specimens' backside was photographed every second minute to trace dampness areas. Based on these results, the following conclusions can be drawn:

1. The amount of absorbed water is highly dependent on not only the water absorption coefficient and absorption capacity of the bricks but also the water spray rate, whereas the mortar joint profile finish had limited influence on the amount of absorbed water.
2. The first dampness patches on the specimens' backside appear in the vicinity of the head joint, at water content levels corresponding to 50%–60% of full saturation level. This corresponds to 5–8 h of exposure at the actual water spray rates.
3. The specimens' backside reached 90% dampness at water content levels corresponding to 95% of full saturation level.
4. As a feature attributed to the actual, relatively low, water application rates, absence of known defects and zero differential air pressure, no measurable amounts of penetrated water could be collected at the specimens' backside.
5. The newly developed test setup might facilitate the verification of moisture simulations as it enables continuous water absorption measurement combined with tracing of dampness areas on the backside of masonry specimens.
6. Time-lapse image analysis could provide useful information in the context of masonry characterization under conditions with indiscernible WDR penetration.

Further improvement of the test setup by application of a differential air pressure in conjunction with water spraying will create conditions that can more realistically reproduce wind-driven rain. Further studies with specimens containing known defects, e.g., cracks or incompletely filled joints, might produce more conclusive results that could support decision-making in practical situations.

Author statement

Seyedmohammad Kahangi Shahreza: Methodology, Validation, Visualization, Writing – Original Draft, Data Curation, Formal Analysis, Investigation **Jonas Niklewski:** Validation, Visualization, Writing – Review and Editing, Supervision, Investigation **Miklós Molnár:** Conceptualization, Supervision, Writing – Review and Editing, Project Administration, Funding acquisition.

Declaration of competing interest

The authors declare that they have no known competing financial

interests or personal relationships that could have appeared to influence the work reported in this paper.

Acknowledgments

The authors gratefully acknowledge financial support from SBUF - The Development Fund of the Swedish Construction Trade (grant 13576) and TMPB - The Masonry and Render Construction Association.

Appendix A

A.1. WDR events characteristic for Swedish conditions

As one of the aims of this study is to expose masonry specimens to water spray that reflects realistic WDR events in Sweden, in this section, we calculated WDR intensities for a multi-story building located in three different geographical locations in Sweden. Notably, Sweden can be a good representative of regions with moderate WDR events. Among available semi-empirical WDR deposition models [52–54], the advanced and widely used ISO model [52] is considered. The climate data is taken from the Swedish Meteorological Hydrological Institute (SMHI) [55]. First, the WDR relationship and ISO model are briefly presented. Second, the hourly rain intensities and wind velocities in Malmö, Gothenburg, and Uppsala for the period 1995–2020 are used to calculate driving rain intensities for the considered building.

A.1.1. WDR calculations

The general equation to calculate WDR intensity, R_{wdr} [mm/h] on a building façade in semi-empirical models can be written as follows:

$$R_{\text{wdr}} = \alpha \times U_{10} \times R_h^{0.88} \times \cos \theta \quad (\text{A.1})$$

where α is WDR coefficient [s/m] to be elaborated in the next paragraph; U_{10} is the reference wind speed (unobstructed streamwise wind speed at 10 m height) [m/s]; R_h is the unobstructed horizontal rainfall intensity (i.e., the intensity of rainfall falling through a horizontal plane, as measured by a standard rain gauge with a horizontal orifice) [mm/h]; and θ is the angle between the wind direction and the normal to the façade [°].

As in free-field conditions, WDR intensity can differ from WDR intensity on a building façade [56], the two factors, α and $\cos \theta$, were introduced in Eq. (A.1).

The WDR coefficient α in the ISO model [52] is given in Eq. (A.2):

$$\alpha = \frac{2}{9} \times C_T \times O \times W \times C_R \quad (\text{A.2})$$

where C_T is the topography coefficient [–]; O is the obstruction factor [–]; W is the wall factor [–]; and C_R is the roughness coefficient [–].

Although the ISO model provides the average annual amount of WDR, it can nevertheless be used to determine WDR intensity for any period during a year [56]. In this regard, based on the ISO model, Blocken and Carmeliet [56] presented Eq. (A.3) to calculate WDR intensity on a building façade by inserting Eq. (A.2) to Eq. (A.1):

$$R_{\text{wdr}} = \frac{2}{9} \times C_T \times O \times W \times C_R \times U_{10} \times R_h^{0.88} \times \cos(\theta) \quad (\text{A.3})$$

A.1.2. WDR for multi-story building

WDR intensities R_{wdr} are calculated for a 15-m high multi-story building with a flat roof. The wind direction is perpendicular to the façade ($\theta = 0^\circ$). Regarding the topography coefficient C_T and obstruction factor O , it is considered that the building is located in a terrain that is flat and free of obstructions. Therefore, C_T and O are equal to one. The wall factor, W , for a multi-story building with a flat roof is 0.5 for the top 2.5 m and 0.2 for the remainder of the exposed façade. In this case, the top part of the façade is considered; thus, W is equal to 0.5. The equation to calculate the roughness coefficient (C_R), dependent on the terrain category, as provided in the ISO model, is as follows:

$$C_R(z) = K_R \cdot \ln\left(\frac{z}{z_0}\right) \quad \text{for } z \geq z_{\min} \quad (\text{A.4})$$

$$C_R(z) = C_R(z_{\min}) \quad \text{for } z < z_{\min} \quad (\text{A.5})$$

where z is the height above ground [m]; K_R is the terrain factor [–]; z_0 is the roughness length [m]; and z_{\min} is the minimum height [m].

It is further assumed that the 15-m high building is neighboring to farmlands, thus belonging to terrain category II, according to the ISO model [52]. Values of K_R , z_0 , and z_{\min} as a function of the terrain category are given in the ISO model [52], in which $K_R = 0.19$, $z_0 = 0.05$ m, and $z_{\min} = 4$ m. Hence, C_R is equal to 1.084, and the WDR coefficient α , for the given building façade is then equal to 0.12.

To calculate the WDR intensity R_{wdr} , the same building with the same terrain and building geometry was considered to be located in Malmö,

Gothenburg, and Uppsala.

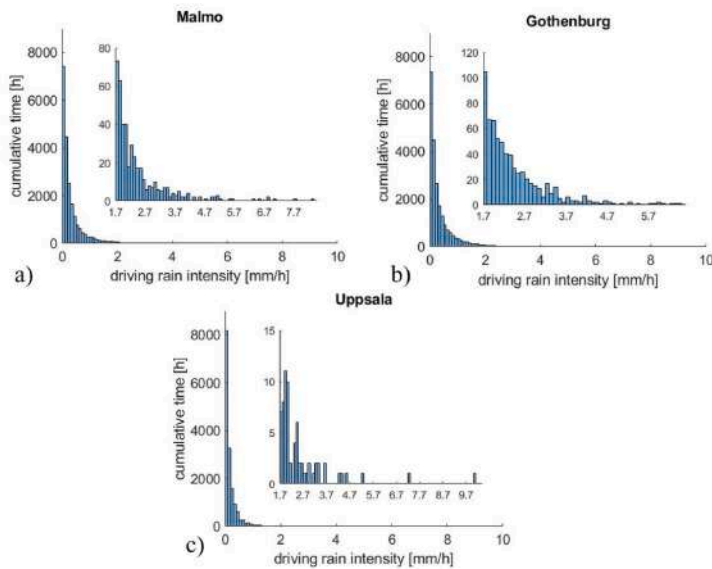


Fig. A.1. Driving rain intensities from 1995 until 2020 for a) Malmö, b) Gothenburg, and c) Uppsala; Small diagrams show highest driving rain intensities.

Fig. A.1 shows that the highest WDR intensity for Malmö, Gothenburg, and Uppsala is equal to 8.4, 6.5, and 10.1 mm/h, respectively. As shown in the figure, the range of the water application rate used in this study, varying between 1.7 and 3.8 l/m²/h, falls within the range of realistic WDR intensities in Sweden, although a clear majority (>99%) of the WDR events has intensities below 1 mm/h. Thus, the test setup should be further developed to reproduce even lower water application rates.

References

- [1] J. Carmeliet, B. Blocken, Driving Rain, Rain Absorption and Rainwater Runoff for Evaluating Water Leakage Risks in Building Envelopes, 2004, 9th International Conference on Performance of Exterior Envelopes of Whole Buildings (Buildings IX).
- [2] A. Day, R. Lacy, J. Skeen, Rain Penetration through Walls, A Summary of the Investigations Made at the UK Building Research Station from 1925 to 1955, Building Research Station Note, 1955.
- [3] M. Pountney, R. Maxwell, A. Butler, Rain penetration of cavity walls: report of a survey of properties in England and Wales, Building Research Establishment Information Paper 2, 1988.
- [4] J.M. Pérez-Bella, J. Domínguez-Hernández, B. Rodríguez-Soria, J.J. del Coz-Díaz, E. Cano-Suñén, Combined use of wind-driven rain and wind pressure to define water penetration risk into building façades: the Spanish case, *Build. Environ.* 64 (2013) 46–56.
- [5] A.S. Kaslegard, Climate Change and Cultural Heritage in the Nordic Countries, Nordic Council of Ministers 2011.
- [6] S. Shahreza, M. Molnár, J. Niklewski, I. Björnsson, T. Gustavsson, Making Decision on Repointing of Clay Brick Facades on the Basis of Moisture Content and Water Absorption Tests Results—A Review of Assessment Methods, *Brick and Block Masonry-From Historical to Sustainable Masonry*, CRC Press 2020, pp. 617–623.
- [7] W. Tang, C.I. Davidson, S. Finger, K. Vance, Erosion of limestone building surfaces caused by wind-driven rain: 1. Field measurements, *Atmos. Environ.* 38 (33) (2004) 5589–5599.
- [8] M.E. Young, Dampness penetration problems in granite buildings in Aberdeen, UK: causes and remedies, *Construct. Build. Mater.* 21 (9) (2007) 1846–1859.
- [9] T. Hines, M. Mehta, The effect of mortar joints on the permeance of masonry walls, in: *Proceedings of the 9th International Brick/Block Masonry Conference*, 1991, pp. 1227–1234. Berlin, Germany.
- [10] C.T. Grimm, Water Permeance of Masonry Walls: a Review of the Literature, *Masonry: Materials, Properties, and Performance*, ASTM International 1982.
- [11] B. Blocken, J. Carmeliet, A review of wind-driven rain research in building science, *J. Wind Eng. Ind. Aerod.* 92 (13) (2004) 1079–1130.
- [12] B. Blocken, D. Derome, J. Carmeliet, Rainwater runoff from building façades: a review, *Build. Environ.* 60 (2013) 339–361.
- [13] H. Ge, Influence of time resolution and averaging techniques of meteorological data on the estimation of wind-driven rain load on building façades for Canadian climates, *J. Wind Eng. Ind. Aerod.* 143 (2015) 50–61.
- [14] B. Blocken, G. Dezso, J. van Beeck, J. Carmeliet, Comparison of calculation models for wind-driven rain deposition on building façades, *Atmos. Environ.* 44 (14) (2010) 1714–1725.
- [15] A. Erkal, D. D'Ayala, L. Sequeira, Assessment of wind-driven rain impact, related surface erosion and surface strength reduction of historic building materials, *Build. Environ.* 57 (2012) 336–348.
- [16] M. Abuku, H. Janssen, J. Poesen, S. Roels, Impact, absorption and evaporation of raindrops on building façades, *Build. Environ.* 44 (1) (2009) 113–124.
- [17] P. Jonell, T. Moller, Moisture Penetration of Solid Facing Brick Walls, National Research Council of Canada, 1956. Technical Translation (National Research Council of Canada); no. NRC-TT-618.
- [18] T. Ritchie, Rain Penetration of Walls of Unit Masonry, *Canadian Building Digest*; No. CBD-6, 1960.
- [19] T. Ritchie, W.G. Plewes, A Review of Literature on Rain Penetration of Unit Masonry, National Research Council of Canada. Division of Building Research, 1957. Technical Paper.
- [20] T. Ritchie, Small-panel Method for Investigating Moisture Penetration of Brick Masonry, Internal Report (National Research Council of Canada. Division of Building Research); No. DBR-IR-160, National Research Council of Canada, 1958.
- [21] T. Ritchie, Influence of Silicone Treatment of Bricks on Moisture Penetration and Bond Strength of Brickwork, Internal Report (National Research Council of Canada. Division of Building Research); No. DBR-IR-207, National Research Council of Canada, 1960.
- [22] T. Ritchie, W.G. Plewes, Moisture penetration of brick masonry panels, *ASTM Bull.* 249 (1961) 39–43.
- [23] C.C. Fishburn, D. Watstein, D.E. Parsons, Water Permeability of Masonry Walls, US Department of Commerce, National Bureau of Standards, 1938.
- [24] C.C. Fishburn, Water Permeability of Walls Built of Masonry Units, US Department of Commerce, National Bureau of Standards 1942.
- [25] C. Groot, J. Gunneweg, The influence of materials characteristics and workmanship on rain penetration in historic fired clay brick masonry, *Heron* 55 (2) (2010) 2010.

- [26] F. Slaps, T. Kvande, N. Bakken, M. Haugen, J. Lohne, Masonry's resistance to driving rain: mortar water content and impregnation, *Buildings* 7 (3) (2017) 70.
- [27] J.C.Z. Piaia, M. Cheriaf, J.C. Rocha, N.L. Mustelier, Measurements of water penetration and leakage in masonry wall: experimental results and numerical simulation, *Build. Environ.* 61 (2013) 18–26.
- [28] J. Ribar, **Water Permeance of Masonry: a Laboratory Study, Masonry: Materials, Properties, and Performance, ASTM International**1982.
- [29] K.B. Anand, V. Vasudevan, K. Ramamurthy, Water permeability assessment of alternative masonry systems, *Build. Environ.* 38 (7) (2003) 947–957.
- [30] R. Cacciotti, Brick masonry response to wind driven rain, *Eng. Struct.* 204 (2020) 110080.
- [31] A. International, ASTM E514/E514M-14a, Standard Test Method for Water Penetration and Leakage through Masonry, ASTM International, West Conshohocken, PA, 2014.
- [32] NEN 2778, 2015 Nl. Vochtwerking in Gebouwen (Moisture Control in Buildings), 2015, Nederlands.
- [33] NBI 29/1983 Mørtler, Tethet Mot Slagregn (Mortars: Resistance to Driving Rain), Norges byggforskningsinstitutt, Oslo, Norway, 1983, pp. 75–76.
- [34] S. Van Goethem, N. Van Den Bossche, A. Janssens, Watertightness assessment of blown-in retrofit cavity wall insulation, *Energy Procedia* 78 (2015) 883–888.
- [35] R.R. Vilaça, WATER PENETRATION TEST ON CONCRETE BLOCK MASONRY, the 15th International Brick and Block Masonry Conference, Florianópolis – Brazil, 2012.
- [36] D. Chiovitti, M. Gonçalves, A. Renzullo, Performance evaluation of water repellents for above grade masonry, *J. Therm. Envelope Build. Sci.* 22 (2) (1998) 156–168.
- [37] R. Forghani, Y. Totoev, S. Kanjanabootra, A. Davison, Experimental investigation of water penetration through semi-interlocking masonry walls, *J. Architect. Eng.* 23 (1) (2017), 04016017.
- [38] S.K. Ghosh, J.M. Melander, Air Content of Mortar and Water Penetration of Masonry Walls, Portland Cement Association Skokie, IL, 1991.
- [39] M.E. Driscoll, R.E. Gates, A Comparative Review of Various Test Methods for Evaluating the Water Penetration Resistance of Concrete Masonry Wall Units, Masonry: Design and Construction, Problems and Repair, ASTM International, 1993.
- [40] L.R. Baker, F.W. Heintjes, Water leakage through masonry walls, *Architect. Sci. Rev.* 33 (1) (1990) 17–23.
- [41] N. Van Den Bossche, M. Lacasse, A. Janssens, Watertightness of Masonry Walls: an Overview, 12th International Conference on Durability of Building Materials and Components (XII DBMC-2011), FEUP Edições, 2011, pp. 49–56.
- [42] M. Lacasse, T. O'Connor, S. Nunes, P. Beaulieu, Report from Task 6 of MEWS project: experimental assessment of water penetration and entry into wood-frame wall specimens-final report, *Inst. Res. Constr. RR-133* (2003) Feb.
- [43] A.J. Rathbone, Rain and Air Penetration Performance of Concrete Block Work, Technical report 553, 5th Ed., Cement and Concrete Association, 1982. ISBN: 978-0-7210-1261-2.
- [44] H. Hens, S. Roels, W. Desadeleer, Rain Leakage through Veneer Walls, Built with Concrete Blocks, CIB W40 meeting, Glasgow, 2004.
- [45] A. International, ASTM C67/C67M-20, Standard Test Methods for Sampling and Testing Brick and Structural Clay Tile, ASTM International, West Conshohocken, PA, 2020.
- [46] A. International, ASTM C1403 - 15, Standard Test Method for Rate of Water Absorption of Masonry Mortars, ASTM International, West Conshohocken, PA, 2015.
- [47] M. Abuku, B. Blocken, J. Poesen, S. Roels, Spreading, Splashing and Bouncing of Wind-Driven Raindrops on Building Facades, 11th Americas Conf. On Wind Engineering, Univ. of Washington, Seattle, 2009, pp. 22–26.
- [48] T. Ritchie, J.I. Davison, Factors Affecting Bond Strength and Resistance to Moisture Penetration of Brick Masonry, vol. 320, ASTM Special Technical Publication, 1963, pp. 16–30.
- [49] C. Hall, A. Kalimeris, Water movement in porous building materials—V. Absorption and shedding of rain by building surfaces, *Build. Environ.* 17 (4) (1982) 257–262.
- [50] C. Hall, W.D. Hoff, **Water Transport in Brick, Stone and Concrete, second ed., CRC Press**2011.
- [51] K.J. Krakowiak, P.B. Lourenço, F.J. Ulm, Multitechnique investigation of extruded clay brick microstructure, *J. Am. Ceram. Soc.* 94 (9) (2011) 3012–3022.
- [52] EN ISO 15927-3, Hygrothermal Performance of Buildings—Calculation and Presentation of Climatic Data. Part 3: Calculation of a Driving Rain Index for Vertical Surfaces from Hourly Wind and Rain Data, European Committee for Standardization, 2009.
- [53] ASHRAE, Standard 160-2016. Criteria for Moisture-Control Design Analysis in Buildings, ASHRAE, Atlanta, GA, 2016.
- [54] J. Straube, E. Burnett, Simplified Prediction of Driving Rain on Buildings, Proceedings of the International Building Physics Conference, Eindhoven University of Technology Eindhoven, the Netherlands, 2000, pp. 375–382.
- [55] <https://www.smbi.se/data>, (Accessed September 2020).
- [56] B. Blocken, J. Carmeliet, Overview of three state-of-the-art wind-driven rain assessment models and comparison based on model theory, *Build. Environ.* 45 (3) (2010) 691–703.

Paper III





14TH CANADIAN MASONRY SYMPOSIUM
MONTREAL, CANADA
MAY 16TH – MAY 20TH, 2021



WATER ABSORPTION AND PENETRATION IN CLAY BRICK MASONRY EXPOSED TO UNIFORM WATER SPRAY

Kahangi Shahreza, Seyedmohammad¹; Molnár, Miklós² and Niklewski, Jonas³

ABSTRACT

This experimental study investigates the effect of brick absorption properties and mortar joint profiles on water absorption and penetration in clay brick masonry. A test setup is presented, making continuous measurements of absorbed and penetrating water possible. Further, damp patches on the backside of the specimens are tracked by utilizing a digital camera and image analysis. Twenty-four masonry specimens are prepared using three different brick types with two different types of mortar joint profile: flush and raked. The tests are performed with a water application rate of $6.3 \text{ l/m}^2/\text{h} \pm 5 \%$ and zero differential air pressure. Results indicate that water absorption and penetration are mostly dependent on brick absorption properties, and the main way for water to penetrate is through brick-mortar interfacial zone. Additionally, the effect of joint profile on water absorption and penetration in specimens is negligible. The first visible damp patches on the backside of specimens appeared close to the head joint, indicating the difficulty of workmanship in filling the head joints and the brick-mortar interface as the primary water penetration path.

KEYWORDS: *brick masonry, water absorption, water penetration, damp patches, mortar joint profile, wind-driven rain, sorptivity*

¹ PhD Student, Department of Building and Environmental Engineering, Division of Structural Engineering, Lund University, John Ericssons väg 1, SE-223 63 Lund, Sweden, mohammad.kahangi@kstr.lth.se

² Associate Professor, Department of Building and Environmental Engineering, Division of Structural Engineering, Lund University, John Ericssons väg 1, SE-223 63, Lund, Sweden, miklos.molnar@kstr.lth.se

³ Assistant Professor, Department of Building and Environmental Engineering, Division of Structural Engineering, Lund University, John Ericssons väg 1, SE-223 63, Lund, Sweden, jonas.niklewski@kstr.lth.se

INTRODUCTION

Clay brick masonry façades have been used frequently for centuries because of their high longevity and long-term durability. Nevertheless, deterioration of masonry façades exposed to climate agents such as wind-driven rain (WDR) is inevitable [1]. Since moisture is one of the main causes of the damage to the buildings' façades and WDR is the primary source of moisture, the resistance of masonry veneer walls against WDR penetration has been a design issue for several decades [2-4].

Several experimental studies are available in the literature investigating masonry's response to WDR [3, 5-12]. Water penetration through the masonry façade depends on brick and mortar absorption properties, the profile of mortar joints, mortar consistency, presence of cracks, the compatibility of units and mortar, thickness of mortar joint, and workmanship [9, 10, 12-17]. Accordingly, there are several test methods available in standards to assess the water penetration in masonry walls [18-20], where ASTM E514 is one of the most frequently used test methods [3, 11, 21]. In the ASTM E514 standard, the specimens should be tested at a water spray rate of 138 l/m²/h and 500 Pa pressure difference.

The test condition of ASTM E514 standard is, in most cases, more severe than natural exposures, as stated by Fishburn et al. [5], and can only occur at specific locations, with very low probabilities, as analyzed by Cornick and Lacasse [22]. Additionally, a comparative study reviewing existing water penetration test methods, conducted by Driscoll and Gates [23], identifies a need for a simple test method to complement existing ones. Furthermore, Ribar [8] suggests that current test standards need to be revised to incorporate a realistic exposure condition approach. Thus, Forghani et al. [11] adjusted the air pressure of 500 Pa in ASTM E514 [18] to 45 Pa, a reduction of 91 %. Further, performing tests with zero pressure was considered in studies conducted by Shahreza et al. [12], Slapø et al. [10], Anand et al. [21], and Lacasse et al. [24]. Besides, Gigla [4] developed a test setup to study the water absorption of veneer masonry walls without evaluating air pressure. Additionally, Shahreza et al. [12] developed a test setup to expose masonry specimens to a uniform water spray rate varying between 1.7 and 3.8 l/m²/h, a reduction of 95 % with respect to the ASTM E514 [18] test condition. Yet, as no water penetration that could be collected from the backside of the specimens was observed, that study focused on the measurement of water absorption and the analysis of damp patches on the backside of specimens.

In this experimental study, water absorption and penetration in brick masonry are studied using a newly developed test setup. Instead of the other test methods where a water film is maintained on the specimen surface [3, 6, 7], the present test applies a uniform and adjustable water spray to the surface. In addition to continuous water absorption and penetration measurements, the area and location of damp patches on the backside of specimens during the entire test period are monitored. The experimental campaign includes three Series of clay brick masonry specimens, prepared with three different types of bricks and two different mortar joint profiles, namely flush and raked. Since the overall objective of the present study is to investigate the WDR-related effects of mortar joint erosion on increased water uptake and penetration in clay brick masonry, raked specimens were chosen to be studied as a representative of eroded mortar joints. The comparison between water

absorption and penetration of flush and raked specimens can facilitate understanding of how WDR-related water absorption and penetration might be affected in eroded mortar joints. The tests were conducted at zero differential air pressure, at a water spray rate of $6.3 \text{ l/m}^2/\text{h} \pm 5 \%$, approximately 90% lower than the water application rate in current standards and studies [3, 11, 18, 21].

MATERIALS AND METHODS

Test setup

A test setup was designed to expose masonry specimens to a uniform water spray. The specimen was mounted on a scale to allow for continuous monitoring of weight. Any water penetrating through the backside of the specimen was led to a collector mounted on a second scale. A nozzle with a conical spray pattern was mounted in a fixed position at a horizontal distance of 50 cm from the specimen's exposed surface. In order to minimize variation and monitor the water flow, two water pressure regulators and a water flow meter were mounted between the water supply and the nozzle. A digital camera was mounted behind the specimen to record any visible dampness. The resulting time-lapse image sequence was analyzed through image analysis to obtain the location of the first visible dampness and the relative damp area over time. A more detailed description of the test setup is presented in Reference [12]. A schematic illustration of the test setup is shown in Figure 1.

Each specimen was tested over a period of 23 hours, including six consecutive cycles; each cycle consisted of 210 min of water spraying and 20 min of drying. Tests were done with zero pressure, whereas the water application rate was maintained at $6.3 \text{ l/m}^2/\text{h} \pm 5 \%$.

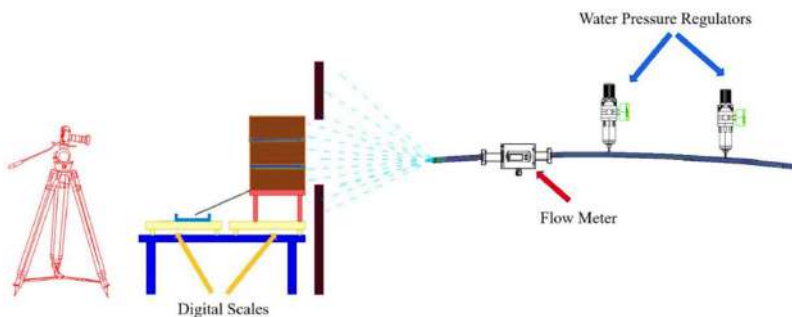


Figure 1: Schematic of the test setup

Bricks and mortar

In this study, three types of bricks, type I, II, and III with different absorption properties, were tested. Twenty bricks from each type were studied to characterize their initial rate of absorption (IRA) and 24-h water absorption properties. Ten bricks of each type were tested to characterize the sorptivity of the bricks. Table 1 summarizes the results of IRA, 24-hour cold water absorption,

and sorptivity tests. Brick types I and II are both classified as medium suction bricks, whereas type III is categorized as low suction. Note that the absorption capacity of type I and II differ by a factor of 2.

Mortar M 2.5, widely used in Northern Europe for masonry façades, was used in this study. Twelve 100 mm-side cubes were cast to characterize the mortar. Table 1 summarizes the average results of the IRA and sorptivity properties of mortar. It should be noted that all tests to characterize brick and mortar properties were conducted according to ASTM C67 [25] and ASTM C1403 – 15 [26] standards.

Table 1: Average water absorption properties, including initial rate of absorption, 24-hour absorption, and sorptivity of bricks and mortars

Materials	Dimensions (mm×mm×mm)	Density ρ (kg/m ³)	Average IRA (kg/m ² /min.)	Average IRA (g/30in ² /min.)	CoV (%)	Average 24-h water absorption (%)	CoV (%)	Average sorptivity mm/min ^{1/2}	CoV (%)
Bricks type I	250×120×62	1800	1.95	37.7	2.3	16.0	1.6	1.495	0.6
Bricks type II	250×120×62	1990	1.81	35.0	5.1	8.6	14.5	1.028	18.4
Bricks type III	240×115×62	2235	0.71	13.7	23.0	4.0	38.6	0.268	22.8
Mortar M 2.5	100×100×100	1869	0.3	5.8	19.7	-	-	0.159	8.7

Masonry specimens

This study aimed to study water absorption and penetration in clay brick masonry exposed to a uniform water spraying. Three different types of bricks and two different joint profiles were considered. In total, 24 triplet specimens were built consisting of three courses of brick, with the length of one brick and the thickness of half-brick length.

Specimens herein presented are divided into three Series according to the brick absorption properties. Each Series is divided into two groups according to the joint profile (Table 2). Group G1 includes twelve specimens pointed with mortar M 2.5 with a tooled flush joint profile, whereas Group G2 consists of twelve specimens pointed with mortar M 2.5 with a raked joint profile. To eliminate uncertainties regarding workmanship, a single craftsman built all specimens. Extra effort went into ensuring that the same amount of water was added to each batch of mortar mix, i.e., eliminating the effect of mortar flow on water penetration.

Specimens of group G1, with mortar M 2.5, were tooled with a wooden stick to have a flush profile. For specimens with the raked joint profile, group G2, the specimens were pointed with mortar M 2.5, and then a 5 mm screw was used to remove extra mortar to reach the depth of 5 mm (Figure 2). The workmanship technique used for bricklaying in this study was the so called pushing of the head joints. Figure 3 shows the backside of the representative specimens.

The specimens are named according to the notation A-B-C, where A, B, and C correspond to the brick type (I = medium suction [I], II = medium suction [II], III = low suction), mortar joint profile (F = flush and R = raked), and specimen number, respectively. For example, specimen I-R-2 belongs to Series I, was built with medium suction bricks, with a raked joint, and it is the second specimen of group G2.

Table 2: Specimen designation and configurations

Series	Group	Brick	Mortar	Joint profile finishes	No. of specimens
Series I (250 mm × 215 mm × 120 mm)	G1	Medium Suction I	M 2.5	Flush	4
	G2			Raked	4
Series I (250 mm × 215 mm × 120 mm)	G1	Medium Suction II	M 2.5	Flush	4
	G2			Raked	4
Series III (240 mm × 215 mm × 120 mm)	G1	Low Suction	M 2.5	Flush	4
	G2			Raked	4

After bricklaying, the specimens were cured for 28 days under plastic sheets. Subsequently, all sides of the specimens except the exposed surface and backside were sealed using a two-component sealant producing a flexible waterproof coating. Prior to testing, all specimens were kept in a climate room under controlled conditions (temperature of 20 °C and relative humidity of 60 %). Figure 2 shows a representative sealed specimen of each group within each Series.

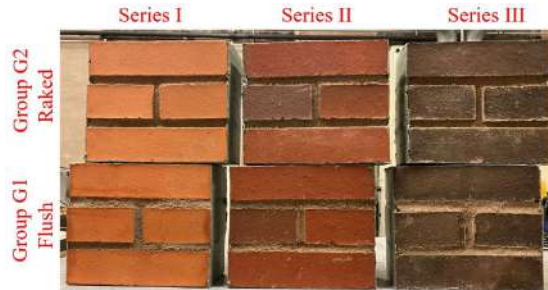


Figure 2: Representative specimens from each group and Series after sealing



Figure 3: Backside of the representative specimens

RESULTS AND DISCUSSION

Water absorption

As the test setup was capable of measuring the amount of absorbed water, i.e., mass gain continuously, it provides the opportunity to study each specimen's absorption behavior during testing. The absorption herein is defined as the ratio between the mass gain, i.e., the difference between measured weight and initial weight, and the initial weight. Figure 4 shows the average absorption of each group within each Series during 23-h of the test. The linear branch of the absorption curve indicates that surface saturation was not yet attained, as most sprayed water is absorbed. The point when surface saturation occurs can be seen from the deviation from a linear slope of the absorption curve. Surface saturation is attained during the 1st cycle for all groups of each Series. The obtained results suggest that there is a strong correlation between brick's sorptivity and the time to attain surface saturation. Accordingly, a high sorptivity allows rapid moisture transport and postpones surface saturation, as shown by Van Den Bossche et al. [27] and Shahreza et al. [12]. As can be seen in Figure 1, surface saturation takes a shorter time to occur for Series III than Series I and II. Thus, the higher the brick's sorptivity is, the shorter time it takes to attain surface saturation.

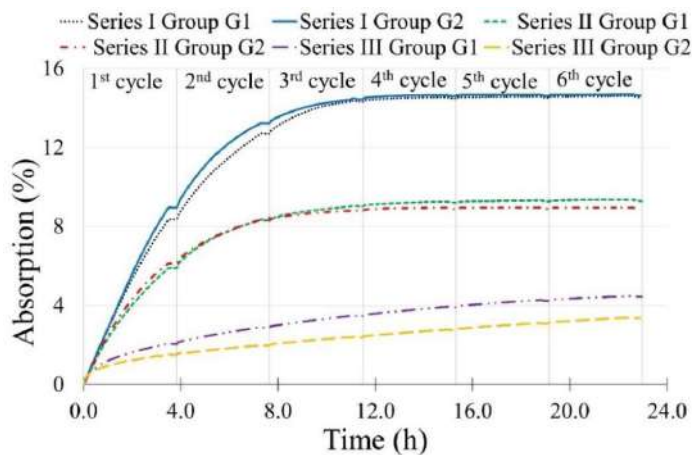


Figure 4: Average water absorption vs. time response for each group within each Series

As the test progressed beyond surface saturation, the slope of the absorption curve decreases. For Series I and II, specimens prepared with medium suction bricks type I and II, the absorption ends during the 4th cycle, whereas for Series III, specimens built by low suction bricks, the absorption continues until the end of the test. The results indicate that the rate of absorption in masonry specimens during 23-h of the test is highly dependent on the sorptivity of the bricks, whereas the amount of absorbed water at the end of the test is mostly correlated to the absorption capacity of the masonry.

Further, in Series I and II, in spite of the relatively high absorption capacity of bricks, full saturation of specimens occurred during the 4th cycle because of the relatively high sorptivity properties of bricks (the sorptivity of medium suction bricks type I and II was roughly 5.5 and 3.8 times more those of low suction bricks). In contrast, for Series III, specimens prepared with relatively low water absorption capacity, the low sorptivity of bricks resulted in continuous absorption during the test, indicating that the specimens did not attain full saturation.

The absorption in each specimen after the 1st cycle and the 6th cycle is summarized in Table 3. It can be seen that the difference in the average total absorption between each group within Series I and II is negligible. In contrast, after performing the 1st cycle, for both Series I and II, the average absorption of group G1, specimens with flush joint profile, is roughly 7.0 % smaller than that of group G2, specimens with raked joint profile. However, it can be observed that after the 6th cycle, the total absorption is consistent with the absorption capacity of the corresponding brick type and the effect of joint profile is negligible, e.g., the absorption is equal to roughly 14.5 % for both groups G1 and G2 of Series I, whereas for groups G1 and G2 of Series II, the absorption is equal to 9.3 % and 8.9 %, respectively. The difference between the total absorption of group G1 and G2 of Series III is related to the large variability in bricks' absorption properties (CoV = 38.6 %).

Table 3: Water absorption of specimens after the 1st and the 6th cycle

	Specimens	Initial weight (g)	1 st cycle Absorp (%)	Ave (%)	Total Absorp (%)	Ave (%)	CoV (%)
Series I Group G1	I-F-1	11746	8.1	8.4	14.4	14.5	1.9
	I-F-2	11766	8.6		14.3		
	I-F-3	11558	8.4		14.9		
	I-F-4	11731	8.4		14.4		
Series I Group G2	I-R-1	11668	8.8	9.0	14.5	14.6	0.9
	I-R-2	11718	9.3		14.4		
	I-R-3	11628	9.1		14.6		
	I-R-4	11585	8.8		14.8		
Series II Group G1	II-F-1	12664	5.5	5.9	9.1	9.3	10.1
	II-F-2	12623	4.3		7.9		
	II-F-3	12591	7.5		9.7		
	II-F-4	12637	6.3		10.4		
Series II Group G2	II-R-1	12762	7.3	6.1	10.1	8.9	10.2
	II-R-2	12575	5.3		8.6		
	II-R-3	12628	6.1		9.3		
	II-R-4	12720	5.7		7.6		
Series III Group G1	III-F-1	12405	1.3	2.1	3.1	4.4	20.2
	III-F-2	12356	2.4		4.3		
	III-F-3	12469	2.4		5.5		
	III-F-4	12219	2.1		4.9		
Series III Group G2	III-R-1	12184	1.7	1.5	3.9	3.3	11.0
	III-R-2	12134	1.5		3.4		
	III-R-3	12010	1.5		2.9		
	III-R-4	12320	1.4		3.2		

Based on the available results, water absorption in brick masonry depends on the brick absorption properties, particularly sorptivity, whereas the impact of joint profile is negligible, particularly after a long exposure to driving rain, as already noted by Shahreza et al [12].

Damp patches

Figure 5 shows the location of the 1st damp patch on the backside of the specimens. With some exceptions, the first patch appeared in close proximity to the head joint. Exceptions include specimens III-F-4, III-R-2, and III-R-4. Due to the difficulty of workmanship in filling and compacting the head joint, the vertical joints can be the primary path for water penetration and leakage.

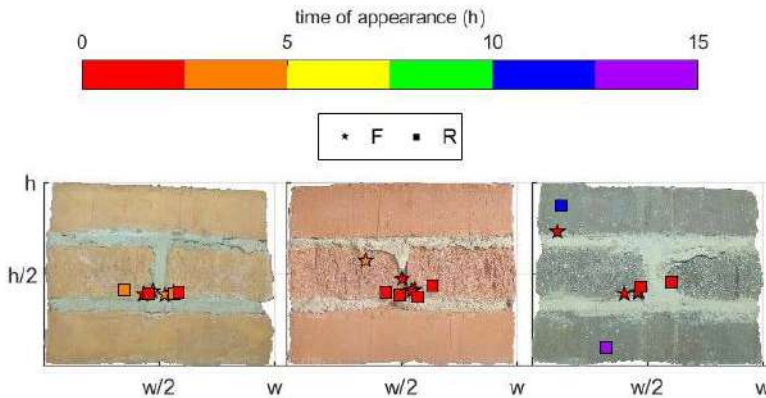


Figure 5: Location of the first visible damp patch on the backside of specimens

The first visible damp patch appeared after 2.5, 2.6, 2.0, and 1.5 hours for groups G1 and G2 of Series I and II, respectively (Table 4). Whereas, for group G1 and G2 of Series III, the dampness appeared after 1.0 and 6.9 hours (Table 4). In Series III, the first dampness appeared after 0.1 h for specimen III-R-1, whereas it took 14 h for specimen III-R-2. This large variability is attributed to the relatively large variability of the bricks' properties and the effects of workmanship.

Additionally, the time when the backside of the specimens reached a relative dampness of 15 % and 50 % are summarized in Table 4. As can be seen, the backside of the specimens in Series I and II reached 15 % dampness roughly 2 hours after the apparition of the 1st visible dampness. The corresponding time in Series III varied between 5 – 10 hours, indicating the importance of the sorptivity on water transport in masonry. A similar trend is discernible when it comes to reach 50 % dampness as it takes roughly 5 hours more in the case of Series I and II and 14 hours in the case of Series III. It should be further observed that for Series III Group G2, 50 % dampness was not reached during the 21 hours of water spray exposure.

Moreover, it can be observed that the adequate filling of the head joint might affect the location and the time to the appearance of the first visible damp patch, as demonstrated for Series III (Figure 5).

Table 4: Time to the first damp patch, 15 % dampness, and 50 % dampness on the backside of specimens, and total water penetration of tested specimens

	Specimen	time to the 1 st patch	time to reach 15 % dampness		time to reach 50 % dampness		Water penetration (g)	Ave (g)
		(h)	Ave (h)	(h)	Ave (h)	(h)		
Series I Group G1	I-F-1	2.0		4.4		8.0	60	108
	I-F-2	3.3	2.5	5.2	5.0	7.5	120	
	I-F-3	1.7		5.5		7.2	150	
	I-F-4	3.0		4.8		7.5	102	
Series I Group G2	I-R-1	2.0		4.7		6.8	190	182
	I-R-2	2.8	2.6	4.3	4.7	5.7	156	
	I-R-3	3.2		5.0		6.8	344	
	I-R-4	2.3		4.8		7.3	32	
Series II Group G1	II-F-1	1.6		4.0		7.2	198	206
	II-F-2	3.2	2.0	4.7	4.0	11.7	30	
	II-F-3	1.3		3.3		4.8	250	
	II-F-4	1.8		3.8		7.0	346	
Series II Group G2	II-R-1	2.3		3.3		5.8	216	146
	II-R-2	1.2	1.5	3.3	3.4	6.2	154	
	II-R-3	1.3		4.0		6.7	16	
	II-R-4	1.2		2.8		6.5	196	
Series III Group G1	III-F-1	0.6		3.3		11.8	50	14
	III-F-2	0.7	1.0	5.0	5.7	15.7	0	
	III-F-3	0.3		6.8		15.4	2	
	III-F-4	2.3		7.5		16.5	2	
Series III Group G2	III-R-1	0.1		13.3		-	0	1
	III-R-2	14.0	6.9	21.0	17.5	-	2	
	III-R-3	2.5		14.0		-	0	
	III-R-4	10.8		21.7		-	2	

Water penetration

The amount of water penetration that could be collected from the backside of specimens after 21 hours of exposure to water spraying is summarized in Table 4. As can be seen, the average amount of penetrated water of group G1 and G2 of Series I and II is equal to 108 g, 182 g, 206 g, and 146 g, respectively. In contrast, there is no considerable water penetration for specimens of Series III except specimen III-F-1. The results suggest that water penetration is highly dependent on the water absorption properties of bricks.

The importance of brick-mortar interface on masonry's resistance to WDR is also noticeable, as most of the collected water from the backside of the specimens, penetrated through the interfacial zone. For instance, in seven out of eight specimens in Series III, the amount of water penetration was limited to between 0 – 2 g. The sharp contrast compared to Series I and II is attributed to continuous contact in the brick-mortar interface and absence of known defects. Yet, in specimen

III-F-1, a water penetration of 50 g was registered, indicating that the quality of the workmanship might not have been as high as in the case of the previously mentioned specimens. It should be further observed that the amount of penetrated water varied within a considerable range also in Series I and II – between 32 – 344 g and 16 – 346 g respectively.

In addition, comparing water penetration of Series I and II with Series III highlights the impact of brick water absorption properties, particularly sorptivity, on the leakage through specimens, as already noted by Ritchie and Plewes [14]. Moreover, comparing water penetration of groups G1 and G2 within each Series indicates the negligible effect of mortar joint profile on water penetration.

Based on the available results, several factors might influence water penetration in brick masonry. Firstly, the primary path for water to penetrate masonry walls is through the brick-mortar interface for low to medium suction bricks, as already noted by Groot and Gunneweg [9] and Slapø et al. [10]. Secondly, although specimens were prepared without any known defects and voids, the difficulty of filling head joints can lead to leakage through masonry specimens. Nevertheless, Jonell and Moller [15] believe on the difficulty of complete filling of the head joint with the pushing technique, as the head joint of specimens in this study were prepared with this technique.

CONCLUSIONS

The presented experimental study was aimed to study water absorption and penetration in clay brick masonry exposed to a uniform water spray by employing a modified test setup. A digital camera was employed to monitor damp patches on the backside (the protected side) of the specimens, and continuous water absorption and penetration measurements were carried out using two digital scales. Parameters investigated were: three different types of bricks and two different mortar joint profiles: flush and raked. The tests were performed with zero differential air pressure between the specimens' exposed side (the front side) and protected side (the backside) with a water application rate of $6.3 \text{ l/m}^2/\text{h} \pm 5 \%$.

Based on the obtained results, the effect of mortar joint profiles on water absorption is negligible, whereas the water absorption in masonry specimens is highly dependent on the water spray rate and sorptivity of bricks prior to the surface saturation. Once the surface saturation was attained, the behavior was dependent on both sorptivity and water absorption capacity of the bricks. Moreover, the first visible damp patch appeared close to the brick-mortar interface, indicating low resistance of the head joint to WDR attributed to low compaction and difficulty in filling the vertical joints.

Furthermore, the main way for water to penetrate a brick masonry was the brick-mortar interface and the water penetration in masonry specimens was influenced by the bricks' absorption properties, whereas the mortar joint profiles did not affect water penetration considerably. The average penetrated water of group G1 and G2 of Series I and II is equal to 108 g, 182 g, 206 g, and 146 g, respectively. However, the water penetration in Series III specimens was roughly zero

except for specimen III-F-1, indicating the high resistance of masonry specimens built with low sorptivity and low absorption capacity bricks to WDR.

Nevertheless, the effect of workmanship to achieve non-open brick-mortar interface on the water penetration in all three Series is noteworthy; a) the difference between the water penetration of individual specimens in Series I and II is substantial, with a minimum of 16 g and a maximum of 346 g; and b) water penetration in specimen III-F-1 was around 50 g despite near zero penetration for the rest of the specimens in Series III.

Eventually, the newly developed test setup might facilitate the verification of moisture simulations as it enables continuous water absorption and penetration measurements combined with tracing of damp areas on the backside of masonry specimens.

ACKNOWLEDGEMENTS

The authors gratefully acknowledge financial support from SBUF - The Development Fund of the Swedish Construction Trade (grant 13576) and TMPB - The Masonry and Render Construction Association.

REFERENCES

- [1] S. Shahreza, M. Molnár, J. Niklewski, I. Björnsson, and T. Gustavsson, "Making decision on repointing of clay brick facades on the basis of moisture content and water absorption tests results—a review of assessment methods," in *Brick and Block Masonry-From Historical to Sustainable Masonry*: CRC Press, 2020, pp. 617-623.
- [2] T. Ritchie, "Rain penetration of walls of unit masonry," (in eng), *Canadian Building Digest*; no. CBD-6, 1960/06 1960, Art no. 5 p., doi: 10.4224/40000794.
- [3] J. C. Z. Piaia, M. Cheriaf, J. C. Rocha, and N. L. Mustelier, "Measurements of water penetration and leakage in masonry wall: Experimental results and numerical simulation," *Build. Environ.*, vol. 61, pp. 18-26, 2013.
- [4] B. Gigla, "RESISTANCE OF MASONRY VENEER WALLS AGAINST RAIN PENETRATION," in *13th CANADIAN MASONRY SYMPOSIUM*, Halifax, Canada, 2017.
- [5] C. C. Fishburn, D. Watstein, and D. E. Parsons, *Water permeability of masonry walls*. US Department of Commerce, National Bureau of Standards, 1938.
- [6] P. Jonell and T. Moller, "Moisture Penetration of Solid Facing Brick Walls," in "Technical Translation (National Research Council of Canada); no. NRC-TT-618," National Research Council of Canada, 0077-5606, 1956 1956.
- [7] T. Ritchie and W. G. Plewes, "Moisture penetration of brick masonry panels," (in eng), *ASTM Bulletin*, no. 249, pp. 39-43, 1961.
- [8] J. Ribar, "Water permeance of masonry: a laboratory study," in *Masonry: Materials, Properties, and Performance*: ASTM International, 1982.
- [9] C. Groot and J. Gunneweg, "The influence of materials characteristics and workmanship on rain penetration in historic fired clay brick masonry," *Heron*, 55 (2), 2010.
- [10] F. Slapø, T. Kvande, N. Bakken, M. Haugen, and J. Lohne, "Masonry's Resistance to Driving Rain: Mortar Water Content and Impregnation," *Buildings*, vol. 7, no. 3, p. 70, 2017.

- [11] R. Forghani, Y. Totoev, S. Kanjanabootra, and A. Davison, "Experimental investigation of water penetration through semi-interlocking masonry walls," *Journal of Architectural Engineering*, vol. 23, no. 1, p. 04016017, 2017.
- [12] S. Kahangi Shahreza, J. Niklewski, and M. Molnár, "Experimental investigation of water absorption and penetration in clay brick masonry under simulated uniform water spray exposure," *Journal of Building Engineering*, vol. 43, p. 102583, 2021/11/01/ 2021, doi: <https://doi.org/10.1016/j.jobe.2021.102583>.
- [13] C. C. Fishburn, *Water permeability of walls built of masonry units*. US Department of Commerce, National Bureau of Standards, 1942.
- [14] T. Ritchie and W. G. Plewes, "A review of literature on rain penetration of unit masonry," (in eng), *Technical Paper (National Research Council of Canada. Division of Building Research)*, 1957/05 1957, Art no. iii, 72 p., doi: 10.4224/40001176.
- [15] T. Ritchie and J. I. Davison, "Factors affecting bond strength and resistance to moisture penetration of brick masonry," (in eng), *ASTM Special Technical Publication*, no. 320, pp. 16-30, 1963/07/01 1963.
- [16] C. T. Grimm, "Water permeance of masonry walls: a review of the literature," in *Masonry: Materials, Properties, and Performance*: ASTM International, 1982.
- [17] T. Hines and M. Mehta, "The Effect of Mortar Joints on the Permeance of Masonry Walls," in *in proceedings of the 9th International Brick/Block Masonry Conference*, Berlin, Germany, October 13-16 1991, pp. pp. 1227-1234.
- [18] *ASTM E514 / E514M-14a, Standard Test Method for Water Penetration and Leakage Through Masonry*, A. International, West Conshohocken, PA, 2014.
- [19] M. Y. L. Chew, "A modified on-site water chamber tester for masonry walls," *Construction and Building Materials*, vol. 15, no. 7, pp. 329-337, 2001/10/01/ 2001, doi: [https://doi.org/10.1016/S0950-0618\(01\)00011-3](https://doi.org/10.1016/S0950-0618(01)00011-3).
- [20] *NEN 2778:2015 nl. Vochtwerking in gebouwen (Moisture control in buildings)*, Nederlands, 2015.
- [21] K. B. Anand, V. Vasudevan, and K. Ramamurthy, "Water permeability assessment of alternative masonry systems," *Build. Environ.*, vol. 38, no. 7, pp. 947-957, 2003/07/01/ 2003, doi: [https://doi.org/10.1016/S0360-1323\(03\)00060-X](https://doi.org/10.1016/S0360-1323(03)00060-X).
- [22] S. Cornick and M. Lacasse, "An Investigation of Climate Loads on Building Façades for Selected Locations in the United States," *Journal of ASTM International*, vol. 6, no. 2, pp. 1-22, 2009.
- [23] M. E. Driscoll and R. E. Gates, "A Comparative Review of Various Test Methods for Evaluating the Water Penetration Resistance of Concrete Masonry Wall Units," in *Masonry: Design and Construction, Problems and Repair*: ASTM International, 1993.
- [24] M. Lacasse, T. O'Connor, S. Nunes, and P. Beaulieu, "Report from Task 6 of MEWS project: Experimental assessment of water penetration and entry into wood-frame wall specimens-final report," *Institute for Research in Construction, RR-133, Feb*, 2003.
- [25] *ASTM C67 / C67M-20, Standard Test Methods for Sampling and Testing Brick and Structural Clay Tile*, A. International, West Conshohocken, PA, 2020.
- [26] *ASTM C1403 - 15, Standard Test Method for Rate of Water Absorption of Masonry Mortars*, A. International, West Conshohocken, PA, 2015.
- [27] N. Van Den Bossche, M. Lacasse, and A. Janssens, "Watertightness of masonry walls: an overview," in *12th International conference on Durability of Building Materials and Components (XII DBMC-2011)*, 2011, vol. 1: FEUP Edições, pp. 49-56.



LUND
UNIVERSITY

Lund University
Faculty of Engineering
Division of Structural Engineering
Report: TVBK-1055
ISBN: 978-91-87993-20-6
ISSN: 0349-4969
ISRN: LUTVDG/TVBK-21/1055 (63)

